UNIVERSITEIT VAN PRETORIA
UNIVERSITY OF PRETORIA
YUNIBESITHI YA PRETORIA

The Use of Metabolomical Analyses for Fungal Phytopathological Diagnosis

Gabriel Chirundu

Submitted in partial fulfilment of the requirements for the degree

MSc (Medicinal Plant Science)

Department of Plant and Soil Sciences

Faculty of Natural and Agricultural Sciences

University of Pretoria

Supervisor: Professor J.J.M. Meyer

Co-Supervisor: Professor D.K. Berger

Co-Supervisor: Professor Q. Kritzinger

October 2023

Title: The Use of Metabolomical Analyses for Fungal Phytopathological Diagnosis

Name of Author: G. Chirundu (16135114)

Name of supervisor: Prof. Marion Meyer

Names of co-supervisors: Prof. Dave Berger

Prof. Quenton Kritzinger

Institution: Department of Plant and Soil Sciences

Faculty of Natural and Agricultural Sciences

University of Pretoria

Date: 31/10/2023

Abstract

Metabolomic data analysis involves assessing, identifying, and quantifying all metabolites, endogenous and exogenous, within biological samples. It allows the global assessment of the cellular state in the context of the immediate environment as it considers gene expression, genetic regulation, enzyme regulation, altered kinetic activity as well as changes in metabolic reactions. Plants being sessile organisms, depend heavily on metabolites to defend themselves against various pathogen attacks e.g., fungi. Metabolomic analysis has been used to determine the defensive metabolites associated with plant pathogens with the aim of understanding both the defense mechanisms of the plant, and infection mechanisms of the pathogen for better disease control and prevention.

This study aimed to assess whether metabolomic and chemical fingerprint analyses can be used in early disease diagnosis as it analyses the state of the plant's physiological changes due to fungal pathogen infection, its proficiency in measuring disease severity, and identifying possible pathogen-related biomarkers. The fungal pathogens that were a point of focus for this study were *Cercospora zeina* which causes grey leaf spot, a devastating maize foliar disease characterized by necrotic lesions, and *Fusarium verticillioides,* which produces fumonisin mycotoxins that can plant growth. Maize leaf samples showing different stages of disease severity were collected from a field trial by Syngenta in Howick. Some samples were collected from plants grown in a glasshouse and inoculated with *C. zeina in vitro*. Cowpea seeds were inoculated *in vitro* with *F. verticillioides* and grown in a phytotron. Metabolites were extracted from the leaf samples and analysed using NMR and GCMS to detect changes in the plants' metabolome, as these techniques encompass both spectroscopic and volatile organic compounds detection.

Maize samples' NMR results showed significant differences between the infected and healthy plants, in both the field trial and glasshouse trial. The NMR data of cowpea samples showed minor differences. However, the GCMS data for both pathosystems showed significant differences between inoculated and uninoculated samples, and certain potential disease-related biomarkers were observed in the chromatograms. These biomarkers shared similarities to hexadecanoic acid, 1-(hydroxymethyl)-1,2-ethanediyl ester, 9,12,15-octadecatrienoic acid, 1,3-dimethoxypropan-2-yl palmitate and butyl-9,12,15-octadecatrienoate. From the results obtained we can conclude that metabolomic and chemical fingerprint analyses are efficient tools in successfully diagnosing plant fungal diseases by indicating various disease-related biomarkers, that can be used for pathogen infection diagnosis.

Acknowledgements

I would like to thank God for everything I have and the opportunity and privilege to do my post-graduate studies at such a prestigious institute, under the guidance of individuals with great presence in the science field. I would like to also thank my Church and everyone who supported and guided me spiritually.

I would like to also thank my parents for all the sacrifices they made for me to complete my studies. For the trust they put in my passion and letting me follow my dream. They also gave me the support I needed to get this far.

I would like to thank Prof. Marion Meyer for his trust and willingness to give one of the best opportunities ever and helped me have the career I have today. For believing, mentoring, and guiding and giving me the platform to live my dream in this project. Pushing me passionately to always improve and be innovative. The man who made me fall in love with metabolomics.

I would also like to thank Prof. Dave Berger for also taking a chance on a project that was just a dream for me and equipping me with the standards of a true scientist. Making me push boundaries in my thinking, reasoning, and approach. No just by mentorship but by also funding my studies. A gift I will forever be grateful for.

I would also like to thank Prof. Quenton Kritzinger for making my fantasies a reality and letting me build on the research he had initiated. Secondly, for also helping me understand scientific reasoning, open-mindedness and being thorough.

I also want to thank my supervisors collectively for the privilege they gave me to exposed to their great minds that have achieved so much in the science field. To be mentored by individuals of such high stature, honor, integrity and contribution in the scientific field. Shaping me in the trajectory I am embarking on now. Another gift I will always cherish.

I would like to thank Sewes Alberts, for all the knowledge he instilled in me. The patience he showed me since my arrival in the Department of Plant and Soil Science. The guidance, the support, the jokes, the pep talks. For this, you are a true inspiration and someone I will forever hold in the highest regard. Words can never describe how much value you added in my journey to your guidance.

Lastly, I would like to thank Bianca Ibeleme for all her help and support during my studies. Prof. Meyer's research group for their support and creating the great environment for excellence. I would also like to thank the Medicinal Sciences and MPPI groups for all their assistance and help. As well as the plethora of laughter, tears, stress, and resolutions we all shared. To always showing willingness to help regardless of who or what the person did. I will always and forever be GRATEFUL to you all.

Table of contents

List of Figures

List of Tables

List of abbreviations

ANOVA	: Analysis of Variance
ATP	: Adenosine Triphosphate
Chls	: Chlorotic Spots
DIMBOA	: 2,4-dihydroxy-7-methoxy-2H-1,4-benzoxazin-3(4H)-one
DNA	: Deoxyribonucleic Acid
FT	: Field Trial
FB	: Fumonisin B
GCMS	: Gas Chromatography Mass Spectrometry
GH	: Glasshouse
GLS	: Grey Leaf Spot
Ha	: Hectares
HDMBOA-Glc	: 2-hydroxy-4,7-dimethoxy-1,4-benzoxazinoid glucoside
Hr	: Hour
ITS	: Internal Transcribed Spacer
KZN	: KwaZulu-Natal
LCMS	: Liquid Chromatography Mass Spectrometry
MHz	: Megahertz
ML	: Mature Lesions
Mnova	: MestreNova Software
MS	: Mass Spectrometry
NMR	: Nuclear Magnetic Resonance
OPLS-DA	: Orthogonal Projection to Latent Structures Discriminant Analysis
PCA	: Principal Component Analysis
PKS	: Polyketide Synthases
QTOF	: Quantitative Time of Flight
RNA	: Ribonucleic Acid
RT	: Retention Time

TEM : Transmission Electron Microscope

UHPLC-ESI : Ultra High-Performance Liquid Chromatography Electron Spray Ionization

Wap : Weeks After Planting

1. Introduction

1.1 Introduction

The cell is a vast pool filled with a plethora of molecules that co-exist and interact together to carry out different cellular functions. To understand this complex network of molecular interactions, techniques have been developed to assess and analyse some of the characteristics of the vast families of cellular constituents e.g., genes, proteins and metabolites. These techniques classified as 'omics' determine the specific roles, interactions and mode of actions of the different cellular molecules within an organism (Roessner and Bowne, 2009; Brunetti et al., 2018). Examples of these omics' techniques are genomics, transcriptomics, proteomics and metabolomics. Genomics involves the analysis of cellular genes and their respective functions, transcriptomics entails the analysis of genetic transcripts (e.g. mRNA) along with their accompanying functions, proteomics involves the analyses proteins with their respective functions and metabolomics is the comprehensive and quantitative analysis of all metabolites in a biological system (Fiehn, 2002). Metabolomics also involves the quantitative measurement of the dynamic multiparametric metabolic response of living systems to pathophysiological stimuli or genetic modification, often termed metabonomics (Beckonert et al., 2007; Ramsden, 2015).

Plants are susceptible to a variety of fungal pathogens that cause some of the most devastating diseases in the world. With over 20 000 parasitic fungal species in nature with high diversity, fungal pathogens account for approximately 70-80 % of plant diseases (Ray et al., 2017). Fungal diseases have threatened food security for many countries for centuries. For example, in the mid-1840s in Ireland potato late blight caused by *Phytopthora infestans* exposed nearly a million people to starvation and drove many more to migrate elsewhere (Talbot, 2003). Another example is rice blast caused by *Pyricularia oryzae* which led to the loss of more than 700 ha of various rice genotypes in Bhutan in 1995 (Ray et al., 2017). One of the most challenging aspects of fungal disease control is their detection (diagnosis) as they can survive in a dormant state on both living and dead plant tissues until environmental conditions become optimal for their proliferation. Their spores also have a variety of propagators e.g., water, wind, soil and animals thus eliciting their effect over wider areas. Omics techniques have been at the epicenter of both conventional and novel diagnostic techniques of various plant fungal diseases (Brunetti et al., 2018).

Conventional diagnostic techniques of plant fungal diseases focused on morphological, microbiological and biochemical identifications. It is mainly composed of three aspects, i.e., visual examination, culturing

and plating methods and isozyme analysis (Figure 1.1). Visual examination involves analysing and interpreting the disease visual symptoms (e.g. spots, galls, lesions, rots, etc.) (Nutter et al., 2006). Several research guidelines have been implored to improve the efficacy of this technique to make it more accurate, reliable, and easily repeatable. However, it has encountered several shortcomings as it depends heavily on an individual's experience and expertise which may lead to inconclusive results, difficult to repeat consistently and impractical for in-field diagnosis (Ray et al., 2017). Culturing and plating methods involve isolating the pathogen from the infected plants, followed by growing it on suitable artificial media under various conditions and microscopic analysis. This technique uses morphological characteristics to diagnose the pathogen i.e., spore morphology, sporulation patterns and characteristics of sporulating structures producing either asexual or sexual spore forms. This is then complemented by taxonomic classification of the fungus (Narayanasamy, 2011). This method however also has its shortcomings which include the need for experience and necessary expertise to make successful diagnosis and it's also time consuming (Ray et al., 2017). In isozyme analysis, the fungal pathogens are detected, differentiated and identified based on morphological similarities or phylogenetic proximity (Rosendahl and Banke, 2020). This technique has been quite proficient in revealing genetic variability in fungal pathogens. Its main limitation however is the low level of polymorphism found in various fungal taxa that have been examined (Burdon, 1993).

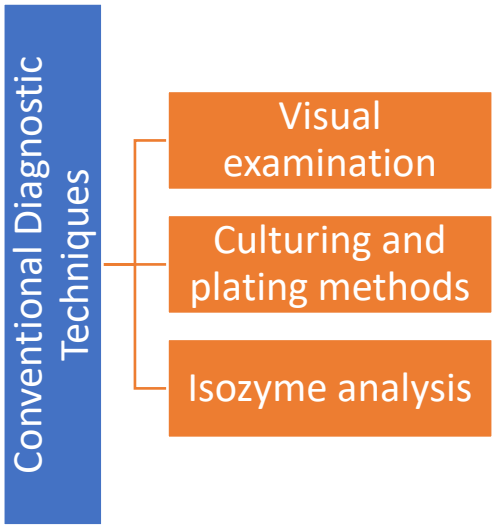

Figure 1.1: Conventional diagnostic techniques (Ray et al., 2017).

Due to the limitations of conventional diagnostic methods which include poor sensitivity and reliability, novel diagnostic methods were developed with the aim of improving detection of fungal pathogens in plants. The novel techniques have been broadly divided into two main categories, direct detection

(pathogen detection) and indirect detection (pathogen-influenced physiological changes) methods (Ray et al., 2017). The direct detection methods are further divided into major categories i.e. immunology-based methods which use antibodies or antibody alternatives and PCR (polymerase chain reaction)- based methods which use nucleic acid probes (Sankaran et al., 2010). Indirect methods of plant disease diagnosis involve detecting the impact of the pathogen on the overall physiological plant response rather than detecting the fungal pathogen itself. It entails plant stress profiling, plant metabolite profiling and gaseous metabolites profiling. It's mainly divided into spectroscopic and imaging techniques with its basis on plant stress response and volatile organic compounds detection which entail identifying specific biomarkers that may indicate infection (Ray et al., 2017). Some examples of direct and indirect fungal diagnostic methods are listed in Figure 1.2.

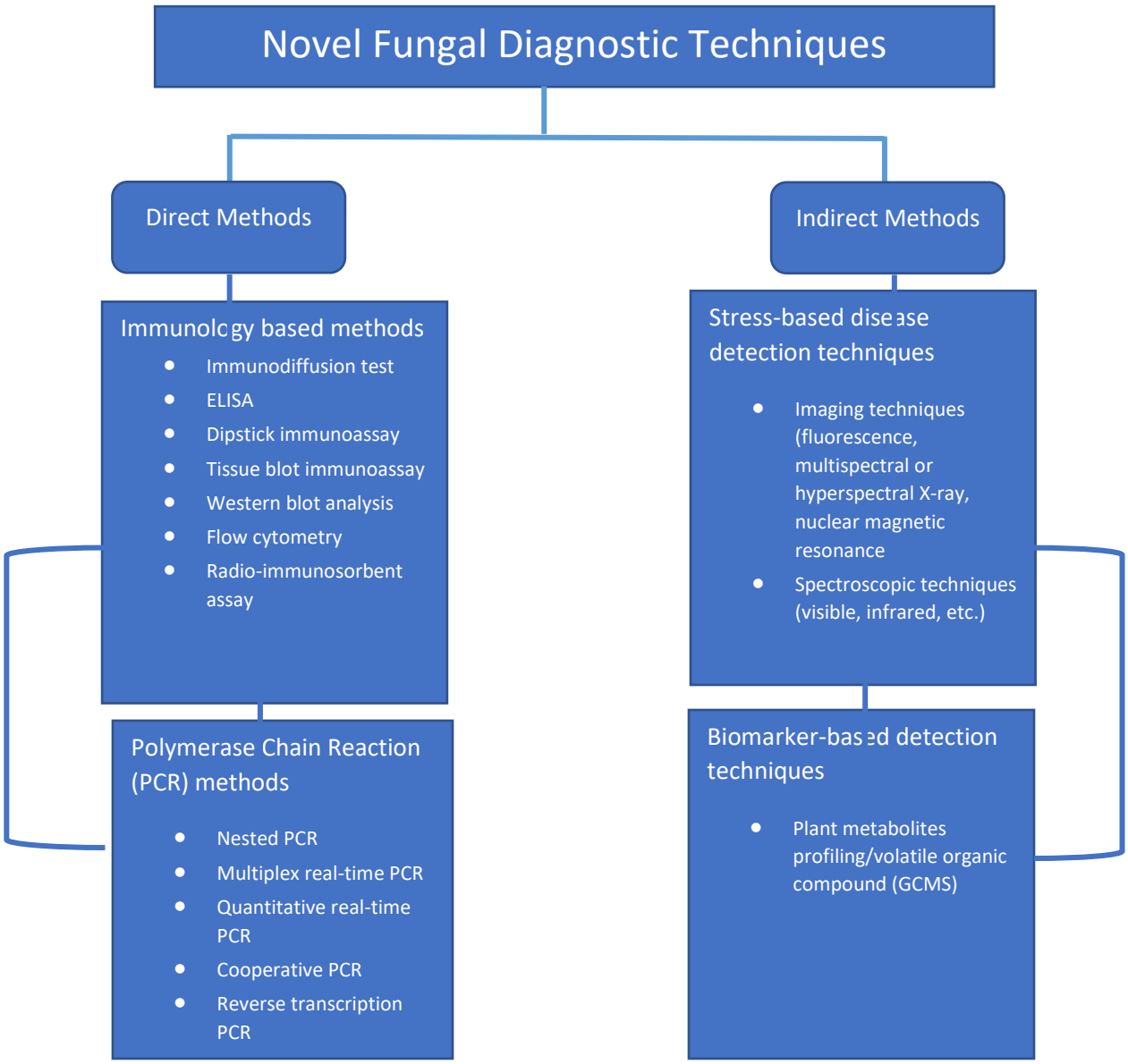

Figure 1.2: Examples of novel disease diagnostic methods used for fungal detection (Ray et al., 2017).

In this study, metabolomic analyses, an indirect detection method that encompasses both spectroscopic and volatile organic compounds detection, will be the point of focus. Metabolomic analyses has been widely used to study the impact of fungal pathogens on the plants' metabolome and as a complementary technique to the preferred direct methods of detection (e.g. PCR) (Chen et al., 2011; Narayanasamy, 2011). This study aims to assess whether metabolomic analyses can be used in early disease diagnosis as it analyses the plant's physiological changes due to fungal pathogen infection. It will also entail assessing the possibility of utilizing metabolomic analysis to directly detect the fungal pathogen's presence in the host plant by detecting the pathogen's metabolomic fingerprint (possibly indicating fungal biomarkers)

within the plant host. Another aspect of this study will be determining the proficiency of metabolomic data in reflecting the degree of disease infection since metabolites are regarded as a direct reflection of a plant's phenotype (Mhlongo et al., 2018).

1.2 Hypothesis

Infected plants will carry the pathogen's metabolite fingerprint in their metabolome, i.e.:

- Presence of metabolites that are known to only be produced by the pathogen.
- Regulation (production/inhibition) of certain metabolites in the plant's metabolome.
- Fluctuations in the concentrations of some metabolites.

1.3 Aims

The main aims of this study were to:

- Successfully diagnose the infected plants through the analysis of their metabolome.
- Determine whether metabolomical analyses can be used for early detection of plant disease.
- Determine the degree of infection of the pathogens in question in the subject plants during certain time intervals.
- Determine whether metabolomical analyses can be used as a direct method of diagnosis.

1.4 Objectives

The main objectives of this study were to:

- Culture fungal pathogens under *in vitro* conditions.
- Obtain the metabolomic data of pure pathogen cultures.
- Successfully inoculate plant species with respective fungal pathogens in a greenhouse and/or collect symptomatic field trial samples.
- Analyses of metabolite profile by NMR and GCMS for fluctuations or changes in the symptomatic plants' metabolome.

1.5 References

Beckonert, O., Keun, H.C., Ebbels, T.M.D., Bundy, J., Holmes, E., Lindon, J.C., Nicholson, J.K., 2007. Metabolic profiling, metabolomic and metabonomic procedures for NMR spectroscopy of urine, plasma, serum and tissue extracts. Nat. Protoc. 2, 2692–2703. https://doi.org/10.1038/nprot.2007.376

Brunetti, A.E., Carnevale Neto, F., Vera, M.C., Taboada, C., Pavarini, D.P., Bauermeister, A., Lopes, N.P., 2018. An integrative omics perspective for the analysis of chemical signals in ecological interactions. Chem. Soc. Rev. https://doi.org/10.1039/c7cs00368d

Burdon, J.J., 1993. The Structure of Pathogen Populations in Natural Plant Communities. Annu. Rev. Phytopathol. 31, 305–323. https://doi.org/10.1146/annurev.py.31.090193.001513

Chen, F., Zhang, J., Song, X., Yang, J., Li, H., Tang, H., Liao, Y.C., 2011. Combined metabonomic and quantitative real-time PCR analyses reveal systems metabolic changes of Fusarium graminearum induced by Tri5 gene deletion. J. Proteome Res. 10, 2273–2285. https://doi.org/10.1021/pr101095t

Fiehn, O., 2002. Metabolomics – the link between genotypes and phenotypes. Plant Mol. Biol. 155–171. https://doi.org/10.1016/j.impact.2017.03.005

Mhlongo, Im.I., Piater, L.A., Madala, N.E., Labuschagne, N., Dubery, I.A., 2018. The Chemistry of Plant – Microbe Interactions in the Rhizosphere and the Potential for Metabolomics to Reveal Signaling Related to Defense Priming and Induced Systemic Resistance. Front. Plant Sci. 9, 1–17. https://doi.org/10.3389/fpls.2018.00112

Narayanasamy, P., Narayanasamy, P., 2011. Introduction, in: Microbial Plant Pathogens-Detection and Disease Diagnosis: Springer Netherlands, pp. 1–4. https://doi.org/10.1007/978-90-481-9735-4_1

Nutter, F.W., Esker, P.D., Netto, R.A.C., 2006. Disease assessment concepts and the advancements made in improving the accuracy and precision of plant disease data, in: European Journal of Plant Pathology. Springer, pp. 95–103. https://doi.org/10.1007/s10658-005-1230-z

Ramsden, J., 2015. Metabolomics and Metabonomics. Springer, London, pp. 265–270. https://doi.org/10.1007/978-1-4471-6702-0_18

Ray, M., Ray, A., Dash, S., Mishra, A., Achary, K.G., Nayak, S., Singh, S., 2017. Fungal disease detection in plants: Traditional assays, novel diagnostic techniques and biosensors. Biosens. Bioelectron. https://doi.org/10.1016/j.bios.2016.09.032

Roessner, U., Bowne, J., 2009. What is metabolomics all about? Biotechniques 46, 363–365. https://doi.org/10.2144/000113133

Rosendahl, S., Banke, S., 2020. Use of Isozymes in Fungal Taxonomy and Population Studies. Chem. Fungal Taxon. 107–120. https://doi.org/10.1201/9781003064626-5

Sankaran, S., Mishra, A., Ehsani, R., Davis, C., 2010. A review of advanced techniques for detecting plant diseases. Comput. Electron. Agric. https://doi.org/10.1016/j.compag.2010.02.007

Talbot, N.J., 2003. On the Trail of a Cereal Killer: Exploring the Biology of Magnaporthe grisea. Annu. Rev. Microbiol. https://doi.org/10.1146/annurev.micro.57.030502.090957

2. Literature Review

2.1 Metabolomics

Metabolites are structurally diverse small molecules that are chemically transformed during cell metabolism and are a direct product of protein activity. In plants, metabolite synthesis pathways are particularly branched since they lead to the production of highly diverse metabolites and minimise the cost put into their production (Ramakrishna and Ravishankar, 2011). Metabolomic data analysis involves the assessment, identification and quantification of all metabolites, endogenous and exogenous, within biological samples (Smolinska et al., 2012). Metabolomics do not function independently of other omics techniques; instead, their interactions with other omics such as functional genomics i.e. DNA sequencing, RNA expression profiling and proteomics provide a better understanding of metabolites (Manzoni et al., 2018). Gene and protein functions are directly subjected to epigenetic regulations and post-translational modifications, respectively. Metabolites are also directly affected downstream by epigenetic factors, however they function as a direct fingerprint of biochemical activity; as such they can easily be correlated with a specific phenotype as illustrated in Figure 2.1 (Jorge et al., 2015). Metabolomics allows the global assessment of the cellular state in the context of the immediate environment as it is a result of gene expression, genetic regulation, enzyme regulation, altered kinetic activity as well as changes in metabolic reactions (Gomez-Casati et al., 2013). Changes in the metabolome are often more amplified relative to the changes in the proteome or transcriptome (Feussner and Polle, 2015).

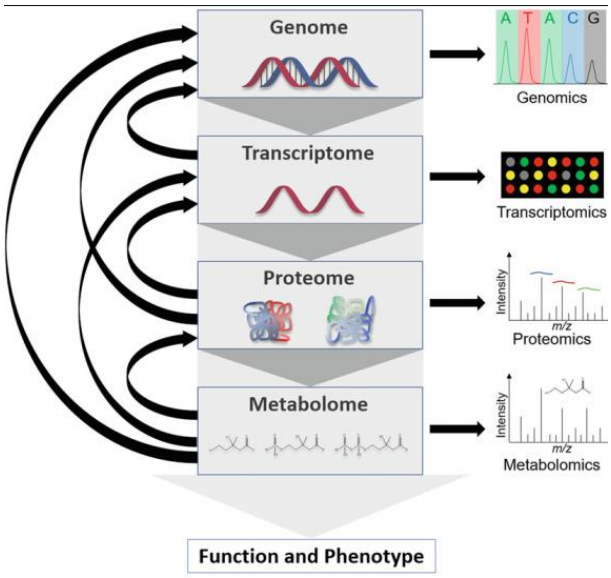

Figure 2.1: General schematic presentation of the omics techniques flowing from genes to transcripts to proteins to metabolites to phenotype as well as the accompanying interactions of the different omics techniques (Baidoo, 2019).

Metabolite analysis provides a new way of analysing functional genomics, as a large number of genes may contribute to the production of a single metabolite and various metabolites may arise from a single or few genes (Smedsgaard and Nielsen, 2005; Luo, 2015). Metabolomics is not dependent on organism-specific genome information for data analysis (Jorge et al., 2015). Metabolomics uses highly sophisticated analytical techniques such as mass spectrometry (MS) and nuclear magnetic resonance (NMR) spectrometry, accompanied by statistical and multivariate analysis for data attainment and interpretation (Heyman and Meyer, 2012).

Metabolites manifest as signals from the genetic architecture and the environment i.e. they are considered to be a direct reflection of the physiological state of an organism (Muji et al., 2015). Studies have shown that certain metabolites are widely distributed in different taxa, while other metabolites are confined to specific clades or taxa e.g. the diterpenoids kaurene and abietane are confined to the Alismataceae (Wink et al., 2018). The metabolomes of organisms are large, complex, and highly dynamic; thus, no specific metabolomics approach can singularly analyse the entire metabolome. Various complementary approaches have to be incorporated for the different stages of metabolomical analysis until the identification of the specific metabolite (Roessner and Beckles, 2009). Metabolomic analyses are focused on metabolite-targeted analysis, metabolite profiling and metabolic fingerprinting (Tan et al., 2009; Worley and Powers, 2013). Targeted analysis is used mainly for screening purposes and analysing compounds that are present at low concentrations, such as phytohormones (Shulaev et al., 2008). Metabolite profiling is an analytical

process that is restricted to identifying and quantifying a specific niche of pre-defined secondary metabolite groups in a biological sample (Roessner and Bowne, 2009). Metabolite profiling is used to determine which class of compounds e.g. lipids, isoprenoids or carbohydrates the metabolites belong to and is often used in drug research (Shulaev et al., 2008). Metabolic fingerprinting is aimed at classification of metabolic samples based on their origin or biological relevance, without identifying classes or compounds. Certain fingerprints have been used to differentiate individual signals that can be attributed to specific sample classification (Worley and Powers, 2013). The types of metabolites obtained from samples is heavily influenced by the type of solvent used for the extraction as shown in Table 2.1. It's therefore a critical decision in a study on which extraction solvent(s) will be used.

Table 2.1: Examples of solvents used for metabolite extractions and the metabolites that can be found in the extract. NB: Compounds in bold are usually extracted using only one solvent (Cowan, 1999).

Water	**Ethanol**	**Ether**	**Dichloromethanol**	**Methanol**	**Chloroform**	**Acetone**
Anthocyanins	Tannins	Alkaloids	Terpenoids	Anthocyanins	Terpenoids	Flavanols
Starches	**Polyphenols**	Terpenoids		Terpenoids	Flavonoids	
Tannins	Polyacetylenes	**Coumarins**		Saponins		
Saponins	Flavanol	**Fatty acids**		Tannins		
Terpenoids	Terpenoids			**Xanthoxyllines**		
Polypeptides	**Sterols**			**Totarol**		
Lectins	Alkaloids			**Quassinoids**		
	Propolis			**Lactones**		
				Flavones		
				Phenones		
				Polyphenols		

Metabolomics have been used substantially in analysing plant responses to abiotic and biotic stress (Hong et al., 2016). They have contributed largely in understanding the metabolites used by plants to overcome biotic stresses i.e. diseases and infections, as well as abiotic stresses such as adverse environmental effects e.g. extremely low temperatures (AbuQamar et al., 2016). This has contributed enormously to the field of biotechnology, specifically genetic modification of plant species to produce metabolites, originally from other plants, to combat stresses that transformed plants were previously susceptible to (Okazaki and Saito, 2012). It can also be used to assess the degree of success of the transformation of the genetically modified plant species (Worley and Powers, 2013).

In summary, metabolomics aims to study metabolomes, the pools of metabolites in a cell at any given point in time (Feussner and Polle, 2015). There are some challenges to this process, particularly for secondary metabolites. Firstly, in comparison to metabolites of primary metabolism, secondary metabolite concentrations vary greatly depending on the environmental conditions (Go, 2010) and through time. Secondly, many secondary metabolites are present at extremely low concentrations; for example, the average secondary metabolite concentration is usually much lower than the highly abundant primary compounds such as those involved in the physiological pathways, e.g. photosynthesis and respiration (Pott et al., 2019). Metabolomic analysis is also relatively new compared to other omics techniques, and reference information for metabolomic analysis is not as abundant as those for proteins or genes, i.e. referencing NMR data for known metabolites (Worley and Powers, 2013). Metabolite concentrations are highly dynamic in both space and time and have an immense range of chemical structures which leads to challenges in their analytical procedures and measurements (Roessner and Bowne, 2009; Gomez-Casati et al., 2013). Linked to this, the complexity of metabolomic data, especially when identifying and analysing biomarker metabolites (i.e. metabolites used as references in identifying and analysing new metabolites in an organism), can lead to misinterpretation of data due to the use of wrong biomarkers (Broadhurst and Kell, 2006). Some metabolites can also have uncontrolled fluctuations in concentrations under the same experimental conditions, termed uninduced biological variations (Van den Berg et al., 2006).

2.2 Metabolomics and Disease Diagnosis

Although metabolomic techniques are more recent compared to other omics techniques, they have been used in a wide range of applications as illustrated in Figure 2.2. Metabolomics offers the same advantages as transcriptomic and proteomic techniques i.e. the ability to analyse biofluids and involves relatively inexpensive, rapid and automated techniques once start-up costs have been settled (Gomez-Casati et al., 2013). Though its role in plant disease diagnosis has been primarily acting as a complementary technique

to conventional methods (genomics, transcriptomics, etc.), studies have shown its capability to distinctively diagnose plant disease independently of other techniques (Chen et al., 2019). The proficiency of metabolomic analysis has been portrayed through its role in human disease diagnosis through the utilization of metabolite biomarkers to diagnose various human diseases e.g. cancer, diabetes, coronary diseases, etc. as shown in Table 2.2 (Gomez-Casati et al., 2013).

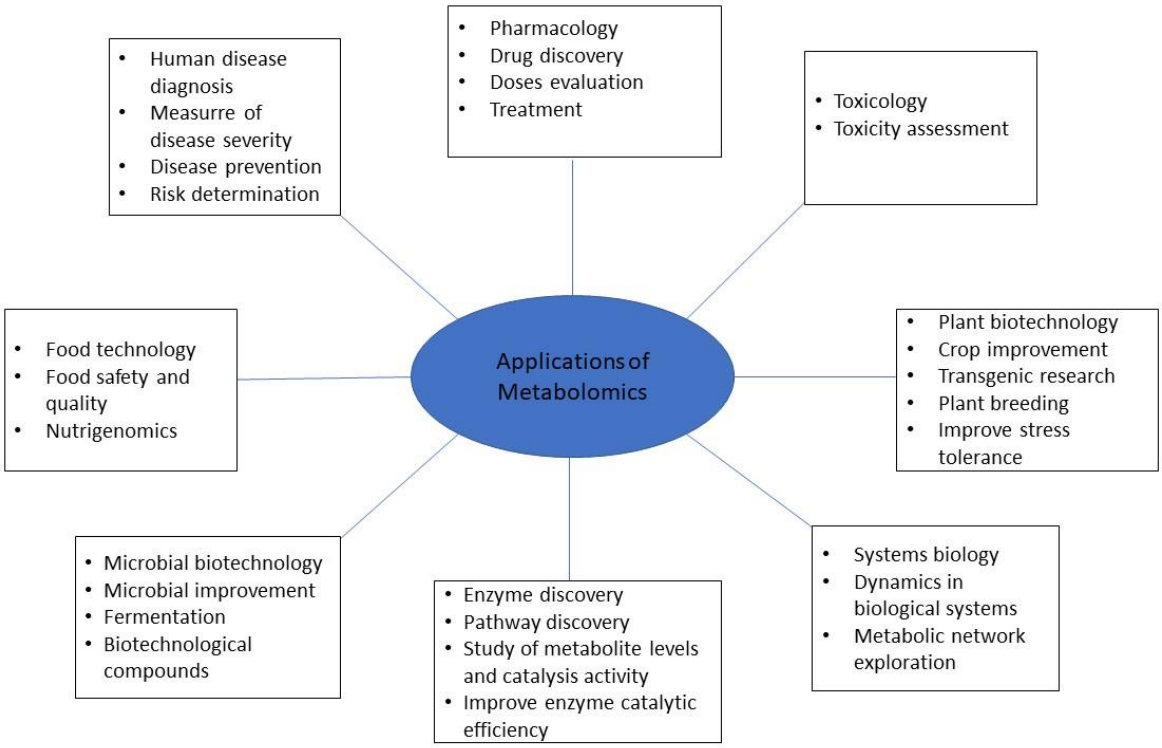

Figure 2.2: Examples of some metabolomics applications (Gomez-Casati et al., 2013).

Table 2.2: Examples of metabolites used as biomarkers of human diseases (Gomez-Casati et al., 2013).

Disease	Metabolite Biomarker
Male Infertility	Citrate, lactate, glycerylphosphorylcholine
Chronic obstructive pulmonary disease	Acetate, leucine, lactate, pyruvate
Huntington disease	3-Nitropropionic acid
Colorectal cancer	Acetycarnine, phenylalanine, tryptophan,
Kidney cancer	Quinolinate, 4-hydroxybenzoate and gentisate
Impaired glucose tolerance	Glycine, acetylcarnitine
Renal-cell carcinoma	Phospholipids, phenylalanine, tryptophan

Like other organisms, secondary metabolites have evolved in fungi over millions of years as chemical signals to defend their habitat as well as inhibit growth of competitors (Yim et al., 2007; Brakhage and Schroeckh, 2011). These secondary metabolites are also used by pathogenic fungi during host infection to induce various changes in the plant's metabolic pathways e.g. *Fusarium* species secrete secondary metabolites called fumonisins that kill plant tissue, which they utilize as a nutrient source infection (Lowe et al., 2010); (Chen et al., 2019). In fungi, many secondary metabolites are non-ribosomal peptides (NRPs) or polyketides. Examples of NRP derivatives are penicillin, cephalosporin and cyclosporines (Hoffmeister and Keller, 2007).

The biosynthetic genes for fungal secondary metabolites are generally located in clusters with a few exceptions e.g. *Aspergillus nidulans* has two separate gene clusters that are located on different chromosomes and are used for the synthesis of meroterpenoids austinol and dehydroaustinol (Lo et al., 2012). These clusters contain one or more central biosynthesis genes encoding large multidomain, multimodular enzymes that belong to the polyketide synthases (PKSs) or non-ribosomal peptide synthetases (Hertweck, 2009). Fungal metabolites mediate regulation of microbial metabolism in response to continuous environmental changes and these regulatory mechanisms are adaptation tools for the organism (Aretz and Meierhofer, 2016). However they must also be reversible as the environmental conditions can revert to the original state, thus metabolites show the fastest response times to changes in the environment (Baidoo, 2019).

Using proton NMR and GCMS it was discovered that *F. oxysporum* infection causes changes in metabolite concentrations by affecting the tricarboxylic cycle, gamma-amino butyric acid (GABA) bypass, the shikimate pathway and various other metabolites (Chen et al., 2011). *Ustilago maydis* is a fungal pathogen that causes tumors in maize. It was discovered that during tumor formation the flavonoid and shikimate pathways were activated leading to the upregulation of metabolites such as phenylpropionic acid, shikimic acid and tyrosine, as well as the levels of anthocyanins and hydroxycinnamic acid. It was also discovered that glutamate concentrations were sharply decreased (Doehlemann et al., 2008). *Rhizoctonia solani* is a causative agent of sheath blight in various plant species, e.g. *Oryza sativa* (rice), *Glycine max* (soybean) etc. (Hayden et al., 2019). Using metabolomic profiling analysis on infected soybean it was shown that the pathogen causes mobilisation of carbohydrates, disturbance of the amino acid pool, as well as the activation of isoflavonoid and phenylpropanoid biosynthetic pathways. These affected pathways have antioxidant effects and bioactivity, as such they assist the soybean to defend itself during *R. solani* infection (Aliferis et al., 2014: Verwaaijen et al., 2019).

Table 2.3 provides a summary of some instances where metabolomic techniques were employed in the study and diagnosis of various fungal diseases. Metabolomic analysis has also been discovered to have potential in studying plant root interaction with various microbes in the rhizosphere from growth promoting to pathogenic organisms. The roots produce various metabolites e.g. flavonoids and lipochitooligosaccharides during their interaction with bacteria (Mhlongo et al., 2018).

Table 2.3: Examples of the application of metabolomics in fungi-plant interaction analysis (Chen et al., 2019).

Fungal pathogen	Plant host	Metabolomic technique	Metabolomic Experiment (summary)	Research Findings (summary)	Citation
Fusarium graminearum	*Arabidopsis thaliana*	^{1}H NMR	The seeds of four lines of *Arabidopsis thaliana* were infected with *F. graminearum*. Metabolites were extracted from the ground plants' powder using aqueous methanol. Plant extract was analysed using ^{1}H NMR.	*F. graminearum* resistance was associated with an upregulation in various secondary metabolites e.g., alkaloids, phenylpropanoids, etc., and various organic osmolytes e.g., betaine, proline, etc., as well as enhanced TCA cycle and GABA shunt.	(Chen et al., 2011)
Fusarium oxysporum	*Cicer arietinum* (chickpea)	^{1}H NMR and UHPLC-ESI-MS/MS	Used non-targeted metabolomics analysis through high resolution LCMS and multivariate data analysis to identify metabolic modulations at various time points in roots of resistant and susceptible chickpea cultivars infected with *F. oxysporum* f. sp. *ciceri.*	Resistant cultivars had increased flavonoid, isoflavonoids and molonyl conjugates expression. Pathogen infection induced the expression of aurantion-obstine and querecitin.	(Kumar et al., 2015)

Fusarium tucumaniae	*Glycine max* (soybean)	GCMS	Leaves of two commercially significant soybean cultivars (one susceptible and one partially resistant) were infected with *F. tucumaniae*. Leaf samples were collected at different time intervals after inoculation. Powdery leaf material was dissolved in methanol and later derivatized using methoxyamine hydrochloride and analysed using GCMS. The aim was to determine cultivar response to pathogen infection.	It was discovered that pathogen infection led to increased amino acid production, a decrease in photosynthesis activity and increased plant specific peroxidase activity in the susceptible cultivars in the asymptomatic stages.	(Rosati et al., 2018)
Magnaporthe oryzae	*Oryza sativa* (rice)	GCMS, ^{1}H NMR, LCMS	Three susceptible plant species were infected with a single strain of the pathogen. The aim was to detect the impact of the pathogen on the plant's physiology during the asymptomatic stages. Metabolomic fingerprinting and targeted metabolite analysis was carried out using various MS techniques.	Results showed an unexpected upregulation of polyamines and malate during the asymptomatic stages. These metabolites were expected to be used in generating defensive oxygen species. Metabolomic profile showed the modulation of various conserved metabolites.	(Parker et al., 2009)

Cercospora beticola	*Beta vulgaris subsp. vulgaris var. altissima* (sugar beet)	(U)HPLC-UV-ESI-MS	Three sugar beet host genotypes with different susceptibility (resistant, tolerant, and susceptible) to the pathogen were selected to determine the plant's metabolites responses to fungal infection, in a non-invasive manner and during asymptomatic periods. The seeds of the hosts were treated and planted; the experiment took place 8 weeks into the plant growth stage. The samples were subjected to hyperspectral image analysis and MS metabolomic analysis.	Metabolomic data showed that pathogen infection stimulated the host to produce L-DOPA, 12-hydrojamonic acid, pantothenic acid and 5-*O*-feruloylquinic acid, to use as their defensive response.	(Arens et al., 2016)
Rhizoctonia solani	*Zeae maydis*	UHPLC-QTOF-MS	The aim was to study the pathogenesis of *R. solani* and its phytotoxin phenylacetic acid (PAA) on various maize leaf components. Maize plants were treated with the pathogen and the phytotoxin. A quality control sample was prepared for all the treatments. The	The metabolomic results showed that disease infection by the respective pathogen led to a change in the concentration of various metabolites e.g., phospholipids, flavonoids, alkaloids, etc. Both treatments caused an upregulation of	(Hu et al., 2018)

			metabolites were extracted using methanol and a combination of centrifugation, vortexing and sonication. The extract was analysed using UPLC and MS.	capsorubin expression and the inhibition of 3-hexaprenyl-4-hydroxy-5-methoxybenzoate expression. In the leaves treated with *R. solani* an increase in the levels of quercitrin, cis-homoaconitate and rutin was observed, as well as the inhibition of L-Glutamate. Many of the upregulated metabolites assist the plants in counteracting stresses and deterring pathogens.	
Botrytis cinerea	*Fragaria x ananassa* (Strawberry)	GCMS	The aim of the study was to determine the metabolome changes during the latent infection periods of *B. cinerea.* Plant leaves were inoculated with *B. cinerea* at a concentration of 10^5 spores/ml. The infected plants and the control plants were grown at the same time. The leaves were harvested at 2,5- and 7-days post inoculation.	Results showed that *B. cinerea* infection caused concentration alterations of 13 metabolites. Among them were the inositol a cell signal metabolite. Other metabolites included hexadecenoic acid and octadecanoic acid which are involved in jasmonic acid synthesis which is also involved in	(Hu et al., 2019)

			The plants were ground into powder and metabolites were extracted using methanol and water solution (4:1) by ultrasonication and centrifugation. The crude extract was analysed in GCMS.	plant defense against pathogens. There was an increase in metabolites such as malic acid, fructose, galactose, and pyruvic acid which are in involved in adjustment of plant morphology during the restraining of pathogens during infections.
Sclerotinia sclerotum	*Phaseolus vulgaris* (common bean)	UPLC-MS and GCMS	The aim of the study was to determine the metabolic responses of common bean to *S. sclerotum* infection. Leaves and stems of plants were inoculated in a cut-stem and detached leaf assays. The plant material was then lyophilized and ground to a fine powder. Metabolites were extracted using a methanol and water solution (80:20) by shaking on a vortex mixer. The extracts were analysed using UPLC-MS and GCMS.	Results showed a decrease in amino acids, except for asparagine. The metabolic change also included the increase in ureides and pyridines, terpenes, flavonoids including bean phytoalexins and some variable shifts in phytohormones.

Most diagnostic studies that have been carried out using metabolomical analysis aimed at understanding or detecting the impact of the plant pathogens on the physiology and metabolome of the plant host, and not detecting the pathogen itself. Mass spectrometry combined by various separation techniques e.g. GC, LC, etc. were commonly used in these studies as they provide easy identification and analysis of individual metabolites involved (Mhlongo et al., 2018).

2.3 *Zea mays L.* (Maize)

Zea mays L., commonly known as maize is considered one of the most important food sources in the world along with rice and wheat (Cai et al., 2020). It belongs to Panicoideae subfamily of the Poaceae (grass family) and its widely cultivated globally due to its adaptability to an array of environmental conditions as well as its rich nutritional value (Borrego and Kolomiets, 2016). Maize is also used for fuel, feed, fibres and scientifically as a model plant for the study of plant genetics due to its unprecedented structural, morphological and nucleotide diversity (Tenaillon et al., 2001; Gore et al., 2009).

Archaeological studies revealed that the earliest evidence of maize domestication was found in the Balsa region of Mexico dating back to 8 700 cal. years BP (calibrated years before the present) (Piperno et al., 2009; Ranere et al., 2009). Maize now has the broadest cultivated varieties farmed globally from latitude ranges of 50°N to 40°S and from altitudes ranging from 3400 m above ground in the Andean Mountains to the Caribbean Islands (Tenaillon and Charcosset, 2011). Maize also uses C4-carbon metabolism making it adaptable to high light intensities, high temperatures and low water availability which also promoted its increased global cultivation (Borrego and Kolomiets, 2016).

This global dissemination of maize resulted in various morphological differentiations from its ancestor, and these include changes in vegetative architecture e.g., decreased branching, kernel morphology and some characteristics (shape, size, hardness, dormancy, protein, and starch content, etc.) and ear morphology (size, shape, etc.) (Tenaillon and Charcosset, 2011). South Africa is considered one of the major producers of maize globally and it's one of the country's major exports. Maize is easily assimilated by different cultures in the country due to its taste and high source of nutrition as well as other reasons that include (Verheye, 2012):

- High yield per person or time of labour spent
- Its adaptation against biotic (birds) and abiotic (rain) stresses
- Easy storage and transportation over long distances

- Easy harvest and durability

According to the census of commercial agricultural report compiled by the South African Department of Statistics in 2017, maize production increased by 46.5% from 2007 (Figure 2.3) and this was mainly attributed to the increase in the production per hectare across various regions in the country as shown in Figure. 2.4.

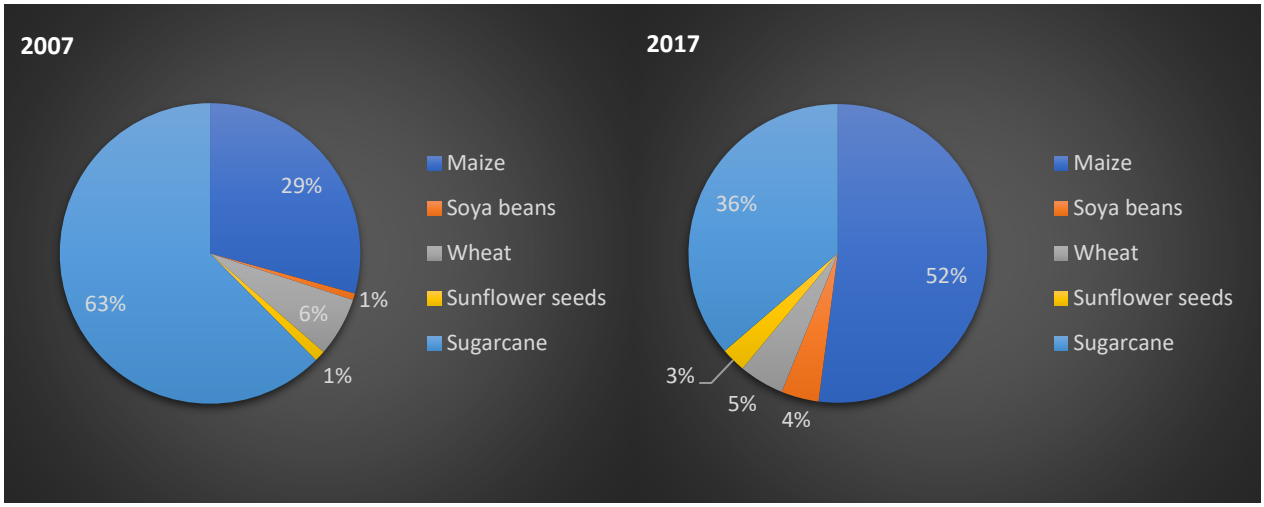

Figure 2.3: Pie charts illustrating the total production of major South African field crops from 2007 (left) to 2017 (right) (in metric-tons) (Statistics South Africa, 2020).

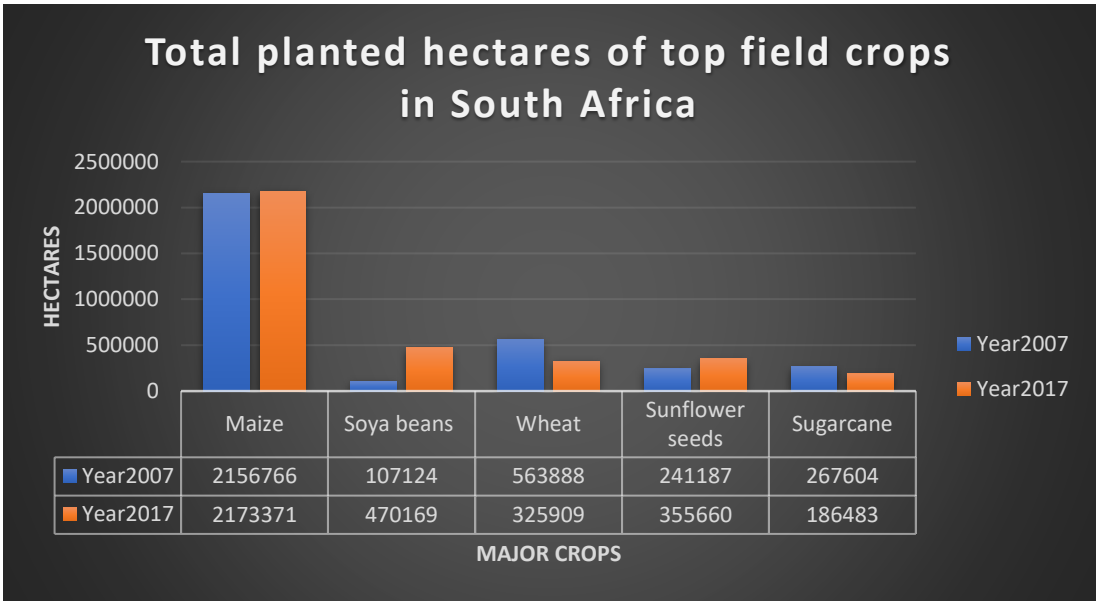

	Maize	Soya beans	Wheat	Sunflower seeds	Sugarcane
Year2007	2156766	107124	563888	241187	267604
Year2017	2173371	470169	325909	355660	186483

Figure 2.4: Illustrates the total amount of hectares used for the cultivation of the top field crops in South Africa (Statistics South Africa, 2020).

2.4 *Cercospora Zeina* (Grey Leaf Spot Pathogen)

C. zeina is the causal agent of grey leaf spot (GLS), one of the deadliest and most devastating maize diseases in the world (Meisel et al., 2009). Initially the disease was known to be caused by *Cercospora zeae-maydis* globally but studies conducted in the US revealed the existence of two genetically distinct yet morphologically similar *C. zeae-maydis* species which were classified as Type I and Type II (Dunkle and Levy, 2000). Dunkle and Levy (2000) came to this conclusion after analyzing the pathogens' internal transcribed spacer (ITS) and 5.8S ribosomal DNA (rDNA) regions. The distinction between the pathogens was further affirmed by Crous et al. (2006) by analysing DNA sequences of different *Cercospora* isolates. The analysed DNA sequences included ITS1 and ITS2 loci, 5.8S rRNA gene, elongation factor 1-α, histone 3, actin and calmodulin regions using a PCR test incorporating species-specific primers. Phylogenetic trees obtained using maximum parsimony illustrated the distinction between *C. zeina* (formerly *C. zeae-maydis* type II) and *C. zeae-maydis* (formerly *C. zeae-maydis* type I). Okori et al. (2003) confirmed the prevalence of *C. zeae-maydis* type II strains in eastern African countries and indicated that its genetic flow was dominant amongst *C. zeae-maydis* populations in Africa. A study done by Mathioni et al. (2006) on type I and type II isolates at different locations in Brazil indicated that the latter was more aggressive. Furthermore, the study also outlined that the degree of fitness of the two isolates differed and was environment specific. Type II was reclassified by Crous et al. (2006) as a distinct species called *C. zeina* and Meisel et al. (2009) affirmed that it was the causal agent of GLS in southern Africa.

C. zeina, is a poor food-base competitor in the soil, thus it is better suited to survive intercrop periods within infested maize crop residue. The primary source of pathogen inoculum are the Infected maize crop debris. Ideal conditions for rapid disease development are moderate/ high temperatures (20-30^{o}C) accompanied by periods of high humidity in early spring. This leads to extensive blighting and leaf tissue necrosis, causing lesion formation on the leaf (Figure. 2.5). Prolonged favorable conditions result in conidiophores contained in early infection lesions producing more spores that are dispersed either by wind or rain and the disease progresses to the upper parts of the plant (Ward et al., 1999; Lyimo et al., 2013). The pathogen has high sporulating potential thus lesion numbers can rapidly increase on developing leaves higher in the canopy. When environmental conditions are unfavorable the fungi may remain dormant and resume rapid development under favorable conditions (Korsman et al., 2012). Infection can also occur later in the season when spores are blown from adjacent fields (Meyer et al., 2017).

Figure 2.5: (A) Maize leaves infected with C. zeina. (B) Microscopic image of C. zeina conidium (42.5 µm). (C) In vitro culture of C. zeina on V8 media.

The symptoms of the disease are initially observed on the lower leaves of the plant. GLS disease lesions assume a rectangular shaped greyish cast, and this is attributed to the name of the disease (Kinyua et al., 2011). Immature lesions are not distinguishable in the earlier stages from the lesions of other foliar pathogens (Muller et al., 2016). GLS disease has a latent period of 14 to 28 days after infection before any visible lesions appear and the fungi begin to sporulate (Meisel et al., 2009: Dhami et al., 2015). GLS disease lesions first appear as small spots that are approximately 1-3 mm in length and rectangular to irregularly shaped. The spots are characterized by a chlorotic border that can be observed when diseased leaves are viewed via transmitted light. In mature GLS disease, the lesions can be easily distinguishable from those of other maize foliar pathogens. A unique feature of GLS disease lesions is that they run parallel to the leaf veins (Ward et al., 1999). In-breds and hybrids that are susceptible show necrotic lesions, while those that are moderately resistant show chlorotic or fleck type lesions (Meisel et al., 2009).

2.5 *Vigna unguiculata* (L.) Walp. (Cowpea)

Vigna unguiculata (L.) Walp. commonly known as cowpea, is an herbaceous crop that is widely cultivated as a grain and vegetable crop. It is a legume plant belonging to the Fabaceae family. It is widely grown in over 100 countries in Africa, Europe, North and South America and Asia, in areas with semi-arid and humid

climate between the latitudes of 35° N and 30°. Africa is considered the largest producer of cowpea attributing approximately 68% to global yield (Nandi et al., 2013; Mfeka et al., 2019), with Nigeria being the largest producer with approximately 2.14 million metric tonnes (Boukar et al., 2019).

Cowpea origins can be traced back to west and central Africa and its cultivation then spread to Latin America and south east Asia around 2 300 years BP (Owade et al., 2020). It was formerly named *Dolichos unguiculatus* L. and it was renamed to *Vigna unguiculata* (L.) Walp. in 1753 (Pasquet, 1998). The wild cowpea *Vigna unguiculata ssp. unguiculata* var. *spontanea* is considered to be the progenitor of the cultivated cowpea and its only found in Africa (Pasquet, 1998). Cowpea domestication evidence can be traced back to north-eastern Africa based on the results from amplified fragment length polymorphism (AFLP) analysis (Coulibaly et al., 2002).

Cowpea's morphology is characterized by dark green compound leaves with a central terminal symmetrical leaflet. The first pair of leaves are opposite, and the subsequent leaves are trifoliate and arranged in alternate patterns (Pottorff et al., 2012). They have thick hairy stems and branches, as well as well-developed tap root system with spreading lateral roots (Timko et al., 2007). Cowpeas develop flowers with a racemose inflorescence which are self-pollinating. The flowers have a variety of colours, which include white, pink, pale blue, dirty yellow or purple. It has rhomboid seeds of 6-12 mm and pedant pods which are 12-30 cm long (Pasquet, 1998). Each pod may contain between 8 to 20 seeds. The pods turn yellow or when they are mature (Boukar et al., 2019).

The global spread of cowpea was highly influenced by its ability to grow in semi-arid regions with low input requirements (Gonçalves et al., 2016). It is able to withstand poor soil fertility, water stress caused by irregular and low rainfall (300 mm or less annually) and tolerates wide ranges of soil pH (Timko et al., 2007). It is a good source of nutritious food with approximately 23 - 25% protein, 50 - 67% carbohydrates and several minerals and vitamins in the grains. The immature cowpea pods and leaves are consumed as fresh vegetables, and they contain 17 – 25% minerals and proteins (Moswatsi et al., 2013). In addition, cowpea has been reported to be a good source of folic acid, a particularly significant nutrient for pregnant women (Boukar et al., 2019).

Cowpea has been predominantly utilized as an intercrop along with cereal crops such as maize, sorghum (*Sorghum bicolor*) and millet (*Pennisetum glaucum*) due to its role in nitrogen fixation in the soil thus contributing to soil fertility and reducing the costs of purchasing commercial nitrogen fertilizers (Sanginga et al., 2003). It has a short growth period which means it can be harvested earlier than most plants; thus

shortening the hunger period (Timko et al., 2007). Furthermore, it's an important source of forage for livestock during dry seasons in some parts of west Africa (Adeyemi et al., 2012).

These traits led to its assimilation as a significant indigenous crop with potential to promote food security in sub-Saharan Africa, a region where many crops perform very poorly (Boukar et al., 2019). In 2020 the global estimates for cowpea production were approximately 8.9 million metric tonnes with Africa having the highest production as shown (Figure 2.6). In South Africa cowpea cultivation occurs particularly in the provinces of Limpopo, KwaZulu-Natal (KZN), North West and Mpumalanga, mainly by subsistence farmers (Mfeka et al., 2019). In 2020, South African cowpea production was estimated at 4,867 metric tonnes, a significant amount but a decline from the estimated 6,400 metric tonnes reported in 1994 (Figure 2.5). This is attributed to lack of funding and interest of researchers to carry out studies on the crop which led to improper production practices by the subsistence farmers and use of old seed varieties (Asiwe, 2009).

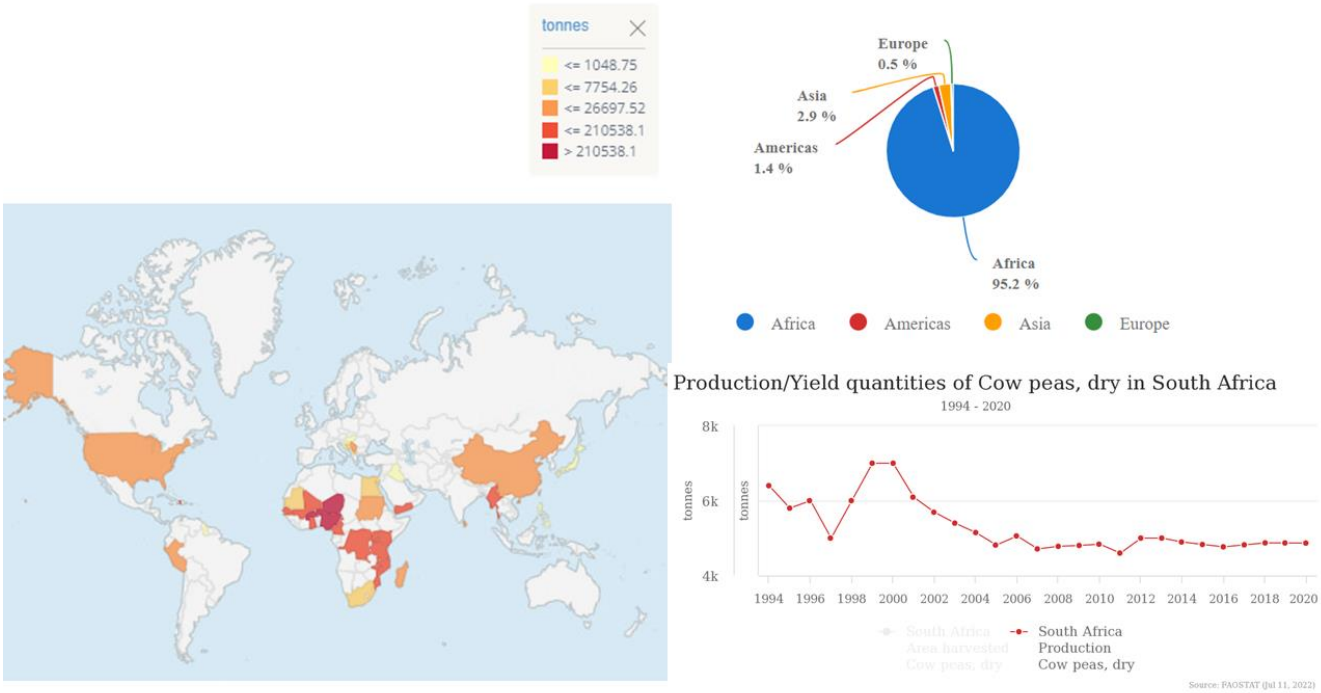

Figure 2.6: Global cowpea production in 2020 and the trend in cowpea production in South Africa from 1994 – 2020 (FAOSTAT, 2022).

2.6 *Fusarium Verticillioides*

Some of the most threatening fungal pathogens belong to the genus *Fusarium* and some species are known to produce mycotoxins e.g., fumonisins. Pathogens belonging to this genus are proficient soil inhabitants with saprophytic growth capabilities (Rheeder et al., 2002). *Fusarium verticillioides* is

considered as one of the most prevalent plant pathogens globally (Stockmann-Juvala and Savolainen, 2008). It was first isolated in 1970 from a batch of moldy maize suspected of causing an outbreak of equine leukoencepholomalacia in horses in South Africa (Marasas, 2001). Extensive studies on the fungus led to the initial isolation and identification of the mycotoxins named fumonisins from *F. verticillioides* MRC 826 cultures in 1988 (Gelderblom et al., 1988). Three years later it was discovered that their mode of action involved disrupting sphingolipid biosynthesis (Wang et al., 1991). *Fusarium verticillioides* is widely regarded as the main producer of fumonisins (Stockmann-Juvala and Savolainen, 2008). Other fumonisin--producing species include *F. proliferatum*, *F. dlamini*, and *Aternaria alternata* f. sp. *lycopersici* (Stockmann-Juvala and Savolainen, 2008).

Fusarium verticillioides is primarily a maize pathogen but studies have shown that it also infects other crops e.g. wheat (*Triticum*), and barley (*Hordeum vulgare*) (Zeng et al., 2020). The infection process of *F. verticillioides* was illustrated by Oren et al. (2003) using green fluorescent protein. Under optimal growth (warm and humid) conditions for the plant, the initial growth of the pathogens hyphae progressed sparsely along the root surface. Approximately 72 hours after planting in infested soil the pathogen penetrated the lateral roots and mesocotyl and proliferated in the intercellular matrix. Approximately, 14 days post infection, there were no visible symptoms, the pathogen could not be detected using a fluorescent microscope. However, it could still be recovered using *in vitro* plating methods. Coincidentally, certain undefined rounded organelles were observed around the mesocotyl and conidophores had developed on the endophytic hyphae. Consequently, 21 days after planting conidia had accumulated in the mesocotyl cells. However, the surrounding cells were unaffected, and the infection was still asymptomatic. Relatively 30 days after planting the fungal pathogen became active and caused necrosis in the mesocotyl and main root. Movement of the conidia through the vascular system allows the pathogen to spread to aerial parts of the plant. Under favourable conditions (low light) the pathogen proliferates aggressively in the roots, mesocotyl and stem (Oren et al., 2003).

2.6.1 Fumonisins

There are 28 fumonisin analogs that have been characterized since 1988 and can be divided into four main groups, namely fumonisin A, B, C, and P (Rheeder et al., 2002). The most abundant naturally occurring analogs amongst these groups are the fumonisin B or FB class (Figure 2.7 and Table 2.4), comprising of FB_1, FB_2 and FB_3, which are considered toxicologically significant, with FB_1 being more prevalent and usually found in higher levels in nature (Blacutt et al., 2018). The molecular structures of FB_2 and FB_3 are almost identical to that of FB_1 thus its reported that their level of toxicity may be similar (Stockmann-

Juvala and Savolainen, 2008). The toxicological significance of other fumonisins remains unknown and most publications focus on FB_1 (Månsson et al., 2010).

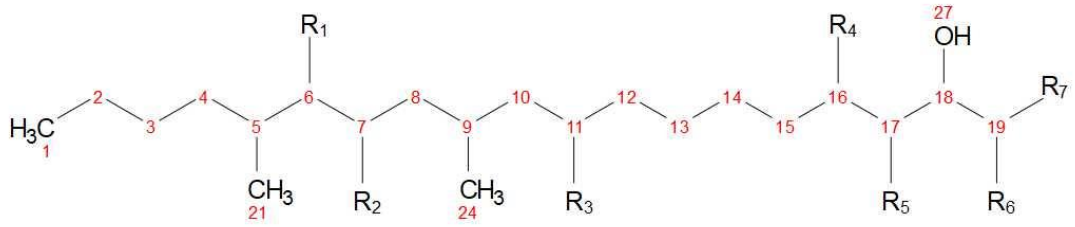

.

Figure 2.7: Basic structure of fumonisins with some of its side chains.

Table 2.4: List of known fumonisin B analogs (TCA – tricarboxylic acid) (Rheeder et al., 2002).

Analogs	**Side chains to fumonisin backbone**						
	R1	**R2**	**R3**	**R4**	**R5**	**R6**	**R7**
FB_1	TCA	TCA	OH	OH	H	NH_2	CH_3
Iso-FB_1	TCA	TCA	OH	H	OH	NH_2	CH_3
HFB_1	OH	TCA	OH	OH	H	NH_2	CH_3
FB_2	TCA	TCA	H	OH	H	NH_2	CH_3
FB_3	TCA	TCA	OH	H	H	NH_2	CH_3
FB_4	TCA	TCA	H	H	H	NH_2	CH_3

FB_1 is a structural analog of sphinganine and sphingosine (Figure 2.8), precursors in ceramide biosynthesis, a sphingolipid (Merrill et al., 2001; Zeng et al., 2020). Sphingolipids is a class of lipids found in all eukaryotic cells where they carry out an array of functions. These functions include acting as structural components for the plasma membrane and endomembrane systems, secondary messengers and bioactive molecules for plant cell signaling for development, stress response (biotic and abiotic) and programmed cell death (apoptosis) (Zeng et al., 2020). Furthermore, sphingolipids also play an essential role in pollen development (Michaelson et al., 2016). Sphingolipid signaling and metabolism in plants is still quite a mystery with many of the participants such as the receptors, mediators, and targets still unknown (Ali et al., 2018).

The main steps in the biosynthesis pathway involve the formation of sphinganine, which is acylated to dihydroceramide and ceramide by the enzyme ceramide synthase. The complex sphingolipids are subsequently hydrolysed to form ceramide and further to sphingosine (Stockmann-Juvala and Savolainen, 2008). FB_1 elicits its phytotoxicity by competitively inhibiting the enzyme ceramide synthase thus blocking the formation of complex sphingolipids (Figure 2.9). Inhibition of ceramide synthase leads to accumulation of sphinganine from the *de novo* ceramide biosynthesis; sphingosine recycled from ceramide; and sphinganine 1-phosphate and sphingosine 1-phosphate due to kinase phosphorylation of the two sphingoid bases. The result is the disruption of the sphingolipid dependent signaling and physiological functions (Riley et al., 1996).

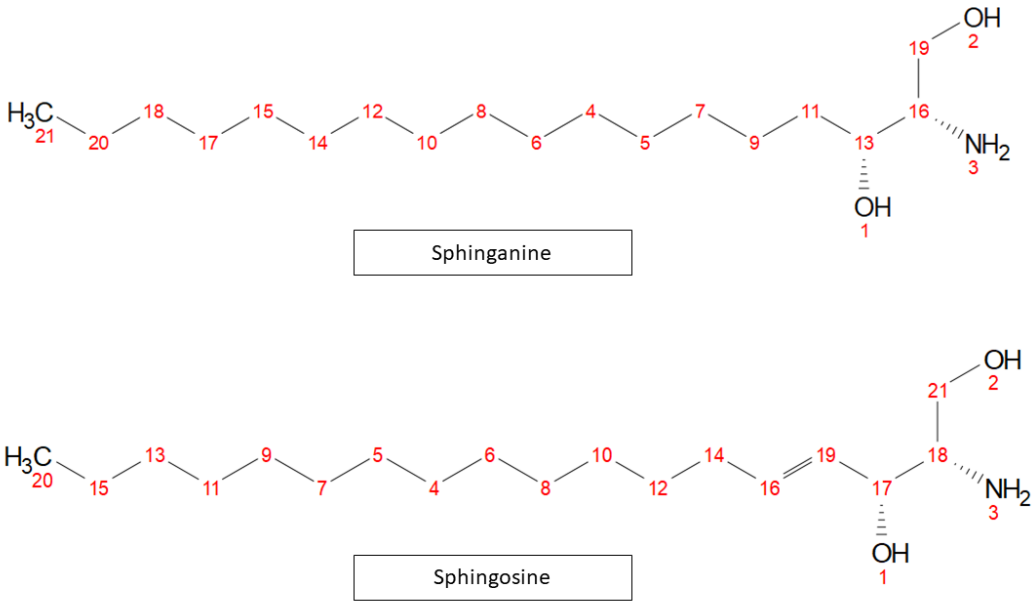

Figure 2.8: Chemical structures of sphinganine and sphingosine.

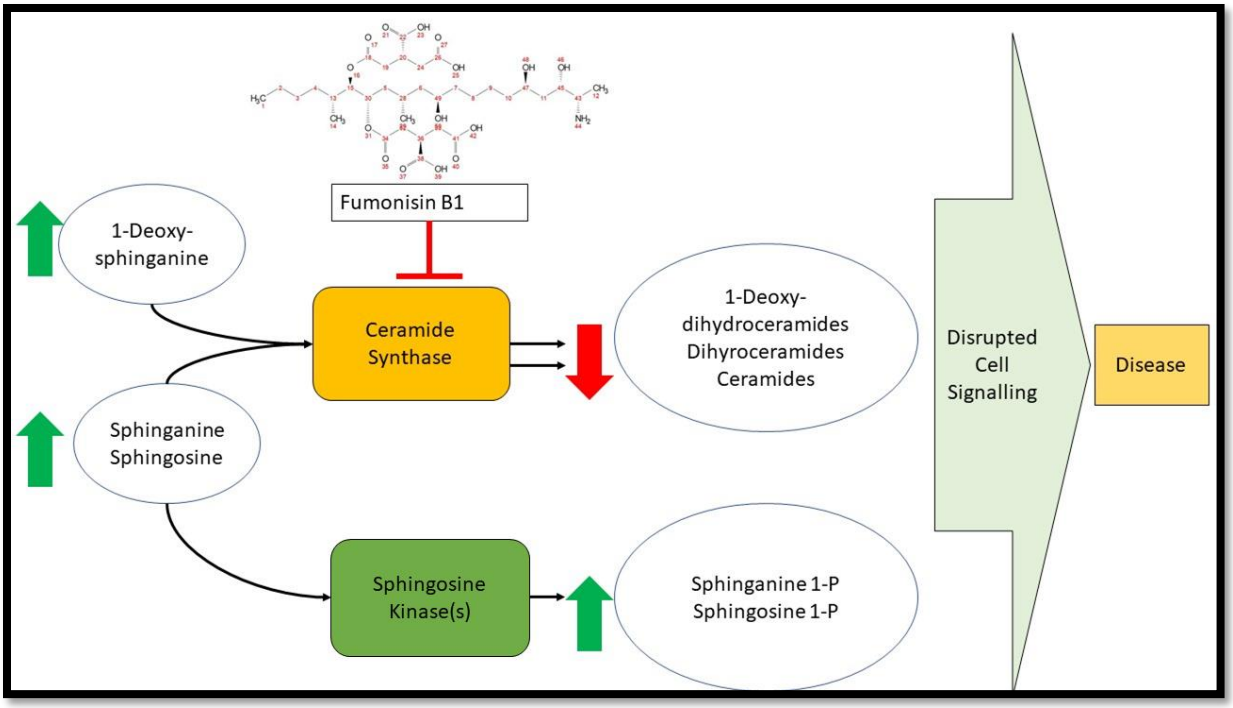

Figure 2.9: Illustration of the effects of ceramide synthase inhibition by fumonisin B_1 leading to disruption in various cell signaling mechanisms (Riley and Merrill, 2019).

Various diseases caused by *F. verticillioides* have been reported in plants, animals and even humans. Comparative studies carried out in parts of China and South Africa indicated a high incidence of esophageal cancer and neural tube defects in maize growing areas with significant high levels of *F. verticillioIdes* (Cornell et al., 1983; Chu and Li, 1994). Fumonisins were attributed to causing porcine pulmonary edema syndrome (PES) and cancer in rodents and swine (Haschek et al., 2001; Riley and Merrill, 2019). Another study done by Gelderblom et al. (2001) illustrated that male rats treated with purified FB_1 or *F. verticillioides* resulted in the formation of cholangiocarcinomas and hepatocellular carcinomas (Stockmann-Juvala and Savolainen, 2008).

Fumonisin B_1 is phytotoxic to a wide range of agriculturally important crops. Its phytotoxic effects in maize include necrosis, wilting, stunted growth, chlorosis and reduced root growth leading to the death of the plant (Williams et al., 2007). Kritzinger et al. (2006) discovered that cowpea seeds artificially treated with varying concentrations of FB_1 had reduced seed germination. Transmission electron microscopy (TEM) demonstrated that FB_1 led to the plasma membrane being separated from the cell wall, formation of irregular sized vacuoles and abundance of lipid bodies next to the cell wall (Kritzinger et al., 2003). In plants FB_1 triggers long chain bases accumulation which serve as secondary messengers and building blocks for sphingolipids (Zeng et al., 2020). This is what inherently leads to induced cell death (Saucedo-

García et al., 2011; Yanagawa et al., 2017). A study done by Coll et al. (2014) indicated autophagy constituted pro-survival mechanisms in plants with unrestricted cell death upon exposure to FB_1. Zeng et al., (2020) concluded that in addition to FB_1 causing cell death, it also damaged the structural components of the cell thus impairing plant development. Gutiérrez-Nájera et al. (2005) discovered that sphingoid intermediates and FB_1 inhibited H^+ ATPase in maize embryos, thus affecting the growth of the plant as ATP is a vital energy molecule.

2.7 References

AbuQamar, S.F., Moustafa, K., Tran, L.-S.P., 2016. 'Omics' and plant responses to *Botrytis cinerea*. Front. Plant Sci. 7, 1658. https://doi.org/10.3389/fpls.2016.01658

Adeyemi, S.A., Lewu, F.B., Adebola, P.O., Bradley, G., Okoh, A.I., 2012. Protein content variation in cowpea genotypes (*Vigna unguiculata* L. Walp.) grown in the Eastern Cape province of South Africa as affected by mineralised goat manure. African J. Agric. Res. 7, 4943–4947. https://doi.org/10.5897/AJAR11.1680

Ali, U., Li, H., Wang, X., Guo, L., 2018. Emerging roles of sphingolipid signaling in plant response to biotic and abiotic stresses. Mol. Plant 11, 1328–1343. https://doi.org/10.1016/J.MOLP.2018.10.001

Aliferis, K.A., Faubert, D., Jabaji, S., 2014. A metabolic profiling strategy for the dissection of plant defense against fungal pathogens. PLoS One 9. https://doi.org/10.1371/journal.pone.0111930

Arens, N., Backhaus, A., Döll, S., Fischer, S., Seiffert, U., Mock, H.P., 2016. Non-invasive presymptomatic detection of *Cercospora beticola* infection and identification of early metabolic responses in sugar beet. Front. Plant Sci. 7, 1–14. https://doi.org/10.3389/fpls.2016.01377

Aretz, I., Meierhofer, D., 2016. Advantages and pitfalls of mass spectrometry based metabolome profiling in systems biology. Int. J. Mol. Sci. https://doi.org/10.3390/ijms17050632

Asiwe, J.A.N., 2009. Needs assessment of cowpea production practices, constraints and utilization in South Africa. African J. Biotechnol. 8, 5383–5388. https://doi.org/10.4314/ajb.v8i20.65978

Baidoo, E.E.K., 2019. Microbial metabolomics: A general overview, in: Methods in Molecular Biology. Humana Press Inc., pp. 1–8. https://doi.org/10.1007/978-1-4939-8757-3_1

Blacutt, A.A., Gold, S.E., Voss, K.A., Gao, M., Glenn, A.E., 2018. *Fusarium verticillioides* : Advancements in understanding the toxicity , virulence , and niche adaptations of a model mycotoxigenic pathogen of maize 312–326.

Borrego, E.J., Kolomiets, M. V., 2016. Synthesis and functions of jasmonates in maize. Plants 5, 1–13. https://doi.org/10.3390/plants5040041

Boukar, O., Belko, N., Chamarthi, S., Togola, A., Batieno, J., Owusu, E., Haruna, M., Diallo, S., Umar, M.L., Olufajo, O., Fatokun, C., 2019. Cowpea (*Vigna unguiculata*): Genetics, genomics and breeding. Plant Breed. 138, 415–424. https://doi.org/10.1111/pbr.12589

Brakhage, A.A., Schroeckh, V., 2011. Fungal secondary metabolites - Strategies to activate silent gene clusters. Fungal Genet. Biol. https://doi.org/10.1016/j.fgb.2010.04.004

Broadhurst, D.I., Kell, D.B., 2006. Statistical strategies for avoiding false discoveries in metabolomics and related experiments. Metabolomics 2, 171–196. https://doi.org/10.1007/s11306-006-0037-z

Cai, F., Zhang, Y., Mi, N., Ming, H., Zhang, S., Zhang, H., Zhao, X., 2020. Maize (Zea mays L.) physiological responses to drought and rewatering, and the associations with water stress degree. Agric. Water Manag. 241. https://doi.org/10.1016/j.agwat.2020.106379

Chen, F., Ma, R., Chen, X., 2019. Advances of metabolomics in fungal pathogen – Plant Interactions.

Chen, F., Zhang, J., Song, X., Yang, J., Li, H., Tang, H., Liao, Y.C., 2011. Combined metabonomic and quantitative real-time PCR analyses reveal systems metabolic changes of Fusarium graminearum induced by Tri5 gene deletion. J. Proteome Res. 10, 2273–2285. https://doi.org/10.1021/pr101095t

Chu, F.S., Li, G.Y., 1994. Simultaneous occurrence of fumonisin B1 and other mycotoxins in moldy corn collected from the People's Republic of China in regions with high incidences of esophageal cancer. Appl. Environ. Microbiol. 60, 847–852. https://doi.org/10.1128/AEM.60.3.847-852.1994

Coll, N.S., Smidler, A., Puigvert, M., Popa, C., Valls, M., Dangl, J.L., 2014. The plant metacaspase AtMC1 in pathogen-triggered programmed cell death and aging: functional linkage with autophagy. Cell Death Differ. 21, 1399–1408. https://doi.org/10.1038/CDD.2014.50

Cornell, J., Nelson, M.M., Beighton, P., 1983. Neural tube defects in the Cape Town area, 1975-1980. South African Med. J. 64, 83–84.

Coulibaly, S., Pasquet, R.S., Papa, R., Gepts, P., 2002. AFLP analysis of the phenetic organization and genetic diversity of Vigna unguiculataL. Walp. reveals extensive gene flow between wild and domesticated types. Theor. Appl. Genet. 104, 358–366. https://doi.org/10.1007/S001220100740

Cowan, M.M., 1999. Plant products as antimicrobial agents. Clin. Microbiol. Rev. https://doi.org/10.1128/cmr.12.4.564

Crous, P.W., Groenewald, J.Z., Groenewald, M., Caldwell, P., Braun, U., Harrington, T.C., 2006. Species of Cercospora associated with grey leaf spot of maize. Stud. Mycol. 55, 189–197. https://doi.org/10.3114/sim.55.1.189

Dettmer, K., Aronov, P.A., Hammock, B.D., 2007. Mass spectrometry-based metabolomics. Mass Spectrom. Rev. https://doi.org/10.1002/mas.20108

Dhami, N.B., Kim, S., Paudel, A., Shrestha, J., Rijal, T.R., 2015. A review on threat of gray leaf spot disease of maize in Asia. J. Maize Res. Dev. 1, 71–85. https://doi.org/10.3126/jmrd.v1i1.14245

Doehlemann, G., Wahl, R., Horst, R.J., Voll, L.M., Poree, F., Stitt, M., Sonnewald, U., Kahmann, R., 2008. Reprogramming a maize plant : transcriptional and metabolic changes induced by the fungal biotroph Ustilago maydis 181–195. https://doi.org/10.1111/j.1365-313X.2008.03590.x

Dunkle, L.D., Levy, M., 2000. Genetic relatedness of African and United States populations of *Cercospora zeae-maydis*. Phytopathology 90, 486–490. https://doi.org/10.1094/PHYTO.2000.90.5.486

Feussner, I., Polle, A., 2015. What the transcriptome does not tell - proteomics and metabolomics are closer to the plants' patho-phenotype. Curr. Opin. Plant Biol. https://doi.org/10.1016/j.pbi.2015.05.023

Gelderblom, W.C., Jaskiewicz, K., Marasas, W.F., Thiel, P.G., Horak, R.M., Vleggaar, R., Kriek, N.P., 1988.

Fumonisins--novel mycotoxins with cancer-promoting activity produced by *Fusarium moniliforme.* Appl. Environ. Microbiol. 54.

Gelderblom, W.C.A., Abel, S., Smuts, C.M., Marnewick, J., Marasas, W.F.O., Lemmer, E.R., Ramljak, D., 2001. Fumonisin-induced hepatocarcinogenesis: mechanisms related to cancer initiation and promotion. Environ. Health Perspect. 109 Suppl 2, 291–300. https://doi.org/10.1289/EHP.01109S2291

Go, E.P., 2010. Database resources in metabolomics : An Overview 18–30. https://doi.org/10.1007/s11481-009-9157-3

Gomez-Casati, D.F., Zanor, M.I., Busi, M. V., 2013. Metabolomics in plants and humans: Applications in the prevention and diagnosis of diseases. Biomed Res. Int. 2013. https://doi.org/10.1155/2013/792527

Gonçalves, A., Goufo, P., Barros, A., Domínguez-Perles, R., Trindade, H., Rosa, E.A.S., Ferreira, L., Rodrigues, M., 2016. Cowpea (*Vigna unguiculata* L. Walp), a renewed multipurpose crop for a more sustainable agri-food system: Nutritional advantages and constraints. J. Sci. Food Agric. 96, 2941–2951. https://doi.org/10.1002/jsfa.7644

Gore, M.A., Chia, J.M., Elshire, R.J., Sun, Q., Ersoz, E.S., Hurwitz, B.L., Peiffer, J.A., McMullen, M.D., Grills, G.S., Ross-Ibarra, J., Ware, D.H., Buckler, E.S., 2009. A first-generation haplotype map of maize. Science 326, 1115–1117. https://doi.org/10.1126/SCIENCE.1177837

Gutiérrez-Nájera, N., Muñoz-Clares, R.A., Palacios-Bahena, S., Ramírez, J., Sánchez-Nieto, S., Plasencia, J., Gavilanes-Ruíz, M., 2005. Fumonisin B1, a sphingoid toxin, is a potent inhibitor of the plasma membrane H+-ATPase. Planta 221, 589–596. https://doi.org/10.1007/S00425-004-1469-1

Haschek, W.M., Gumprecht, L.A., Smith, G., Tumbleson, M.E., Constable, P.D., 2001. Fumonisin toxicosis in swine: an overview of porcine pulmonary edema and current perspectives. Environ. Health Perspect. 109, 251. https://doi.org/10.1289/EHP.01109S2251

Hayden, H.L., Rochfort, S.J., Ezernieks, V., Savin, K.W., Mele, P.M., 2019. Metabolomics approaches for the discrimination of disease suppressive soils for *Rhizoctonia solani* AG8 in cereal crops using ^{1}H NMR and LC-MS. Sci. Total Environ. 651, 1627–1638. https://doi.org/10.1016/j.scitotenv.2018.09.249

Hertweck, C., 2009. The biosynthetic logic of polyketide diversity. Angew. Chemie - Int. Ed. https://doi.org/10.1002/anie.200806121

Heyman, H.M., Meyer, J.J.M., 2012. NMR-based metabolomics as a quality control tool for herbal products. South African J. Bot. 82, 21–32. https://doi.org/10.1016/j.sajb.2012.04.001

Hoffmeister, D., Keller, N.P., 2007. Natural products of filamentous fungi: Enzymes, genes, and their regulation. Nat. Prod. Rep. https://doi.org/10.1039/b603084j

Hong, J., Yang, L., Zhang, D., Shi, J., 2016. Plant Metabolomics: An indispensable system biology tool for plant science. Int. J. Mol. Sci. 17, 767. https://doi.org/10.3390/ijms17060767

Hu, W., Pan, X., Li, F., Dong, W., 2018. UPLC-QTOF-MS metabolomics analysis revealed the contributions of metabolites to the pathogenesis of *Rhizoctonia solani* strain AG-1-IA. PLoS One 13. https://doi.org/10.1371/journal.pone.0192486

Hu, Z., Chang, X., Dai, T., Li, L., Liu, Panqing, Wang, G., Liu, Pengfei, Huang, Z., Liu, X., 2019. Metabolic profiling to identify the latent infection of strawberry by *Botrytis cinerea*. Evol. Bioinforma. 15. https://doi.org/10.1177/1176934319838518

Jorge, T.F., Rodrigues, J.A., Caldana, C., Schmidt, R., Dongen, J.T. van, Thomas-Oates, J., Antonio, C., 2015. Mass spectrometry-based plant metabolomics: Metabolite responses to abiotic stress. Wiley Online Libr. 19, 173–181. https://doi.org/10.1002/mas

Kinyua, Z., Smith, J., Kibata, G., Simons, S., Langat, B., 2011. Status of grey leaf spot disease in Kenyan maize production ecosystems. African Crop Sci. J. 18. https://doi.org/10.4314/acsj.v18i4.68647

Korsman, J., Meisel, B., Kloppers, F.J., Crampton, B.G., Berger, D.K., 2012. Quantitative phenotyping of grey leaf spot disease in maize using real-time PCR. Eur. J. Plant Pathol. 133, 461–471. https://doi.org/10.1007/s10658-011-9920-1

Kritzinger, Q., Aveling, T.A.S., Marasas, W.F.O., Rheeder, J.P., Van Der Westhuizen, L. V., Shephard, G.S., 2003. Mycoflora and fumonisin mycotoxins associated with cowpea [Vigna unguiculata (L.) Walp] seeds. J. Agric. Food Chem. 51, 2188–2192. https://doi.org/10.1021/jf026121v

Kritzinger, Q., Aveling, T.A.S., Van Der Merwe, C.F., 2006. Phytotoxic effects of fumonisin B1 on cowpea seed. Phytoparasitica 34, 178–186. https://doi.org/10.1007/BF02981318

Kumar, Y., Dholakia, B.B., Panigrahi, P., Kadoo, N.Y., Giri, A.P., Gupta, V.S., 2015. Metabolic profiling of chickpea-*Fusarium* interaction identifies differential modulation of disease resistance pathways. Phytochemistry 116, 120–129. https://doi.org/10.1016/j.phytochem.2015.04.001

Lo, H.C., Entwistle, R., Guo, C.J., Ahuja, M., Szewczyk, E., Hung, J.H., Chiang, Y.M., Oakley, B.R., Wang, C.C.C., 2012. Two separate gene clusters encode the biosynthetic pathway for the meroterpenoids austinol and dehydroaustinol in Aspergillus nidulans. J. Am. Chem. Soc. 134, 4709–4720. https://doi.org/10.1021/ja209809t

Lowe, R.G.T., Allwood, J.W., Galster, A.M., Urban, M., Daudi, A., Canning, G., Ward, J.L., Beale, M.H., Hammond-Kosack, K.E., 2010. A Combined 1H nuclear magnetic resonance and electrospray ionization-mass spectrometry analysis to understand the basal metabolismof plant-pathogenic Fusarium spp. Mol. Plant-Microbe Interact. 23, 1605–1618. https://doi.org/10.1094/MPMI-04-10-0092

Luo, J., 2015. Metabolite-based genome-wide association studies in plants. Curr. Opin. Plant Biol. https://doi.org/10.1016/j.pbi.2015.01.006

Lyimo, H.J.F., Pratt, R.C., Mnyuku, R.S.O.W., 2013. Infection process in resistant and susceptible maize (Zea mays L.) Genotypes to Cercospora zeae-maydis (Type II). Plant Prot. Sci. 49, 11–18. https://doi.org/10.17221/57/2011-pps

Månsson, M., Klejnstrup, M.L., Phipps, R.K., Nielsen, K.F., Frisvad, J.C., Gotfredsen, C.H., Larsen, T.O., 2010. Isolation and NMR characterization of fumonisin B2 and a new fumonisin B6 from *Aspergillus niger*. J. Agric. Food Chem. 58, 949–953. https://doi.org/10.1021/jf902834g

Manzoni, C., Kia, D.A., Vandrovcova, J., Hardy, J., Wood, N.W., Lewis, P.A., Ferrari, R., 2018. Genome, transcriptome and proteome: the rise of omics data and their integration in biomedical sciences. Brief. Bioinform. 19, 286. https://doi.org/10.1093/bib/bbw114

Marasas, W.F.O., 2001. Discovery and occurrence of the fumonisins: a historical perspective. Environ.

Health Perspect. 109, 239. https://doi.org/10.1289/EHP.01109S2239

Mathioni, S.M., Venceslau De Carvalho, R., Kátia, ;, Brunelli, R., Beló, A., Luis, ;, Camargo, E.A., 2006. Aggressiveness between genetic groups I and II of isolates of *Cercospora zeae-maydis*. Sci. Agric 547–551.

Meisel, B., Korsman, J., Kloppers, F.J., Berger, D.K., 2009. *Cercospora zeina* is the causal agent of grey leaf spot disease of maize in southern Africa. Eur. J. Plant Pathol. 124, 577–583. https://doi.org/10.1007/s10658-009-9443-1

Meyer, J., Berger, D.K., Christensen, S.A., Murray, S.L., 2017. RNA-Seq analysis of resistant and susceptible sub-tropical maize lines reveals a role for kauralexins in resistance to grey leaf spot disease, caused by Cercospora zeina. BMC Plant Biol. 17, 1–20. https://doi.org/10.1186/s12870-017-1137-9

Mfeka, N., Mulidzi, R.A., Lewu, F.B., 2019. Growth and yield parameters of three cowpea (*Vigna unguiculata* L. Walp) lines as affected by planting date and zinc application rate. S. Afr. J. Sci. 115, 1–8. https://doi.org/10.17159/sajs.2019/4474

Mhlongo, Im.I., Piater, L.A., Madala, N.E., Labuschagne, N., Dubery, I.A., 2018. The chemistry of plant – microbe interactions in the rhizosphere and the potential for metabolomics to reveal signaling related to defense priming and induced systemic resistance. Front. Plant Sci. 9, 1–17. https://doi.org/10.3389/fpls.2018.00112

Michaelson, L. V., Napier, J.A., Molino, D., Faure, J.D., 2016. Plant sphingolipids: Their importance in cellular organization and adaption. Biochim. Biophys. Acta - Mol. Cell Biol. Lipids 1861, 1329–1335. https://doi.org/10.1016/j.bbalip.2016.04.003

Moswatsi, M.S., Kutu, F.R., Mafeo, T.P., 2013. Response of cowpea to variable rates and methods of zinc application under different field conditions. African Crop Sci. Conf. Proc. 11, 757–762.

Muji, I., Šertovi, E., Joki, S., Sari, Z., Alibabi, V., Vidovi, S., Živkovi, J., Paul, A., Bennet, R.N., Wallsgrove, R.M., Yang, L., Ning, Z.S., Shi, C.Z., Chang, Z.Y., Huan, L.Y., Londrina, U.E. De, Londrina, U.E. De, Warta, D. De, Wink, M., Hartmann, T., Singh, G., Vinod, A.K.V., Tiwari, R., Rana, C.S., 2015. Plant secondary metabolites : a review. J. Agric. Food Chem. 3, 3–19. https://doi.org/10.5511/plantbiotechnology.14.1002a

Muller, M.F., Barnes, I., Kunene, N.T., Crampton, B.G., Bluhm, B.H., Phillips, S.M., Olivier, N.A., Berger, D.K., 2016. Cercospora zeina from maize in South Africa exhibits high genetic diversity and lack of regional population differentiation. Phytopathology 106, 1194–1205. https://doi.org/10.1094/PHYTO-02-16-0084-FI

Nandi, S., Dutta, S., Mondal, A., Nath, A.A.R., Chattopadhaya, A., Chaudhuri, S., 2013. Biochemical responses during the pathogenesis of *Sclerotium rolfsii* on cowpea. African J. Biotechnol. 12, 3968–3977. https://doi.org/10.5897/AJB2013.12405

Okazaki, Y., Saito, K., 2012. Recent advances of metabolomics in plant biotechnology. Plant Biotechnol. Rep. 6, 1–15. https://doi.org/10.1007/s11816-011-0191-2

Okori, P., Fahleson, J., Rubaihayo, P.R., Adipala, E., Dixelius, C., 2003. Assessment of genetic variation among East African *Cercospora zeae-maydis* populations. African Crop Sci. J. 11. https://doi.org/10.4314/acsj.v11i2.27520

Oren, L., Ezrati, S., Cohen, D., Sharon, A., 2003. Early events in the *Fusarium verticillioides*-maize interaction characterized by using a green fluorescent protein-expressing transgenic isolate. Appl. Environ. Microbiol. 69, 1695–1701. https://doi.org/10.1128/AEM.69.3.1695-1701.2003

Owade, J.O., Abong', G., Okoth, M., Mwang'ombe, A.W., 2020. A review of the contribution of cowpea leaves to food and nutrition security in East Africa. Food Sci. Nutr. 8, 36–47. https://doi.org/10.1002/fsn3.1337

Parker, D., Beckmann, M., Zubair, H., Enot, D.P., Caracuel-Rios, Z., Overy, D.P., Snowdon, S., Talbot, N.J., Draper, J., 2009. Metabolomic analysis reveals a common pattern of metabolic re-programming during invasion of three host plant species by *Magnaporthe grisea*. Plant J. 59, 723–737. https://doi.org/10.1111/j.1365-313X.2009.03912.x

Pasquet, R.S., 1998. Morphological study of cultivated cowpea Vigna unguiculata (L.) Walp. Importance of ovule number and definition of cv gr Melanophthalmus. Agronomie 18, 61–70. https://doi.org/10.1051/AGRO:19980104

Piperno, D.R., Ranere, A.J., Holst, I., Iriarte, J., Dickau, R., 2009. Starch grain and phytolith evidence for early ninth millennium B.P. maize from the Central Balsas River Valley, Mexico. Proc. Natl. Acad. Sci. 106, 5019–5024. https://doi.org/10.1073/PNAS.0812525106

Pott, D.M., Osorio, S., Vallarino, J.G., 2019. From central to specialized metabolism: An overview of some secondary compounds derived from the primary metabolism for their role in conferring nutritional and organoleptic characteristics to fruit. Front. Plant Sci. https://doi.org/10.3389/fpls.2019.00835

Pottorff, M., Ehlers, J.D., Fatokun, C., Roberts, P.A., Close, T.J., 2012. Leaf morphology in Cowpea [*Vigna unguiculata* (L.) Walp]: QTL analysis, physical mapping and identifying a candidate gene using synteny with model legume species. BMC Genomics 13, 1–12. https://doi.org/10.1186/1471-2164-13-234/FIGURES/4

Ramakrishna, A., Ravishankar, G.A., 2011. Influence of abiotic stress signals on secondary metabolites in plants. Plant Signal. Behav. 6, 1720–1731. https://doi.org/10.4161/psb.6.11.17613

Ranere, A.J., Piperno, D.R., Holst, I., Dickau, R., Iriarte, J., 2009. The cultural and chronological context of early Holocene maize and squash domestication in the Central Balsas River Valley, Mexico. Proc. Natl. Acad. Sci. 106, 5014–5018. https://doi.org/10.1073/PNAS.0812590106

Rheeder, J.P., Marasas, W.F.O., Vismer, H.F., 2002. Production of fumonisin analogs by *Fusarium* species. Appl. Environ. Microbiol. 68, 2101. https://doi.org/10.1128/AEM.68.5.2101-2105.2002

Riley, R.T., Merrill, A.H., 2019. Ceramide synthase inhibition by fumonisins : a perfect storm of perturbed sphingolipid metabolism , signaling , and disease 60, 1183–1189. https://doi.org/10.1194/jlr.S093815

Roessner, U., Beckles, D.M., 2009. Metabolite measurements, in plant metabolic networks. Springer New York, New York, NY, pp. 39–69. https://doi.org/10.1007/978-0-387-78745-9_3

Roessner, U., Bowne, J., 2009. What is metabolomics all about? Biotechniques 46, 363–365. https://doi.org/10.2144/000113133

Rosati, R.G., Lario, L.D., Hourcade, M.E., Cervigni, G.D.L., Luque, A.G., Scandiani, M.M., Spampinato, C.P., 2018. Primary metabolism changes triggered in soybean leaves by *Fusarium tucumaniae* infection. Plant Sci. 274, 91–100. https://doi.org/10.1016/j.plantsci.2018.05.013

Sanginga, N., Dashiell, K.E., Diels, J., Vanlauwe, B., Lyasse, O., Carsky, R.J., Tarawali, S., Asafo-Adjei, B., Menkir, A., Schulz, S., Singh, B.B., Chikoye, D., Keatinge, D., Ortiz, R., 2003. Sustainable resource management coupled to resilient germplasm to provide new intensive cereal-grain-legume-livestock systems in the dry savanna. Agric. Ecosyst. Environ. 100, 305–314. https://doi.org/10.1016/S0167-8809(03)00188-9

Saucedo-García, M., González-Solís, A., Rodríguez-Mejía, P., Olivera-Flores, T. de J., Vázquez-Santana, S., Cahoon, E.B., Gavilanes-Ruiz, M., 2011. Reactive oxygen species as transducers of sphinganine-mediated cell death pathway. Plant Signal. Behav. 6, 1616. https://doi.org/10.4161/PSB.6.10.16981

Shulaev, V., Cortes, D., Miller, G., Mittler, R., 2008. Metabolomics for plant stress response. Physiol. Plant. 132, 199–208. https://doi.org/10.1111/j.1399-3054.2007.01025.x

Smedsgaard, J., Nielsen, J., 2005. Metabolite profiling of fungi and yeast: From phenotype to metabolome by MS and informatics. J. Exp. Bot. 56, 273–286. https://doi.org/10.1093/jxb/eri068

Smolinska, A., Blanchet, L., Buydens, L.M.C., Wijmenga, S.S., 2012. NMR and pattern recognition methods in metabolomics: From data acquisition to biomarker discovery: A review. Anal. Chim. Acta 750, 82–97. https://doi.org/10.1016/J.ACA.2012.05.049

Stockmann-Juvala, H., Savolainen, K., 2008. A review of the toxic effects and mechanisms of action of fumonisin B 1. Hum. Exp. Toxicol. 27, 799–809. https://doi.org/10.1177/0960327108099525

Tan, K.C., Ipcho, S.V.S., Trengove, R.D., Oliver, R.P., Solomon, P.S., 2009. Assessing the impact of transcriptomics, proteomics and metabolomics on fungal phytopathology. Mol. Plant Pathol. 10, 703–715. https://doi.org/10.1111/j.1364-3703.2009.00565.x

Tenaillon, M.I., Charcosset, A., 2011. A European perspective on maize history. C. R. Biol. 334, 221–228. https://doi.org/10.1016/J.CRVI.2010.12.015

Tenaillon, M.I., Sawkins, M.C., Long, A.D., Gaut, R.L., Doebley, J.F., Gaut, B.S., 2001. Patterns of DNA sequence polymorphism along chromosome 1 of maize (*Zea mays* ssp. mays L.). PNAS, 9161–9166. https://doi.org/10.1073/PNAS.151244298

Timko, M.P., Ehlers, J.D., Roberts, P.A., 2007. Cowpea. Genome Mapp. Mol. Breed. Plants 3, 50–67.

Van den Berg, R.A., Hoefsloot, H.C., Westerhuis, J.A., Smilde, A.K., Van der Werf, M.J., 2006. Centering, scaling, and transformations: improving the biological information content of metabolomics data. BMC Genomics 7, 1–15. https://doi.org/10.1186/1471-2164-7-142

Verheye, W., 2012. Growth and production of maize: Tradational low-input cultivation. J. soils, plant growth Crop Prod. II, http://www.eolss.net/Eolss-sampleAllchapter.aspx.

Verwaaijen, B., Wibberg, D., Winkler, A., Zrenner, R., Bednarz, H., Niehaus, K., Grosch, R., Pühler, A., Schlüter, A., 2019. A comprehensive analysis of the *Lactuca sativa*, L. transcriptome during different stages of the compatible interaction with Rhizoctonia solani. Sci. Rep. 9. https://doi.org/10.1038/s41598-019-43706-5

Wang, E., Norred, W.P., Bacon, C.W., Rileygll, R.T., Merrill, A.H., 1991. Inhibition of sphingolipid biosynthesis by fumonisins. Implications for diseases associated with *Fusarium moniliforme*. J. Biol. Chem. 266, 14486–14490. https://doi.org/10.1016/S0021-9258(18)98712-0

Ward, J.M.J., Stromberg, E.L., Nowell, D.C., Nutter Jr, F.W., 1999. Gray leaf spot; A disease of global importance in maize production 83.

Williams, L.D., Glenn, A.E., Zimeri, A.M., Bacon, C.W., Smith, M.A., Riley, R.T., 2007. Fumonisin disruption of ceramide biosynthesis in maize roots and the effects on plant development and *Fusarium verticillioides*-induced seedling disease. J. Agric. Food Chem. 55, 2937–2946. https://doi.org/10.1021/jf0635614

Wink, M., Botschen, F., Gosmann, C., Schäfer, H., Waterman, P.G., 2018. Chemotaxonomy seen from a phylogenetic perspective and evolution of secondary metabolism, Annual Plant Reviews Online. John Wiley & Sons, Ltd, Chichester, UK, pp. 364–433. https://doi.org/10.1002/9781119312994.apr0429

Worley, B., Powers, R., 2013. Multivariate analysis in metabolomics. Curr. Metabolomics 92–107.

Yanagawa, D., Ishikawa, T., Imai, H., 2017. Synthesis and degradation of long-chain base phosphates affect fumonisin B 1-induced cell death in *Arabidopsis thaliana*. J. Plant Res. 130, 571–585. https://doi.org/10.1007/S10265-017-0923-7

Yim, G., Wang, H.H., Davies, J., 2007. Antibiotics as signalling molecules. Philos. Trans. R. Soc. B Biol. Sci. https://doi.org/10.1098/rstb.2007.2044

Zeng, H.Y., Li, C.Y., Yao, N., 2020. Fumonisin B1: A tool for exploring the multiple functions of sphingolipids in plants. Front. Plant Sci. 11, 1649. https://doi.org/10.3389/FPLS.2020.600458/BIBTEX

3. The Use of Metabolomical Analyses As A Potential Tool To Diagnose Grey Leaf Spot In Maize Caused By *Cercospora Zeina*

3.1 Introduction

Cercospora zeina has been known to be the deadliest and most devastating maize pathogen in the world which causes grey leaf spot disease (Meisel et al., 2009). Since maize is one of the most important crops globally (Cai et al., 2020), *C. zeina* poses a great threat to global food security. Due to its extended latency period in the host plant, early detection of the pathogen has proven quite challenging and thus most measures available are to control its damage rather than prevent it (Dhami et al., 2015). Metabolites are the earliest means that maize use to defend against the invasion of pathogens, as such they provide extensive information on the underlying conditions that the plant might be experiencing, i.e, *C. zeina* infection. Suggesting that the monitoring and analyses of these defensive metabolites may provide leeway into the early detection of *C. zeina* as well as its control. Metabolomical analyses provides extensive techniques that can be used for the study of these defensive metabolites to possibly identify a biomarker unique to *C. zeina* infection in maize which will be used in future grey leaf spot diagnostic measures.

Maize (*Zea mays*) fungal infection triggers the formation and accumulation of low molecular weight metabolites (>900 daltons) or phytoalexins for resistance (Pechanova and Pechan, 2015). Phytoalexins represent different classes of specialized metabolites (Jeandet et al., 2014). In maize sesquiterpenoid and diterpenoid phytoalexins have been extensively reported e.g. zealexins, kauralexins and dolabralexins (Huffaker et al., 2011; Ding et al., 2020). Phytoalexin activity in plants can be non-volatile or volatile. It was widely believed that non-volatile chemical defenses in maize were mainly mediated by benzoxazinoids (Huffaker et al., 2011b). However, Schmelz et al. (2011) indicated that a group of kauralexins, non-volatile diterpenoid phytoalexins, had a significant role in maize pathogen defense.

Figure 3.1 illustrates some of the most widely reported defense metabolites found in maize in response to various biotic stresses. Benzoxazinoids involved in maize pathogen defense include DIMBOA (2,4-dihydroxy-7-methoxy-2H-1,4-benzoxazin-3(4H)-one) and HDMBOA-Glc (2-hydroxy-4,7-dimethoxy-1,4-benzoxazinoid

glucoside). DIMBOA is used by maize seedlings in response to fungal pathogens e.g. northern corn leaf blight caused by *Setosphaeria turcica*, and herbivores (McMullen et al., 2009). HDMBOA-Glc is used by plants in response to pathogen infection and herbivory (Oikawa et al., 2001).

Maize also utilize terpenoids that mediate inter-organism interaction leading to the formation of chemical barriers, e.g. terpene olefins serve as precursors to produce non-volatile antibiotic defenses (Schmelz et al., 2014). Kauralexins were observed when *Rhizopus microsporus* inoculated maize induced the production of kauralexin A3 (*ent*-kaur-19-al-17-oic acid) and kauralexin B3 (*ent*-kaur-15-en-19-al-17-oic acid). These metabolites accumulate at the plant-pathogen interface displaying antimicrobial activity against various maize fungal pathogens e.g., *R. microsporus* and *Colletotrichum graminicola* which causes anthranose stalk rot (Schmelz et al., 2011). Ahuja et al. (2012) reported that the accumulation of non-volatile terpenoid end products e.g., dolabradiene limit the impact of fungal pathogens, oxidative stresses and herbivores. Doehlemann et al. (2008) observed that *Ustilago maydis* infection induced the expression of terpene synthases TPS6 and TPS11 and this preceded the accumulation of zealexins. A GCMS analysis done in a study by Meyer et al. (2017) showed that *C. zeina* infection stimulated an accumulation of both kauralexins and zealexins with the latter being more abundant.

Flavonoids also constitute a significant part of phytoalexins (De Souza et al., 2020; Ube et al., 2021). The role of flavonoids in plant pathogen resistance has been observed in various cereal plants e.g., 3-deoxyanthocyadinins in sorghum (*Sorghum bicolor*). A sub-group of O-methylated flavonoids has been reported to have a role in plant disease resistance. Kodama et al. (1992) and Park et al. (2014) discovered that 7-methoxyapigenin and 7-methoxynaringenin had antifungal and antibacterial activity *in vitro*. Examples of various metabolites that have been reported to be involved in maize pathogen resistance are shown in Figure 3.1.

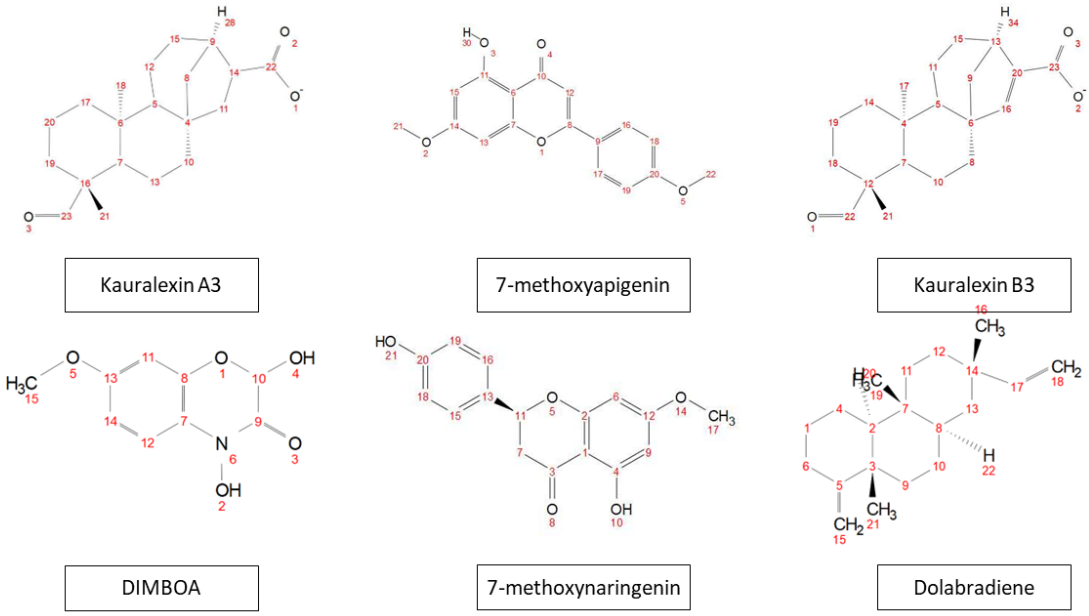

Figure 3.1: Examples of maize secondary metabolites used in pathogen and disease resistance.

3.2 Aim

The aim of this chapter was to investigate the efficacy of metabolomical analyses in successfully diagnosing maize infected with GLS caused by *C. zeina*, by identifying disease related metabolite biomarkers in the maize leaf metabolome. For this investigation, two main strategies were implored which were metabolomic fingerprinting using NMR and GCMS analyses and biomarker target analyses using GCMS. The objective was to observe any metabolomic changes that may occur in the maize metabolome due to the infection and to identify potential biomarker metabolites that may be associated with *C. zeina* infection. Grey leaf spot is a significant maize disease with considerable impact on the food security and economy of South Africa. Metabolomical analyses can be used as an additional tool for early diagnosis prompting execution of quick control measures give ref or refer to previous section.

3.3 Materials and Methods

3.3.1 Maize Field Trial

Maize leaves from six plants (cultivar Hybrid 1), infected by *C. zeina*, were sampled from a 25-ha farm in the Umgungundlovu district, near Howick, KZN. The farm was used by Syngenta South Africa (Pty) Ltd to test the efficacy of different fungicide treatments on GLS. The 12 ha of the farm were demarcated diagonally into three areas where each treatment was applied. The plants were planted on the fifth of November 2020. Approximately five weeks after planting (wap) all regions were sprayed with the

fungicide treatment 1 containing 62.3 g/ha Difenconazole and 100 g/ha Azoxystrobin. Fungicide treatment 2 was applied approximately nine wap. It involved spraying of the demarcated areas on the farm peripheral with fungicide 3 and the middle area was sprayed with Syngenta's new fungicide (fungicide N). At 14 wap, the maize in all regions were sprayed with fungicide treatment 3 containing 60 g/Ha cyperconazole and 188 g/Ha propiconazole. Robertson and Mueller (2007) reported that fungicides are present in the plant for only 14 to 21 days after application and therefore should not be detected chemically since the samples were collected 15 wap and later.

Maize leaf samples showing chlorotic spots (early GLS symptoms) and mature lesions were randomly collected across the farm. Maize leaf samples showing chlorotic spots were collected 15 wap and maize leaves with mature lesions were collected 18 wap. All leaf samples were collected at V14 growth stage and for each set of symptomatic samples, asymptomatic controls (fungicide N sprayed) were collected at the same field. A grading system shown in Figure 3.2 was created to measure the degree of infection based on lesion length and leaf area covered. Leaf samples with chlorotic spots were classified as having a degree of infection of 1 - 2 and those with mature lesions were classified as a grade of 3 - 5. Samples showing no GLS symptoms (control) were graded 0. The maize samples were packaged in an ice box for transportation to the University of Pretoria. The midribs of the leaves were removed, and the samples stored at -80 ^{o}C.

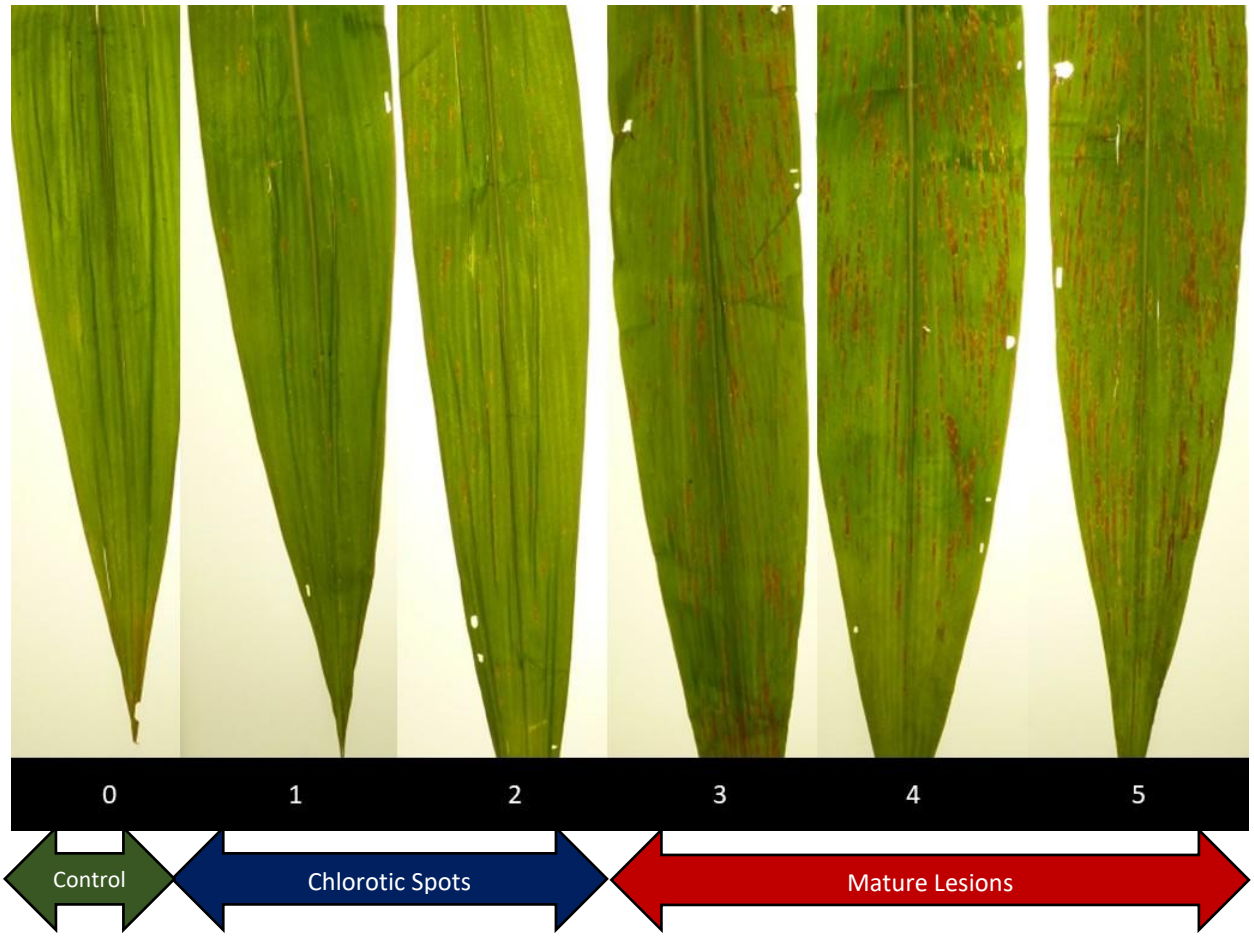

Figure 3.2: Visual scale used to assert degree of infection of collected maize leaf samples based on observed lesions length and area covered on the leaf.

3.3.2 Glasshouse Trial

A glasshouse trial was carried out to compare the field trial results with those of maize grown under controlled environmental conditions with no fungicide treatment. The glasshouse trial was carried out according to the protocol set by Meisel et al. (2009) with a few modifications. Maize seeds (cultivar Hybrid 1) were planted in a glasshouse at the University of Pretoria experimental farm with a 16 hr day length and average temperature of 28±4 °C. *Cercospora zeina* strain CMW 25467 (Meisel et al., 2009) single conidial cultures were collected from 15 % glycerol stocks stored at -80 °C. The glycerol stocks with the pure cultures were transferred onto V8 media plates for proliferation and subsequent multiplication through conidia sub-culturing. The plates were incubated in an incubator kept in the dark at 25 °C for a period of 4-7 days before further subcultured at the conidia phase to bulk up the pathogen culture. The pathogen inoculum was prepared by pouring 0.02 % Tween detergent solution onto V8 media plates and rubbing the conidia using a laboratory glass hockey stick to dissolve it in the detergent. The conidia-

detergent solution was transferred to a Falcon tube for inoculation. The subsequent inoculum was diluted to a concentration of 1.43 x 10^5 spores/ml, using a hemocytometer.

When the maize reached the V9 growth stage (5 wap) they were inoculated with the *C. zeina* spore suspension. Three leaves were selected per plant (V7, V8, V9 growth stages) to be inoculated. The inoculum was applied onto a 15 cm demarcated leaf region on the adaxial and abaxial sides of the leaf using a small paint brush as described by Meisel et al. (2009). The control plants were treated in a similar manner, with the application of detergent only. The plants were left to grow in the glasshouse and observed for symptoms (lesions). Approximately 7 weeks post-inoculation (or 12 wap) mature lesions were observed on the inoculated leaves as shown in Figure 3.4. All leaf samples, both inoculated and control were collected, the midribs removed and stored in a -80 ^oC freezer.

3.3.3 Metabolite Extraction

The frozen maize leaf samples were placed in a Virtis freeze-drier (SP Scientific, USA) to remove the water. The samples were weighed and extracted with distilled methanol using a Büchi E-916 Speed-extractor (Büchi E-916, Switzerland) which can control the extraction pressure and temperature. Plant material (Table 3.1) were placed in 10 ml stainless steel tubes with the pressure set at 100 bar and temperature at 50 ^oC. Each extraction consisted of four cycles, with each one having a 1 min heating phase, 9 min solvent holding phase and a discharge phase of 5 min. A nitrogen gas purge was performed for 8 min at the end and the total extraction time was 1 hr and 32 min. The extracts were vacuum-dried using a Büchi Genevac (EZ-2 plus, England) at 40 ^oC, using the methanol protocol and the dry masses of the crude extracts were recorded.

3.3.4 ^{1}H Nuclear Magnetic Resonance (NMR) Analysis

Maize crude extracts were analysed using proton NMR (^{1}H NMR) with an Oxford 200 MHz NMR instrument (Varian Incorporated, USA). This was done to determine if there were changes in the maize metabolomic fingerprint due to *C. zeina* infection. A leaf extract of 25 mg/ml was prepared and dissolved using 80 % deuterated methanol and 20 % potassium phosphate buffer. Maleic acid (2 mg/ml) was used as an internal standard. From this solution, 700 µl were transferred to a clean NMR glass tube which was placed in the NMR machine. The NMR parameters were set as follows; 512 scans were carried out on the sample consisting of 11 976 data points, an acquisition time of 2 seconds per scan and manual magnetic shimming

was done for each individual sample (Triba et al., 2015). The obtained sample spectra were processed, analysed and compared using MestreNova (Mnova) version 14 (Mestrelab Research, Spain). The spectra were binned (0.04 ppm/bin) and exported to SIMCA-P version 14.1 (Sartorius Stedim Data Analytics AB, Sweden) for multivariate statistical analysis. Principal component analysis plots (PCA) and orthogonal projection to latent structures discriminant analysis (OPLS-DA) plots were generated. PCA plots provide unsupervised data comparison of all samples while OPLS-DA plots generate a supervised or sample group comparison. This was done to establish if a correlation between *C. zeina* infection and a metabolomic change could be observed. Furthermore, multivariate analysis in SIMCA would provide statistical values R2 and Q2 to validate the observed results. R2 indicates how well the analytical model suits the data and Q2 indicates the predictability potential of the data; R2 values of above 0.5 are acceptable and Q2 $\geq$ 0.5 shows that the data has good predictability (Triba et al., 2015).

3.3.5 Gas Chromatography Mass Spectrometry (GCMS) Analysis

Maize leaves crude extracts were analysed using a Shimadzu GCMS-QP2010 SE instrument (Shimadzu Corporation, Japan). This analysis was done to determine if volatile metabolites could be identified in maize that were synthesized after *C. zeina* infection or if metabolite concentration changes can be observed. Such compounds could possibly be used as biomarkers for GLS diagnosis and understanding GLS effects on maize leaves metabolome.

An extract solution of 1 mg/ml was prepared from the crude extract using distilled methanol of which 1 ml was transferred to GCMS glass vials after filtration through 0.45 µm syringe-fitted filters (Merck and Co. Inc., USA). The samples were loaded on to the column using an AOC-20i+s auto-sampler. Compounds were separated in a Rtx- 5MS capillary column with dimensions of 29.3 m x 0.26 µm. Splitless injections of 1 µl were preformed using an AOC-20i+s autosampler and the temperature for both the injector and detector were set at 270 ^{o}C. The oven was programmed at an initial temperature of 50 ^{o}C which was held for 2 min, thereafter the temperature was increased to 300 ^{o}C at a rate of 10 ^{o}C per min and held for 5 min, making the total run time 32 min. The acquisition for mass spectra was set to a mass range of 50.0 to 600.0 m/z. Compound ionizations were carried out using an Electron Ionization Source at -70 eV.

The chromatograms were processed and analysed using the Shimadzu post-run analysis software and Mnova. The chromatograms were binned (0.01 ppm/bin) in Mnova and exported to SIMCA-P version 14.1 for multivariate statistical analysis. Principal component analysis plots (PCA) and orthogonal projection to latent structures discriminant analysis (OPLS-DA) plots were generated. Furthermore, the chromatogram numerical data for the specific identified potential biomarkers was exported to Microsoft Excel (Microsoft

Corporation, USA) and a single factor ANOVA test was carried out on the biomarkers to assess whether the observed change due to grey leaf spot was significant.

3.4 Results

3.4.1 Maize Leaf Samples

Figure 3.3 illustrates the maize samples obtained from the field trial in Howick, KZN. The first images (1A and 1B) are the maize leaf samples with chlorotic spots and their accompanying asymptomatic control samples respectively. Images 2A and 2B show the maize leaf samples with mature lesions and their accompanying asymptomatic control samples respectively. Figure 3.4 illustrates the examples of leaf samples collected from the glasshouse trial at the University of Pretoria experimental farm. The first image (A) illustrates the inoculated leaf samples with mature lesions and (B) shows the uninoculated leaf samples with no observable symptoms. From Table 4.1 it is evident that based on the grading system (Figure 3.2), the maize leaf samples from the field trial had higher mature lesions grades than the inoculated glass house leaf samples.

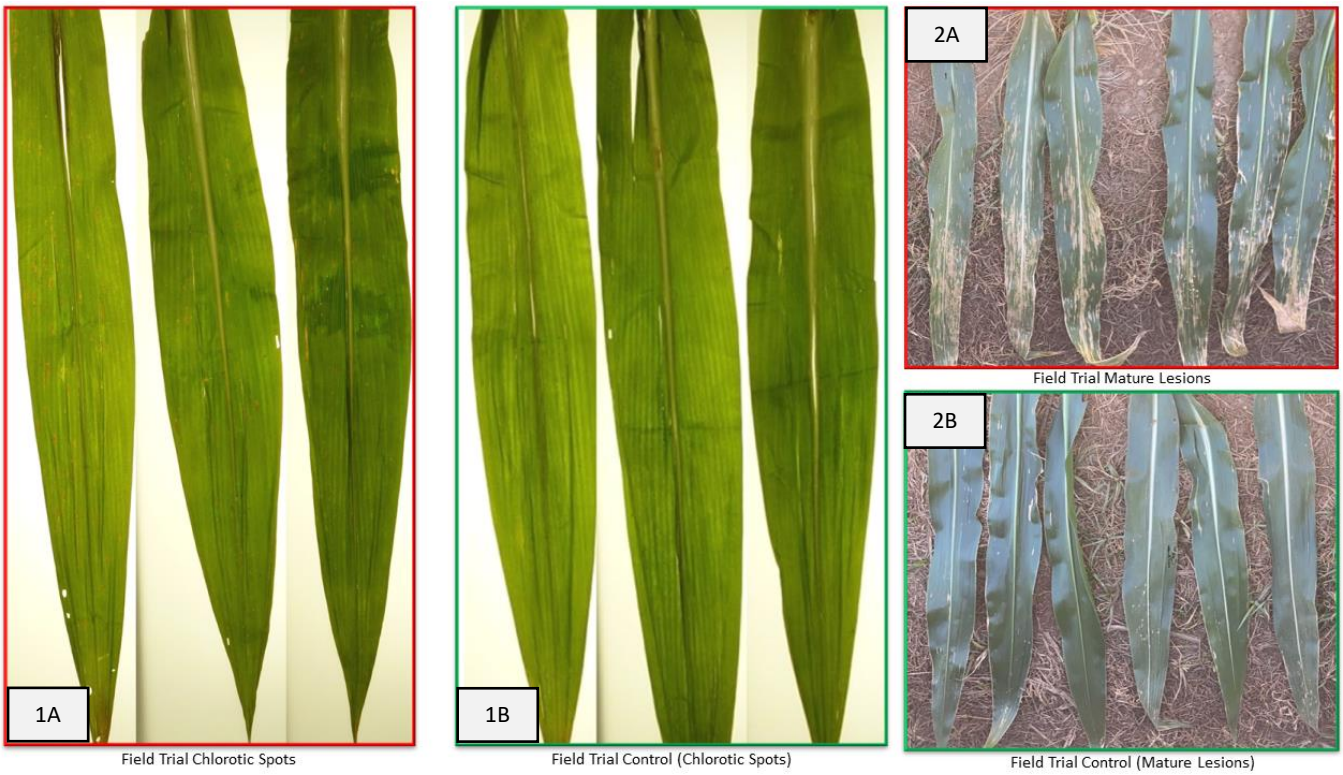

Figure 3.3: Examples of maize leaf samples collected from the field trial in Howick KZN. 1A shows the examples of the maize leaves with chlorotic spots and 1B are the asymptomatic control maize leaves collected along with the chlorotic spots' samples. 2A shows maize leaf samples with mature lesions and 2B shows the asymptomatic controls collected along with the mature lesions' samples.

A B

Figure 3.4: Example of the maize leaves sampled from the glasshouse trial at the University of Pretoria. Image A shows maize leaves with mature lesions and image B shows asymptomatic control maize leaves collected along with the mature lesions' samples from the glasshouse.

Table 3.1: Dry mass of maize leaf samples (in replicates) and the obtained metabolite extract mass. (NB: some samples were spoilt during the storage process hence metabolites could not be extracted from them, and this is indicated by an extract mass of 0). The grading system is meant to illustrate the prevalence of the GLS symptoms.

Sample code	Leaf dry mass (mg)	Extract mass (mg)	Infection grade (see on Figure 3.2)
Chlorotic spots 1	2299.3	607.6	2
Chlorotic spots 2	2353.3	475.0	1
Chlorotic spots 3	1610.3	417.9	1
Chlorotic spots 4	1717.9	422.1	2
Chlorotic spots 5	2225.0	549.8	2
Chlorotic spots 6	1566.0	390.2	1
Average Mass	1961.9	477.1	
Control 1	2321.8	565.9	0
Control 2	1579.3	443.8	0
Control 3	2451.9	616.5	0
Control 4	2716.8	733.5	0
Control 5	2299.6	323.9	0
Control 6	1948.8	570.1	0

Average Mass	2219.7	542.3	
Mature Lesions 1	3265.1	603.7	4
Mature Lesions 2	2387.8	411.9	5
Mature Lesions 3	2320.4	0	5
Mature Lesions 4	2584.7	376.4	3
Mature Lesions 5	2507.0	356.4	4
Mature Lesions 6	2804.1	559.3	3
Average Mass	2644.85	384.6	
Control 1	2207.3	0	0
Control 2	2153.8	425.1	0
Control 3	2798.5	611.9	0
Control 4	2214.8	411.0	0
Control 5	2545.7	656.3	0
Control 6	3184.0	852.8	0
Average Mass	2517.4	492.9	
Inoculated 1	851.6	236.4	3
Inoculated 2	438.4	124.5	3
Inoculated 3	635.5	198.9	3
Inoculated 4	966.8	268.5	3
Inoculated 5	1249.2	317.5	3
Inoculated 6	975.9	321.8	3
Average Mass	852.9	244.6	
Control 1	1264.3	356.7	0
Control 2	1049.5	292.2	0
Control 3	1033.6	265.7	0
Control 4	1443.4	358.7	0
Control 5	1447.3	375.1	0
Control 6	913.6	236.0	0
Average Mass	1191.9	314.1	

3.4.2 ^{1}H Nuclear Magnetic Resonance (NMR) Results

3.4.2.1 Field trial

The leaf extracts were subjected to ^{1}H NMR analysis to determine if the plants' polar (methanol extraction) metabolomic fingerprint changed because of grey leaf spot infection. The samples' NMR spectra were compared in Mnova by stacking them. The NMR spectra of the chlorotic spots' samples did not show any clear differences (Figure 3.5) when compared to their control samples. This suggests that early infection of *C. zeina* does not have a notable influence on the NMR determined metabolomic fingerprint of maize leaves. The PCA plot in Figure 3.7 (A) also showed no clear separation between the infected and control samples. The multivariate statistical values, R2 (0.72) and Q2 (0.43), suggests that the analytical model is good however it cannot be used to predict unknown samples under the same premise as there is no clear difference in the metabolomic fingerprints of the infected and control plants. The supervised OPLS-DA plot (Figure 3.7 B) which considers allocated sample groups, showed slight separations between the infected and control plans. However, the statistical value of Q2 was negative suggesting that the metabolomic differences between the two groups were not definitive enough to be used to predict unknown samples under the same parameters. Furthermore, this reflects that early *C. zeina* infection had little influence in altering the metabolomic fingerprint of the maize leaves.

The NMR spectra of leaf samples with mature lesions showed several differences in their metabolomic fingerprint when compared to their control samples, clearly indicated in Figure 3.6. The chemical shifts of 3.90 – 5.05 ppm are regions where compounds containing functional groups such as hydroxyls, esters, alkyl halides and alkenes are detected. Signals in the region of 0.7 ppm indicates compounds containing long saturated carbon chains (Gable, 2019), including the terpenoids. The unsupervised PCA plot (Figure 3.8 A) showed no definitive separation between the infected and control samples. Furthermore, the Q2 value (0.27) suggests that the samples' data is not reliable in predicting unknown samples under the same premise. However, the OPLS-DA plot in Figure 3.8 (B) showed clear separation between the infected and control samples. This means that the average metabolomic fingerprint of the infected samples differed from the control samples. Furthermore, a Q2 > 0.5 suggested that the data can be used to predict unknown samples under the same premises. The R2 value indicates how well the analytical model suits the data and Q2 indicates the predictability potential of the data; R2 values bigger than 0.5 are acceptable and Q2 $\geq$ 0.5 shows that data has good predictability (Triba et al., 2015).)

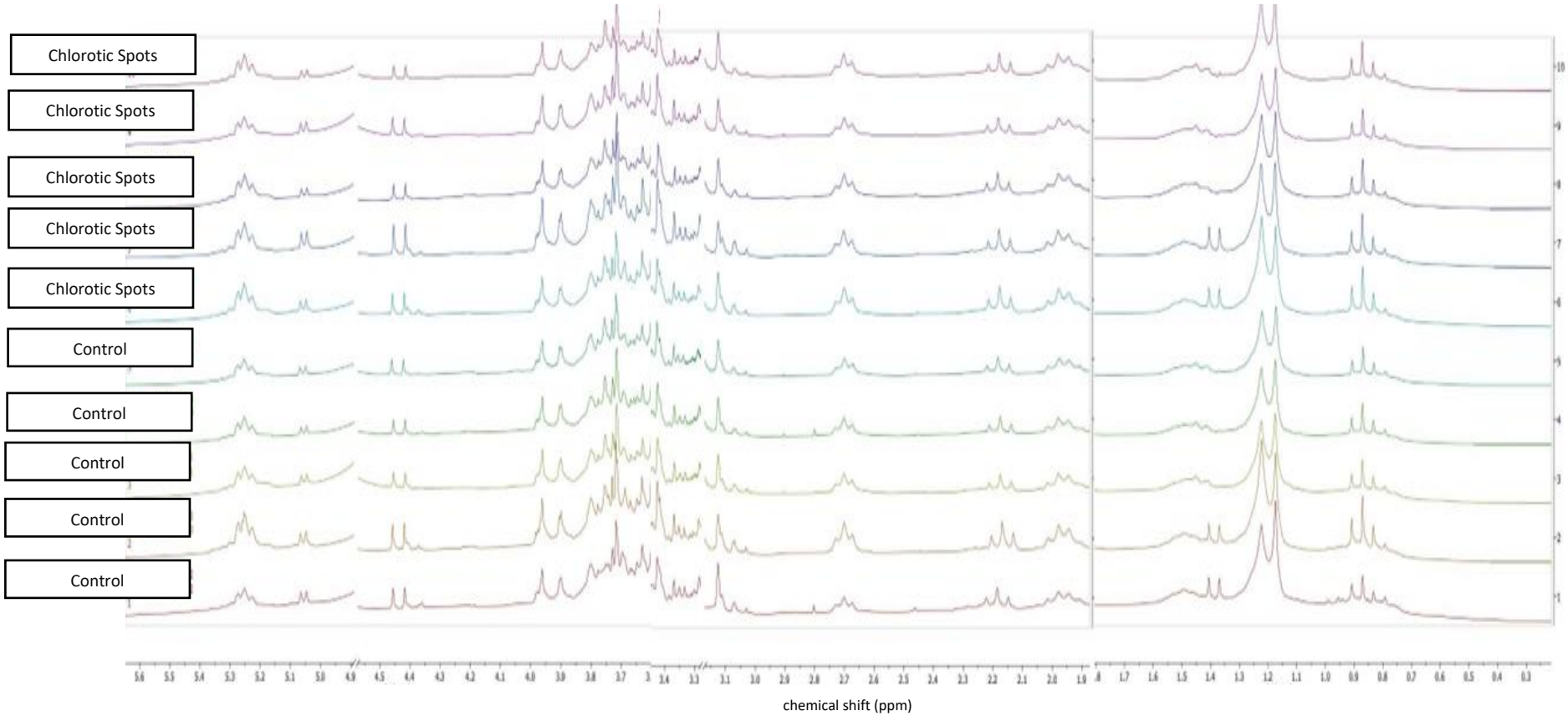

Figure 3.5: Stacked 1H NMR of field trial maize leaves with chlorotic spots and accompanying control samples. No definitive spectra differences were observed between the two sets of samples. The solvent (methanol), water and internal standard (maleic acid) peaks were removed from the NMR spectra by physically cutting out the peaks from the spectra (Chemical shifts 3.4 ppm, 5.1 ppm and 6.2 ppm respectively).

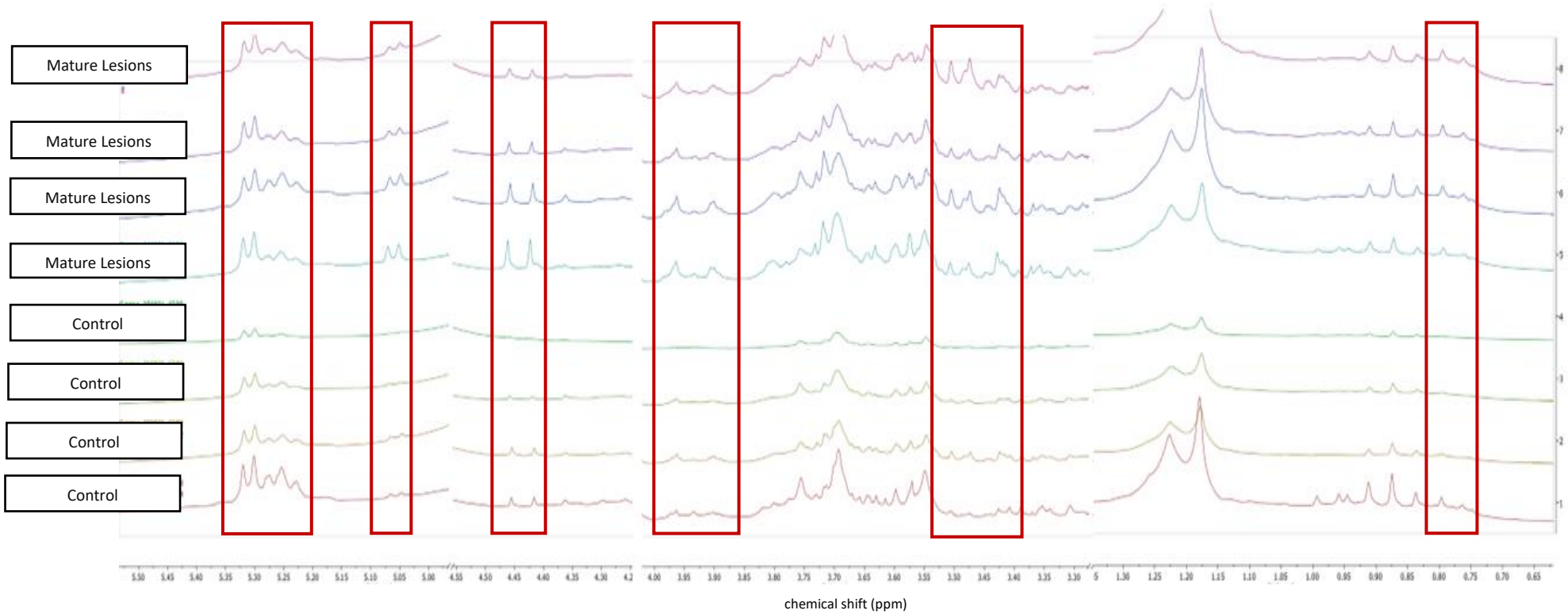

Figure 3.6: Stacked 1H NMR spectra of field trial leaves with mature lesions and their accompanying controls. Most spectral difference between the maize leaves with mature lesions and the control were peak concentration differences. The concentration differences were observed in the following spectral regions (indicated by red boxes from left to right); 5.20-5.35ppm, 5.05-5.10 ppm, 4.40-4.45 ppm, 3.85-4.00 ppm, 3.85-3.95 ppm, 3.40-3.45 ppm and 0.75-0.85 ppm.

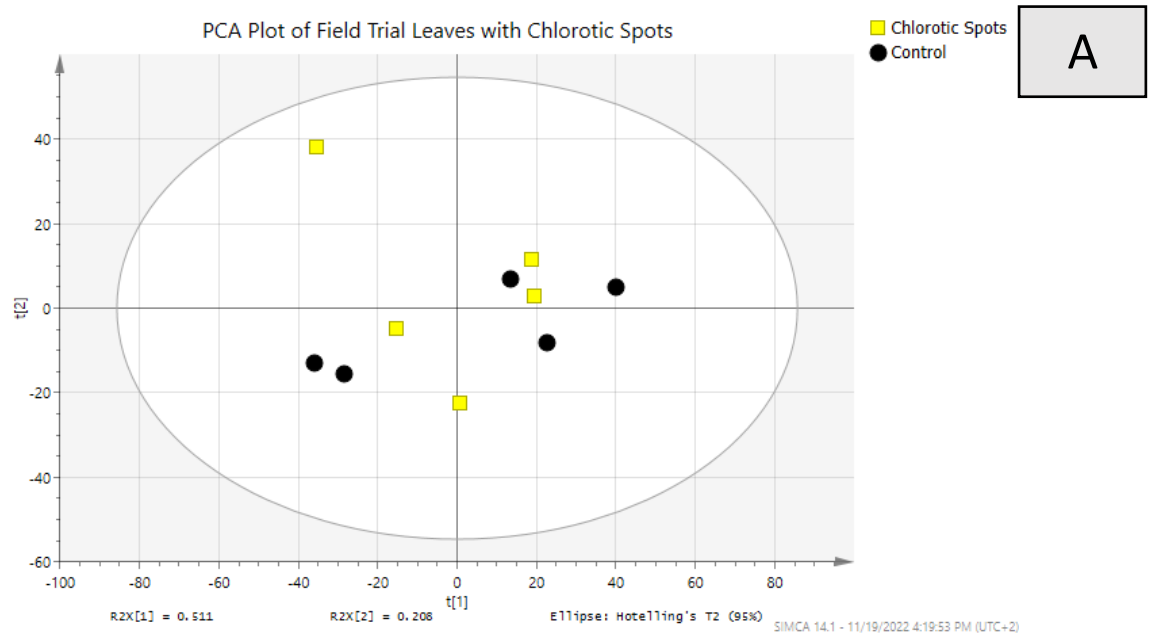

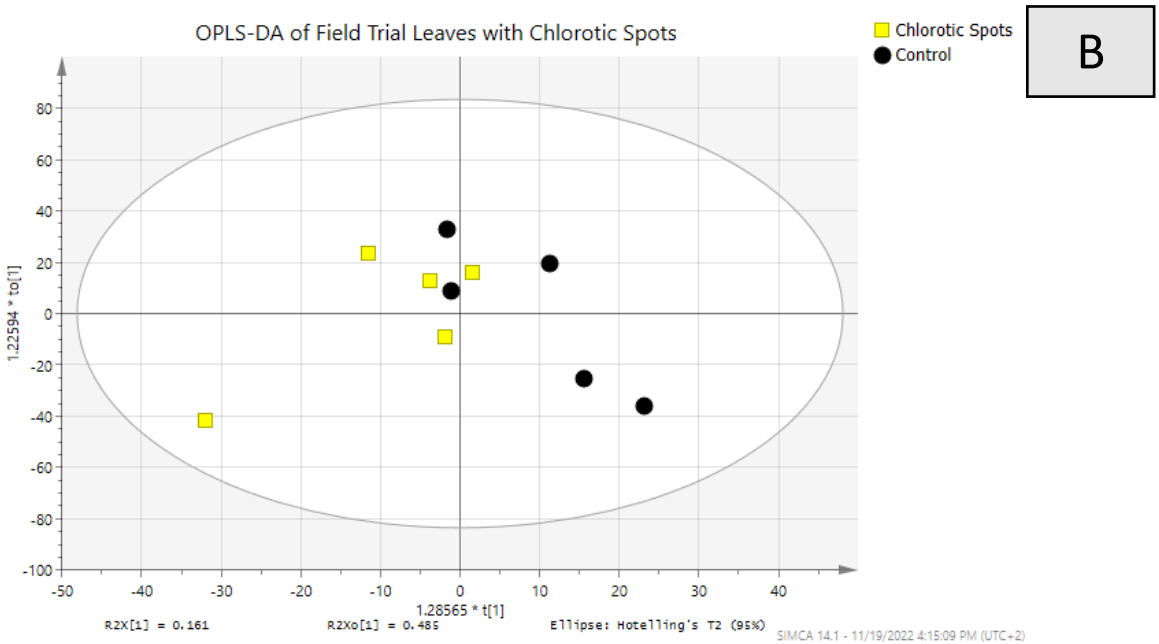

Figure 3.7: (A) 1H NMR PCA score plot of field trial maize leaves with chlorotic spots and corresponding controls. No definitive separation between the two sample sets. Multivariate statistical values: RX2 = 0.72; Q2 = 0.43. (B) 1H NMR OPLS-DA score plot of field trial with chlorotic spots and corresponding controls. No definitive separation between the two sample sets. Multivariate statistical values: R2X = 0.646 and R2Y = 0.43; Q2 = -0.969.

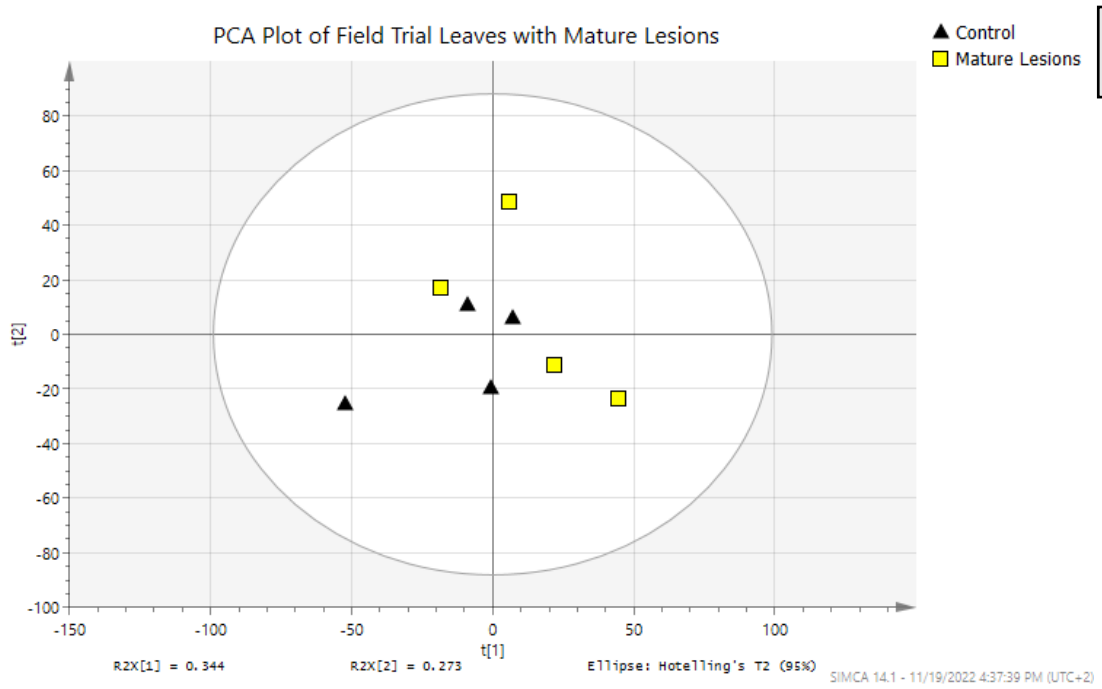

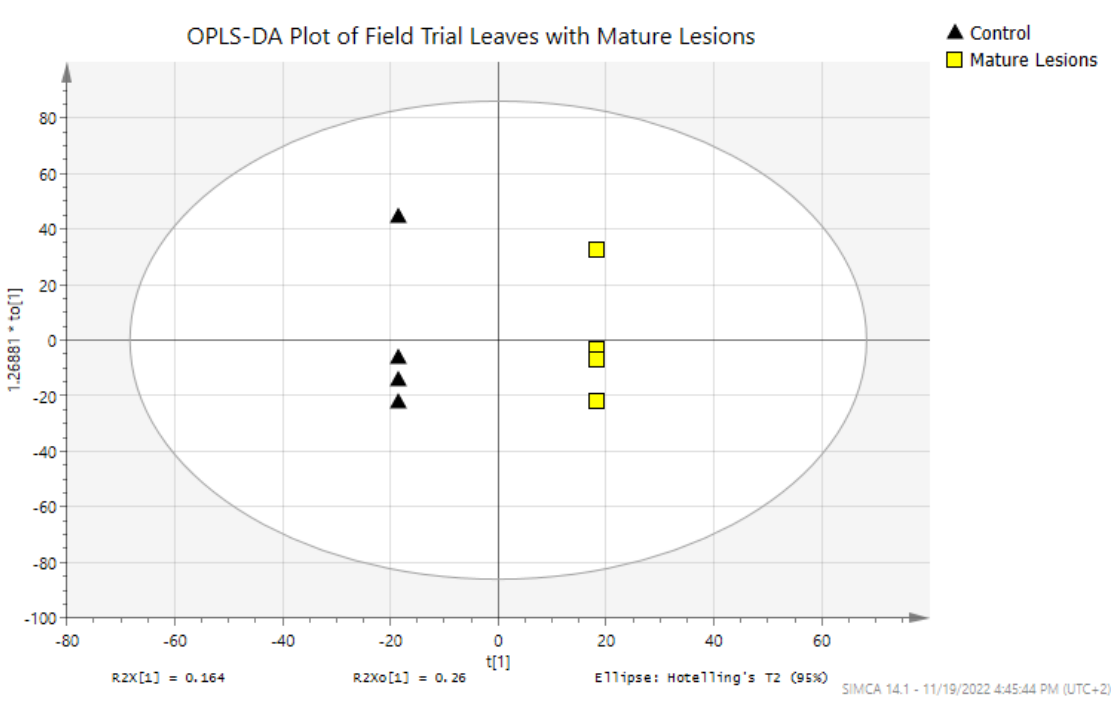

Figure 3.8: (A) ^{1}H NMR PCA score plot of field trial maize leaves with mature lesions and corresponding controls. No definitive separation between the two sample sets. Multivariate statistical values R2X = 0.77; Q2 = 0.27. (B) 1H NMR OPLS-DA score plot of field trial leaves with mature lesions and corresponding controls. Definitive separation between the two sample sets. Multivariate statistical values: R2X = 0.95 and R2Y = 1; Q2 = 0.63.

3.4.2.2 Glasshouse trial

The glasshouse trial's leaf extracts were also subjected to ^{1}H NMR analysis. The stacked spectra of all samples showed differences between the inoculated and the control samples at certain regions indicated in Figure 3.9. This suggested that *C. zeina* inoculation altered the metabolomic fingerprints of the maize leaves. The first difference between the inoculated samples (mature lesions) and the control samples was at the chemical shift region of 1.87 ppm and 2.8 - 3.0 ppm. It was observed that the peaks (functional groups) were only present in the inoculated samples and not the control samples. This suggests a possible *C zeina* related metabolomic fingerprint within the maize leaf metabolome. Furthermore, Gable (2019) reported that the region of 1.8 shows signals of compounds containing allylic, benzylic or ketone functional groups and the region of 2.80 – 3.53 ppm shows the signals of compounds with alkynes, alkyl halides, esters, alcohol, or ethers. Other spectral regions that showed differences between the inoculated and the control were in the regions of 5.2 - 5.4 ppm, 4.4 - 4.5 ppm, 3.1 - 3.5 ppm. In these regions the detected peaks were present in higher concentrations in the inoculated than in the control samples. The chemical shifts of 3.90 – 5.05 ppm are regions where compounds containing functional groups such as alcohols, esters, alkyl halides and alkenes are detected. The functional groups of interest detected may belong to a single compound or various compounds that are upregulated due to *C. zeina* infection.

The unsupervised PCA plot (Figure 3.10 A) shows separation between the infected and the control samples. This indicates that the individual metabolomic fingerprints of the control samples had little intra-variation and differed to that of the inoculated samples. The statistical validation values were high and the Q2 value suggests that the data is reliable in predicting unknown samples. Furthermore, the OPLS-DA plot in Figure 10 (B) showed a clear separation between the two data samples and the statistical values corresponded to those obtained in the PCA plot, indicating a clear metabolomic fingerprint difference between the inoculated and control samples.

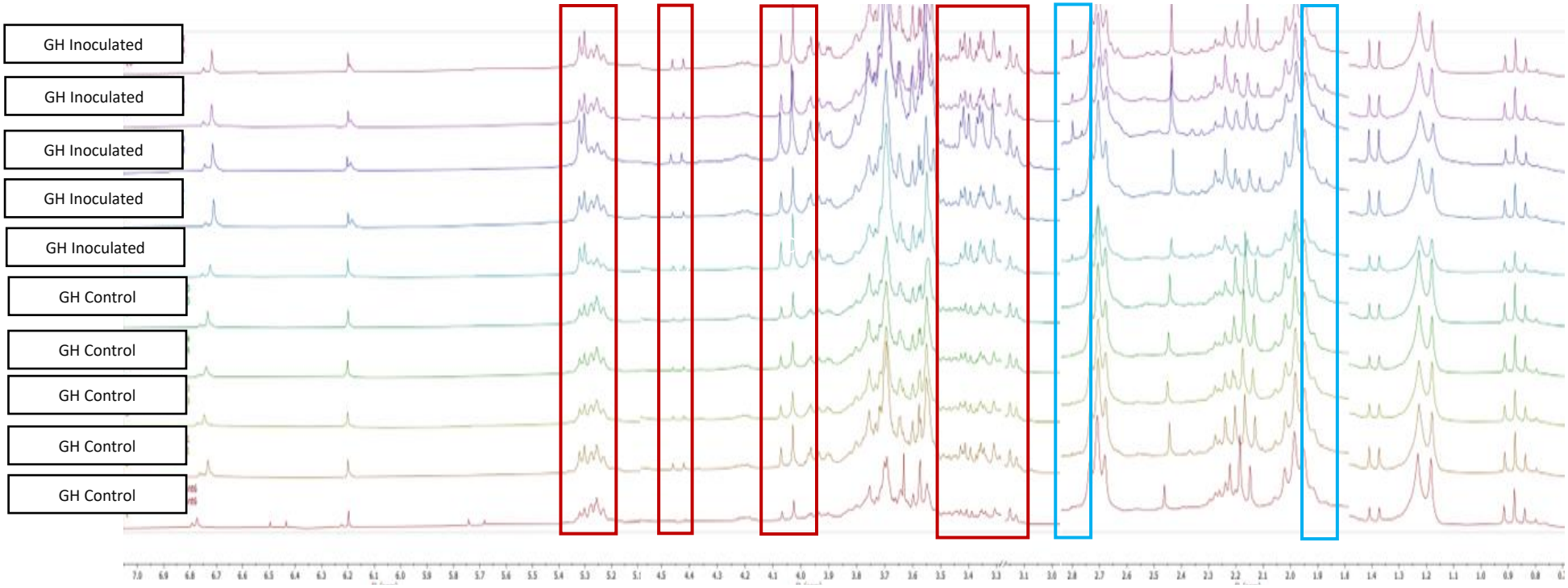

Figure 3.9: Stacked 1H NMR spectra of glasshouse leaves with mature lesions and their accompanying controls. Various concentration differences were observed between the two sets of samples. Peak concentration differences i.e., higher peak intensity in the inoculated were observed at 5.2-5.4 ppm, 4.4-4.5 ppm, 3.1-3.5 ppm (indicated by red boxes from left to right). Peaks unique ONLY the inoculated were identified at 2.8-3.0 ppm and 1.9 ppm (indicated by light blue boxes).

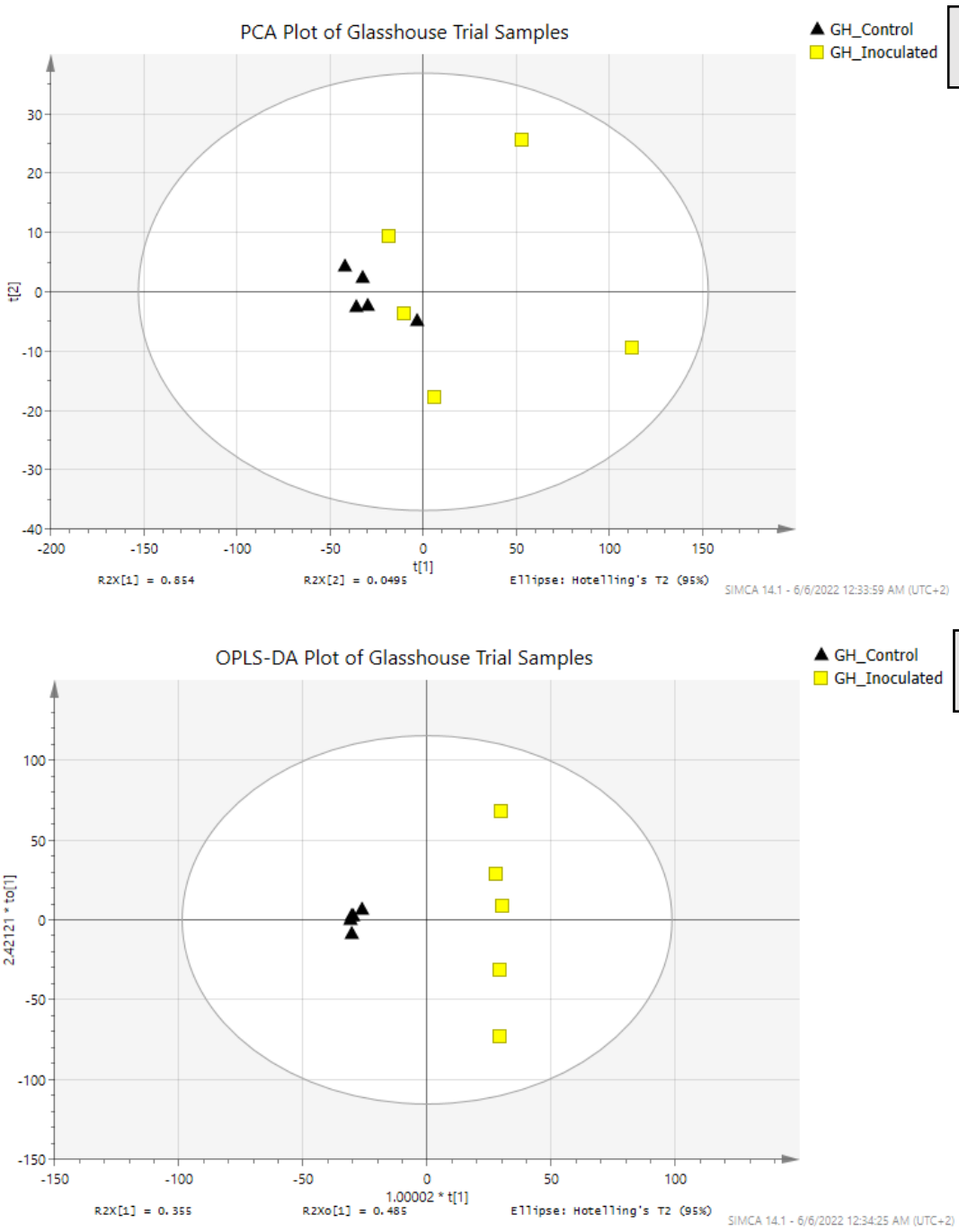

Figure 3.10: (A) 1H NMR PCA Score plot of glasshouse trial inoculated maize leaves with mature lesions and corresponding controls. No definitive separation between the two sample sets. Multivariate statistical values: R2X = 0.95; Q2 = 0.80. (B) OPLS-DA Score plot of glasshouse trial leaves and corresponding controls. Definitive separation between the two sample sets. Multivariate statistical values: R2X = 0.99 and R2Y = 1; Q2= 0.85.

3.4.2.3 Comparison of ^{1}H NMR spectra of field trial chlorotic spots and mature lesions, and glasshouse trial mature lesions leaf samples

The ^{1}H NMR spectra of the all the field and glass house maize leaves were compared to assess similarities and differences in the metabolomic fingerprints of the different sample sets (Figure 3.11). The comparison indicated that all maize samples had the same peak composition (functional) groups in the most parts of their chromatograms. Based on the comparison of the symptomatic samples i.e., field trial chlorotic spots, field trial mature lesions and glasshouse inoculated (mature lesions), the chlorotic spots samples' spectra differed from the mature lesions' samples (both glasshouse and field trial) in the regions of 5.20 -5.35 ppm and 4.00 – 4.10 ppm. In this region the chlorotic spots spectra had some peaks absent that were present in the mature lesions' samples. It was also discovered that in the same regions, though the glasshouse and field trial mature lesions' samples had the same peak composition, the peaks were present in higher concentrations in the glasshouse samples. Another observation made was in the region of 2.40 – 2.47 ppm, where a peak (functional group) was present only in the glasshouse samples and not the field trial samples. This could possibly be attributed to the difference in environment where the samples were collected from (Sardans et al., 2020). Another difference was observed in the region of 2.09 – 2.28 ppm where all symptomatic sample's spectra differed in peak composition. This may be attributed to differences in both the environment of sample collection and time of collection. Coincidentally, upon comparison of the control (asymptomatic) samples' spectra it was discovered they differed in the same regions as the symptomatic samples and in the same way. This suggests that most of the differences observed were due to differences in environment and time of collection.

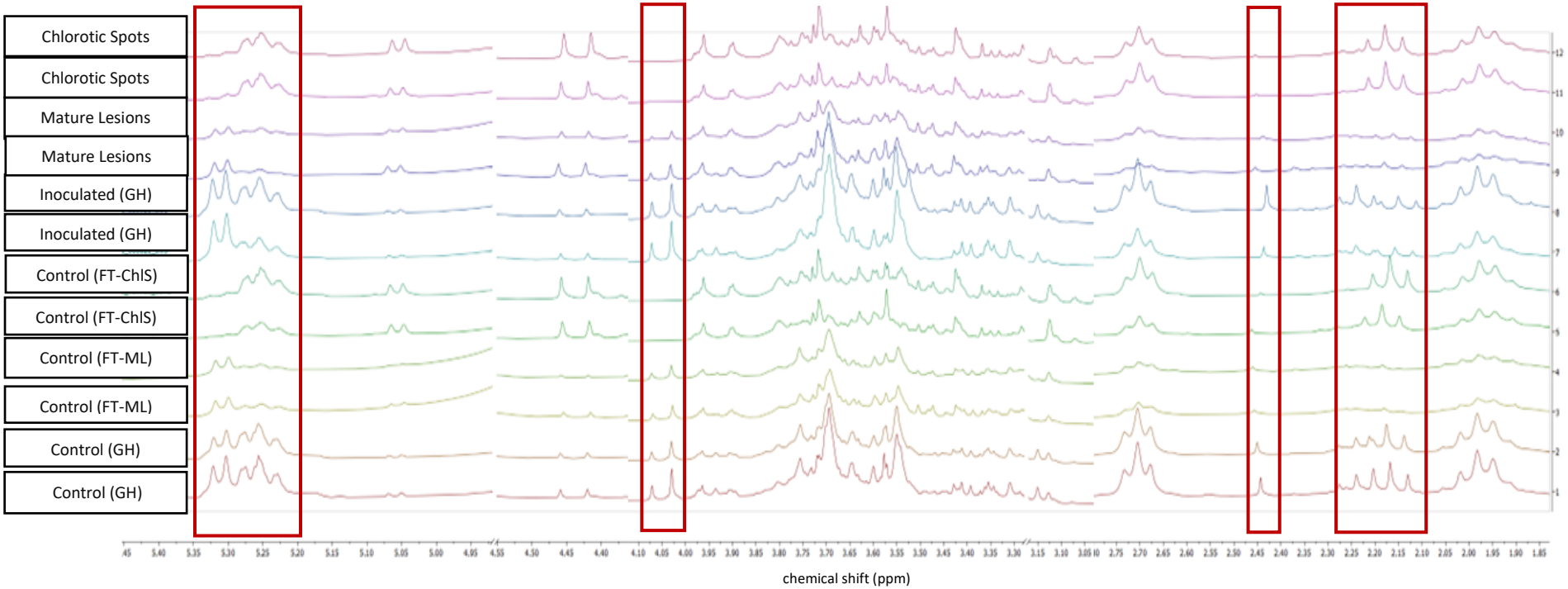

Figure 3.11: Stacked ^{1}H NMR spectra of representatives of field trial maize leaves with chlorotic spots, field trial leaves with mature lesions, inoculated glasshouse leaves with mature lesions and their respective controls. This was to compare the symptomatic samples NMR fingerprint and to compare the control samples' NMR metabolomic fingerprint. The field trial control's spectra are labelled as follows: FT-ML – Field Trial Mature Lesions; FT-ChlS – Field Trial Chlorotic Spots. GH – Glasshouse. Major differences were observed between the symptomatic samples in the regions of 5.20 -5.35 ppm, 4.00 – 4.10 ppm, 2.40 – 2.47 ppm and 2.09 – 2.28 ppm. Coincidentally the control samples also differed in the same regions. (NB: All solvent peaks and internal standard peaks have been removed from the spectra to magnify the peaks of interest).

3.4.3 Gas Chromatography Mass Spectrometry (GCMS) Results

3.4.3.1 Chlorotic spots

Maize leaf extracts with chlorotic spots were also subjected to GCMS analysis to identify possible metabolite changes in the early stages of *C. zeina* infection. It was also aimed at identifying potential biomarkers that can be used to characterize the initial stages of grey leaf spot. The sample chromatograms were stacked for comparison in Mnova as shown in Figure 3.12. A single metabolite's concentration difference was observed between the infected samples and the control samples at retention time of 27.4 mins. as shown in Figure 3.13. Chromatogram numerical data analysis in Microsoft Excel (Figure 3.14) showed that the average metabolite concentration in the chlorotic spots samples was higher than in the control samples. However, the 95% confidence ANOVA statistical test (Figure 3.14) revealed that the concentration of the metabolite in the chlorotic spots leaf samples was not significantly different ($p>0.05$) to that in the control samples. This suggests that early infection of *C. zeina* in maize leaves possibly had no significant detectable metabolite affect. Since the identity of the compound was unknown it was named compound A.

The samples with chlorotic spots were further subjected to multivariate statistical analysis in SIMCA-P. This would allow overall comparison of the chromatograms and possibly elucidate the correlation between the maize leaf metabolome change during early *C. zeina* infection. The unsupervised PCA plot (Figure 3.15) showed no clear grouping between the samples with chlorotic spots and their control. This suggests that there was little inter- and intra-variation between the metabolites found in the two data sets and this is probably supported by the single difference observed in the chromatograms of the control and infected extracts. The supervised OPLS-DA plot (Figure 3.16) showed groupings between the treatments, though not quite distinctive. This suggests that the average chromatogram data of the two sample sets differ to a certain degree, though not definitive or significant. The model fit values ($R2X=0.84$, $R2Y=0.81$) suggested that the model was well suited for the data, however the predictability value ($Q2 < 0.5$) suggested that the data could not be used to predict unknown samples under the same premise (Triba et al., 2015).

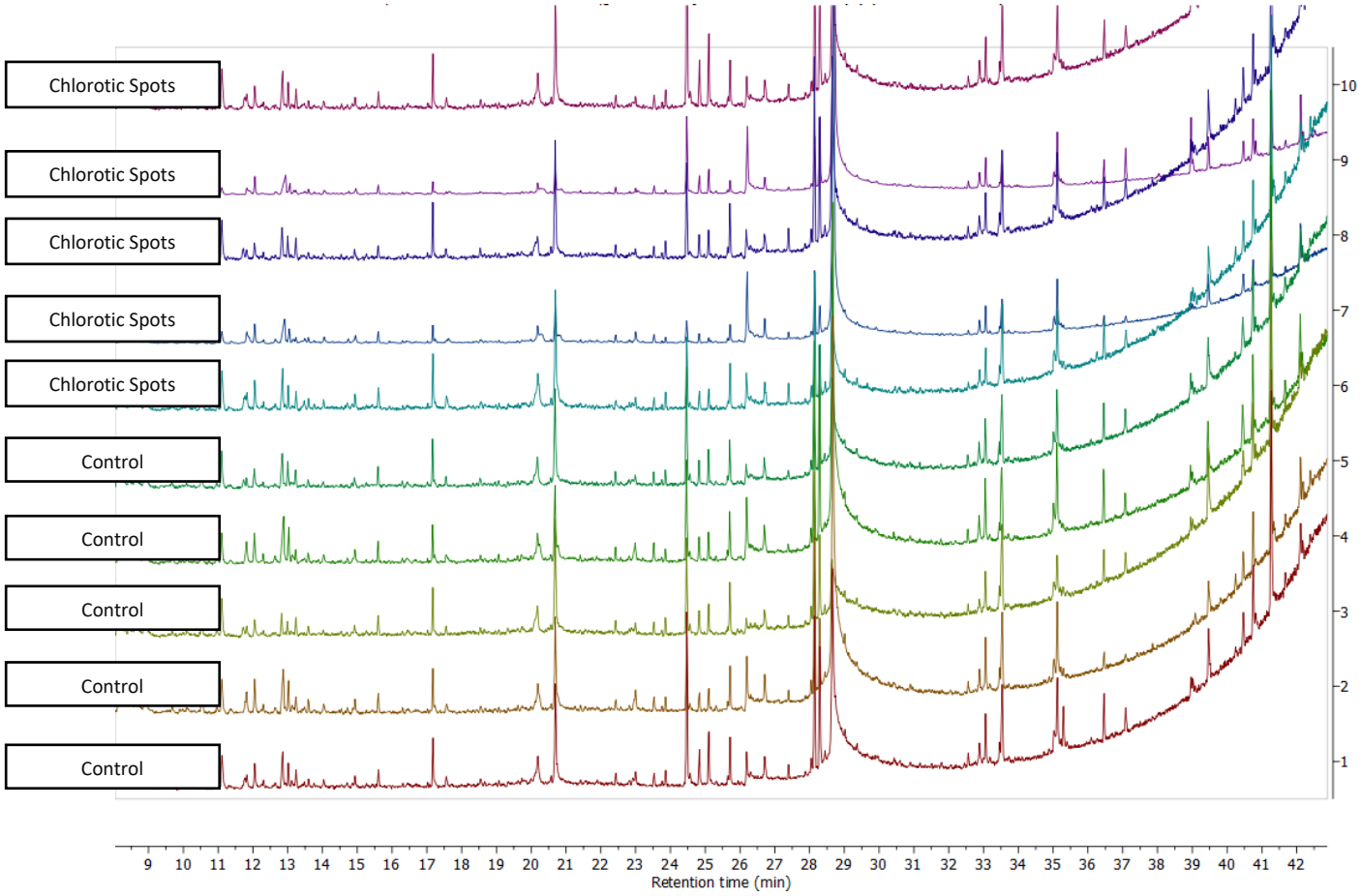

Figure 3.12: Stacked GCMS chromatograms of field trial leaf samples with chlorotic spots and their accompanying controls. At first glance, no clear definitive metabolite differences were observed in the chromatograms of the leaves with chlorotic spots and the asymptomatic controls.

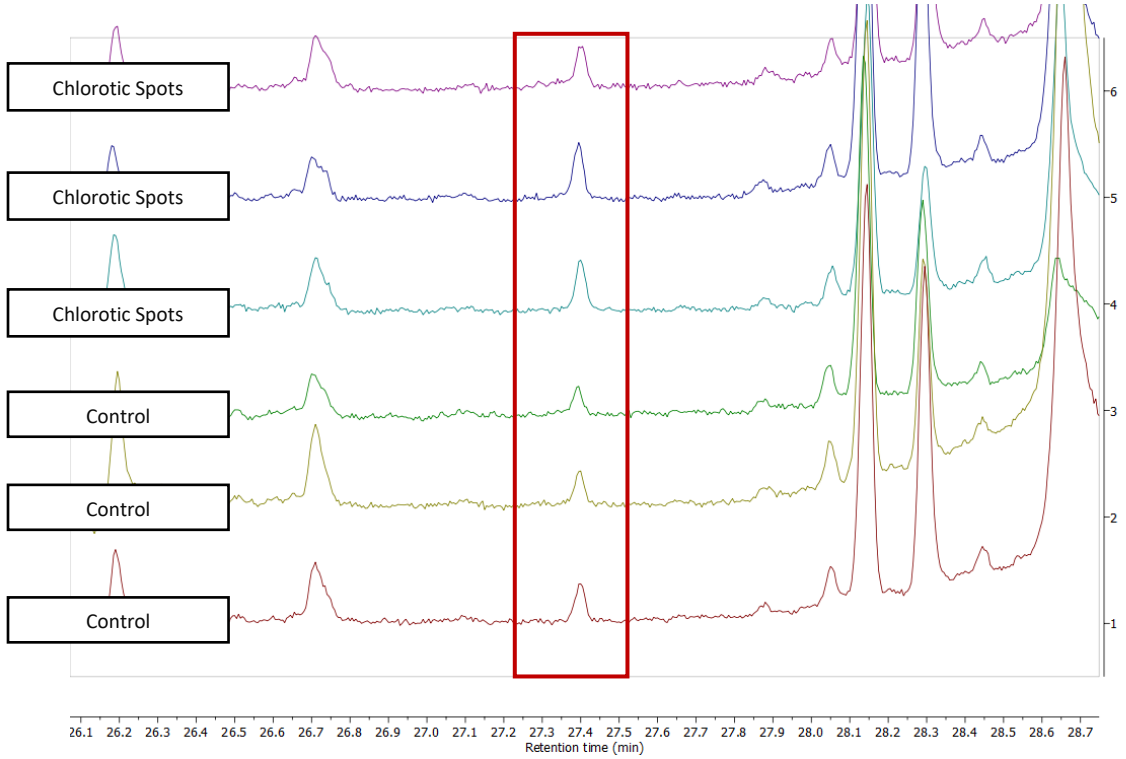

Figure 3.13: Expanded part of the chromatogram region showing the metabolite concentration change observed in the chlorotic spots leaf samples at retention time 27.4 mins. (red box) identified as a potential pathogen related biomarker. The metabolite concentration (peak intensity) is higher in the chlorotic spots' samples than in the asymptomatic control samples.

Statistical analysis of compound A (27.4 mins) in chlorotic spots leaf samples

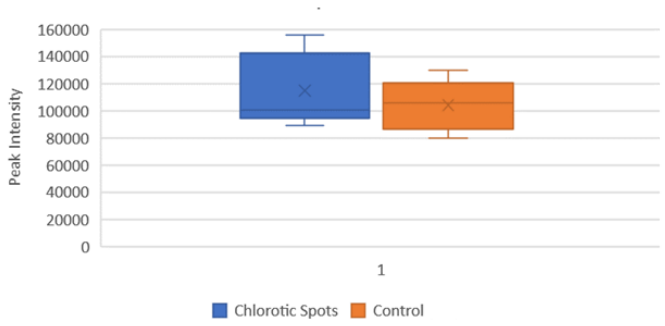

SUMMARY

Groups	Count	Sum	Average	Variance
Chlorotic Spots	5	574101.7	114820.3	7.45E+08
Control	5	520202.3	104040.5	3.54E+08

ANOVA

Source of Variation	SS	df	MS	F	P-value	F crit
Between Groups	2.91E+08	1	2.91E+08	0.528626	0.487913	5.317655
Within Groups	4.4E+09	8	5.5E+08			
Total	4.69E+09	9				

Figure 3.14: Statistical analysis of the concentration of compound A in maize leaf samples with chlorotic spots and their control. Average metabolite concentration difference of compound A between the chlorotic spots and the asymptomatic controls was not significant, p-value > 0.05.

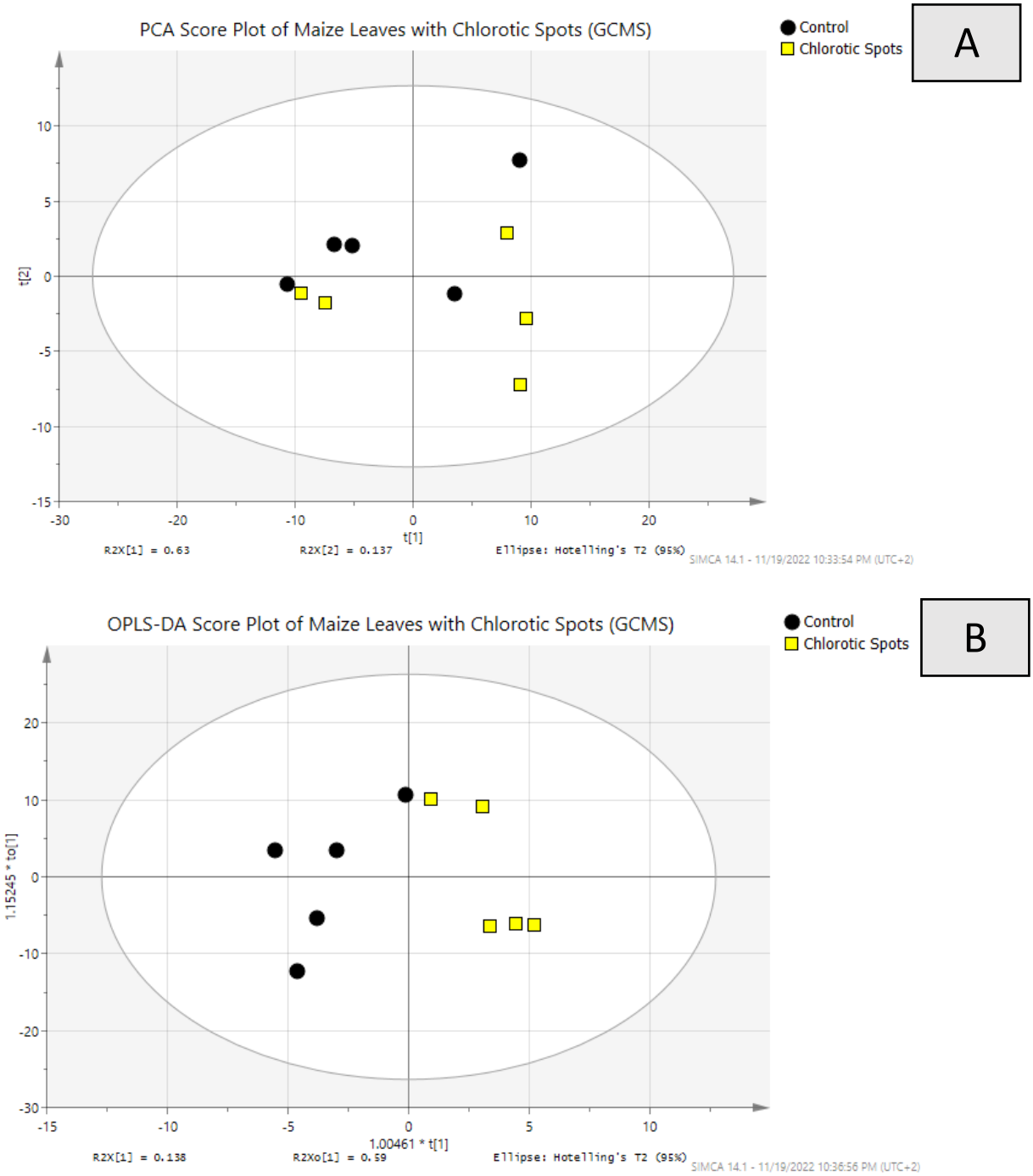

Figure 3.15: (A) GCMS chromatograms PCA score plot of leaf samples with chlorotic spots and accompanying asymptomatic controls. No definitive separation between the sample sets. Multivariate statistical values R2 = 0.77, Q2 = 0.60. (B) GCMS chromatograms OPLS-DA score plot of leaf samples with chlorotic spots and accompanying asymptomatic controls. Multivariate statistical values R2X = 0.84, R2Y = 0.81, Q2 = 0.37. Samples sets separated but not definitively.

3.4.3.2 Mature lesions

The maize leaves with fully developed lesions were also further subjected to GCMS analysis. The sample chromatograms were stacked in Mnova for comparison as shown in Figure 3.16. Several metabolite differences were observed in the mature lesions samples' chromatogram and were identified as potential biomarkers. The first metabolite concentration change was observed at retention time 24.5 min. as shown in Figure 3.17. The metabolite (named compound B) was observed to have a higher peak intensity in the symptomatic leaves. Further chromatogram numerical data analysis (Figure 3.18) revealed that the average concentration of the metabolite in symptomatic leaves was higher than the asymptomatic leaves. A univariate ANOVA test (Figure 3.18) yielded a p-value lower than 0.05, indicating that the concentration of the metabolite in the symptomatic (mature lesions) samples was significantly higher than in the control samples. Suggesting that *C. zeina* infection possibly induced the upregulation of the metabolite.

Another metabolite concentration difference between the symptomatic and the control samples in the chromatogram was observed at retention time 27.4 mins, as illustrated in Figure 3.19. The metabolite peak was present in higher concentrations in the mature lesions' chromatograms than the control samples'. The same observation was made in the chromatogram of chlorotic spots samples and the metabolite was named **Compound A**. Univariate statistical analysis of the chromatogram numerical data (Figure 3.20) revealed that based on the p-value, which was smaller than 0.05, the concentration of the metabolite in the maize leaf samples with mature lesions was significantly higher than in the asymptomatic control samples, suggesting that the metabolite change was influenced by *C. zeina* infection. Subsequent chromatogram differences were identified at retention times of 29.0 mins (Figure 3.21) which was named **Compound C**, and 30.2 mins (Figure 3.22) which was named **Compound D**. Compound C had a reduced peak intensity in the symptomatic samples, and this was highlighted by the statistical analysis of the chromatogram numerical data shown in Figure 3.23. This suggested that *C. 61eina* infection hindered or negatively impacted the production and expression of this metabolite. However, the univariate statistical analyses yielded a p-value larger than 0.05 suggesting that the concentration reduction of the metabolite in the symptomatic samples was not significantly different from that observed in the asymptomatic control samples. This meant that the observation could not be definitively asserted as a biomarker for *C. 61eina* diagnosis. Metabolite. Univariate statistical analysis of the chromatogram numerical data (Figure 3.31) yielded a p-value less than 0.05 indicating that the metabolite concentration was significantly higher in the maize leaves with mature lesions.

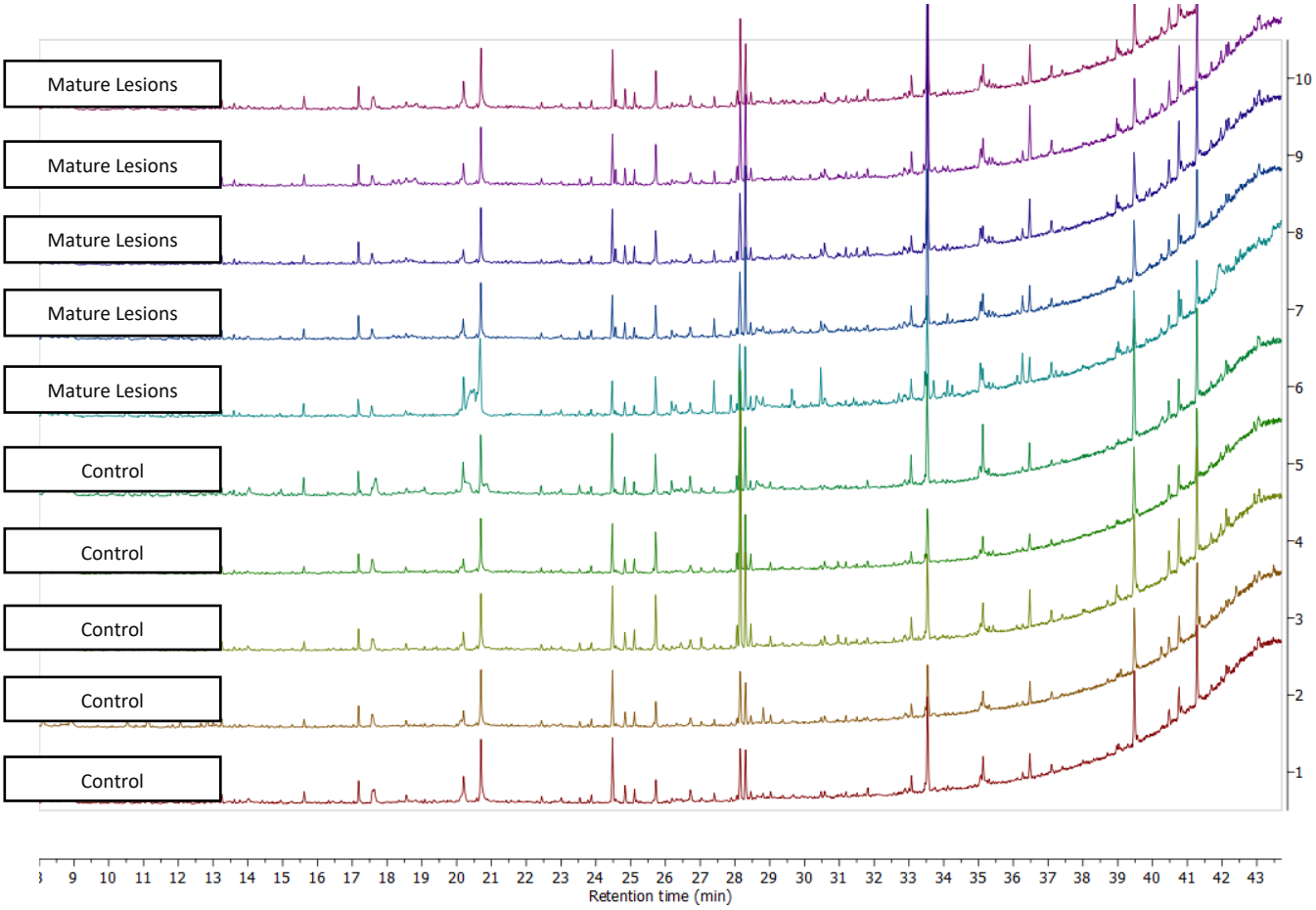

Figure 3.16: Stacked GCMS chromatograms of field trial leaf samples with mature lesions and the accompanying controls. At first glance, very few metabolite differences were observed in the chromatograms of the leaves with mature lesions and the asymptomatic controls. (These will be shown in subsequent expanded chromatogram regions).

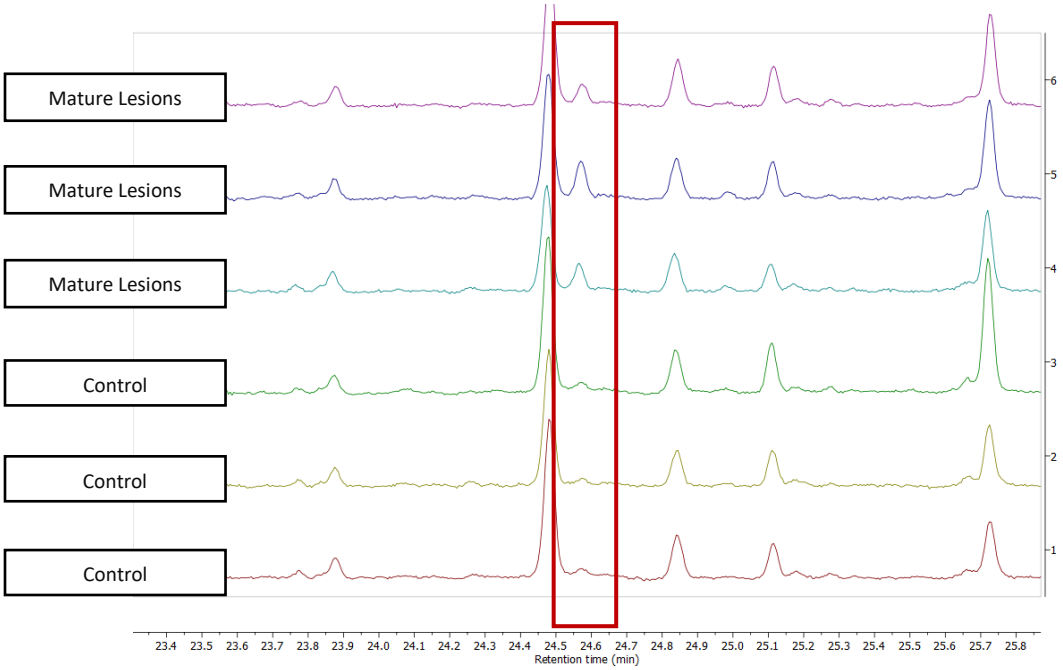

Figure 3.17: Expanded chromatogram region showing metabolite concentration change observed in the mature lesions leaf samples at retention time 24.5 mins. (red box) identified as a potential pathogen related biomarker. The metabolite concentration (peak intensity) is higher in the mature lesions' samples than in the asymptomatic control samples.

Statistical analysis of compound B (24.5 mins) in field trial mature lesions leaf samples

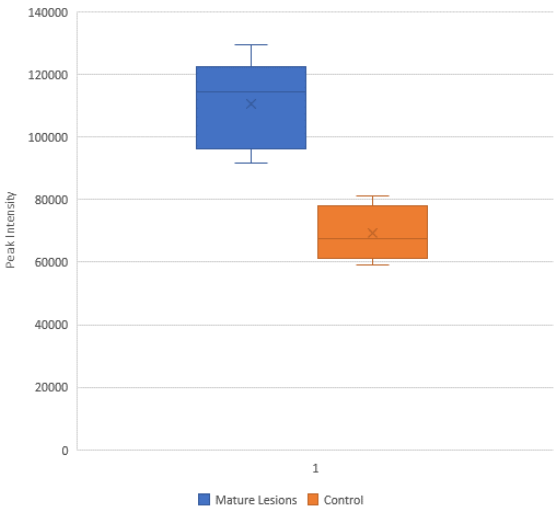

SUMMARY

Groups	Count	Sum	Average	Variance
Mature Lesions	5	552325.58	110465.12	2.14E+08
Control	5	345863.83	69172.77	77324921

ANOVA

Source of Variation	SS	df	MS	F	P-value	F crit
Between Groups	4.26E+09	1	4.26E+09	29.24445	0.00064	5.317655
Within Groups	1.17E+09	8	1.46E+08			
Total	5.43E+09	9				

Figure 3.18: Statistical analysis of the concentration of compound B in maize leaf samples with mature lesions and their control. Average metabolite concentration difference of compound B in leaves with mature lesions was significantly higher than the asymptomatic controls; p-value < 0.05.

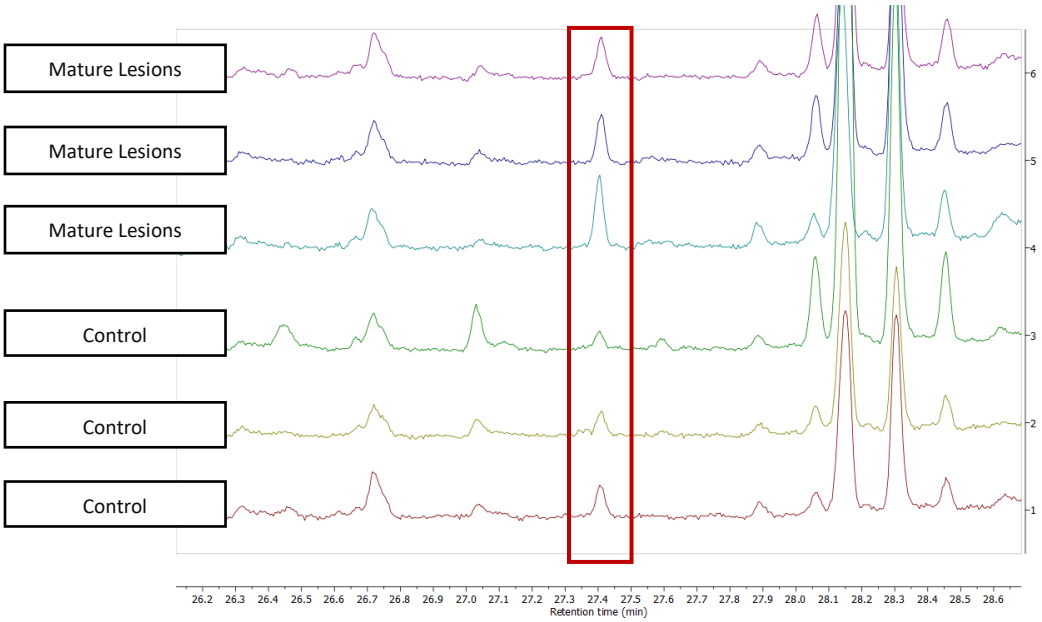

Figure 3.19: Expanded chromatogram region showing metabolite concentration change observed in the mature lesions leaf samples at retention time 27.4 mins. (red box) identified as a potential pathogen related biomarker. The metabolite concentration (peak intensity) is higher in the mature lesions' samples than in the asymptomatic control samples.

Statistical analysis of compound A (27.4 mins) in field trial mature lesions leaf samples

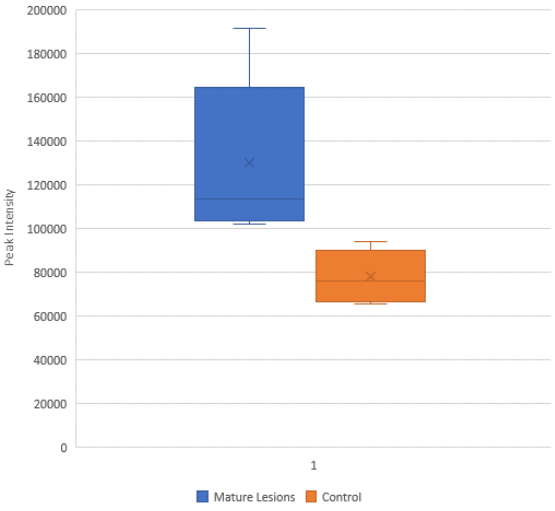

SUMMARY

Groups	Count	Sum	Average	Variance
Mature Lesions	5	649290.47	129858.09	1.38E+09
Control	5	388583.33	77716.67	1.49E+08

ANOVA

Source of Variation	SS	df	MS	F	P-value	F crit
Between Groups	6.8E+09	1	6.8E+09	8.910303	0.017466	5.317655
Within Groups	6.1E+09	8	7.63E+08			
Total	1.29E+10	9				

Figure 3.20: Statistical analysis of the concentration of compound A in maize leaf samples with mature lesions and their control. Average metabolite concentration difference of compound A in leaves with mature lesions was significantly higher than the asymptomatic controls; p-value < 0.05.

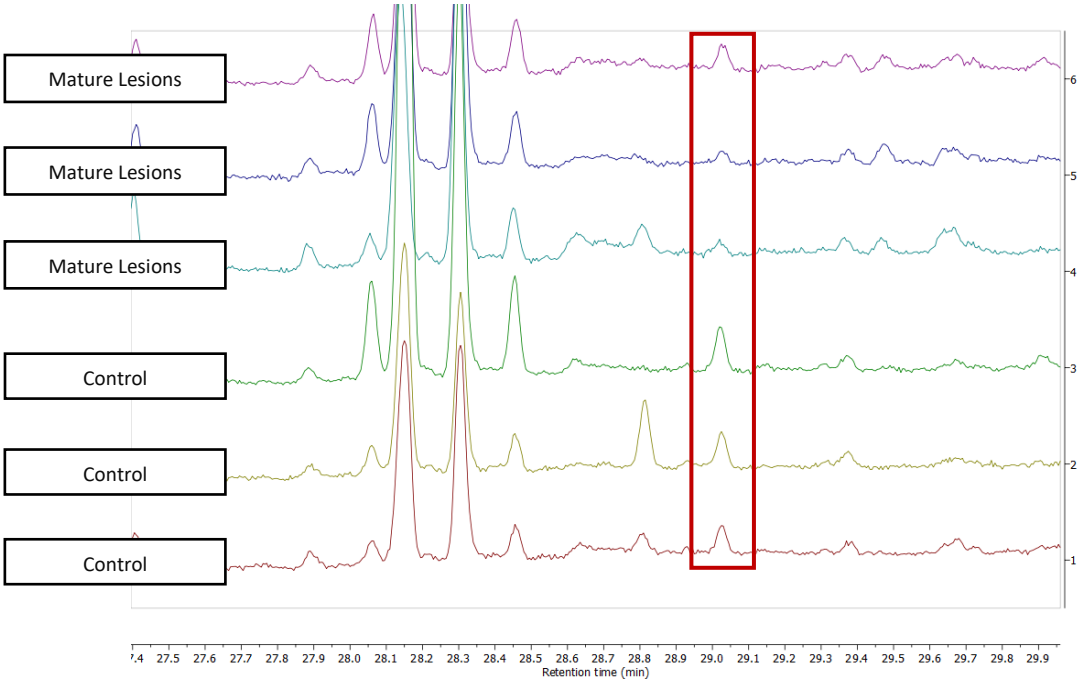

Figure 3.21: Expanded chromatogram region showing metabolite concentration change observed in the mature lesions leaf samples at retention time 29.0 mins. (red box) identified as a potential pathogen related biomarker. The metabolite concentration (peak intensity) is lower in the mature lesions' samples than in the asymptomatic control samples.

Statistical analysis of compound C (29.0 mins) in field trial mature lesions leaf samples

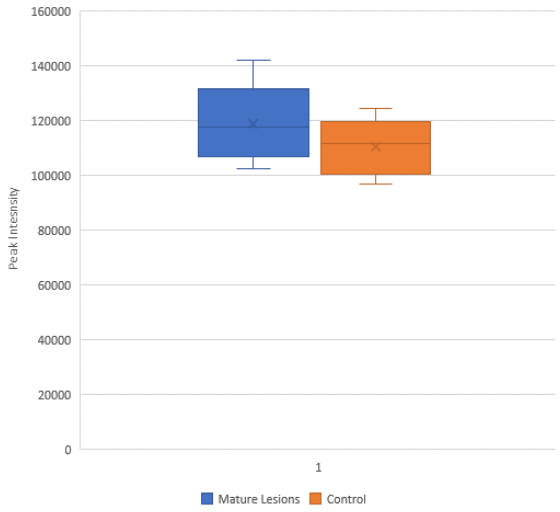

SUMMARY

Groups	Count	Sum	Average	Variance
Mature Lesions	5	594215.8	118843.15	2.18E+08
Control	5	551639.8	1.10E+05	1.09E+08

ANOVA

Source of Variation	SS	df	MS	F	P-value	F crit
Between Groups	1.81E+08	1	181271578	1.109215	0.323021	5.317655
Within Groups	1.31E+09	8	163423361			
Total	1.49E+09	9				

Figure 3.22: Statistical analysis of the concentration of compound C in maize leaf samples with mature lesions and their control. Average metabolite concentration difference of compound C in leaves with mature lesions was not significantly lower than the asymptomatic controls; p-value > 0.05.

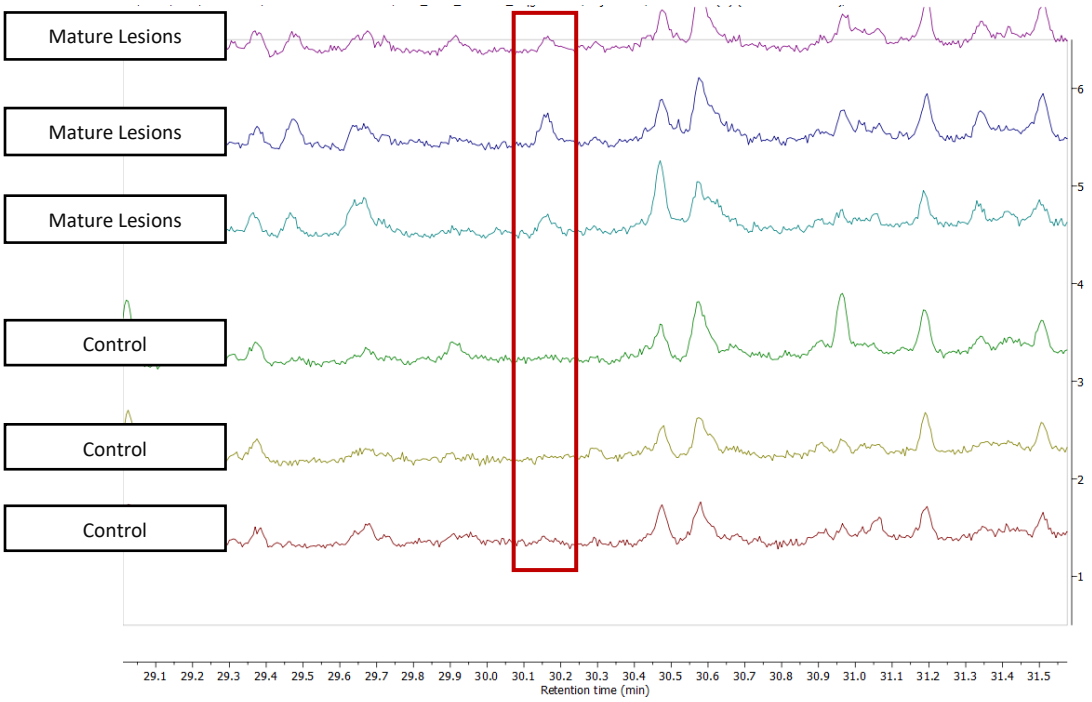

Figure 3.23: Expanded chromatogram region showing metabolite concentration change observed in the mature lesions leaf samples at retention time 30.2 mins. (red box) identified as a potential pathogen related biomarker. The metabolite concentration (peak intensity) is higher in the mature lesions' samples than in the asymptomatic control samples. The metabolite appears to be absent in the asymptomatic control samples.

Statistical analysis of compound D (30.2 mins) in field trial mature lesions leaf samples

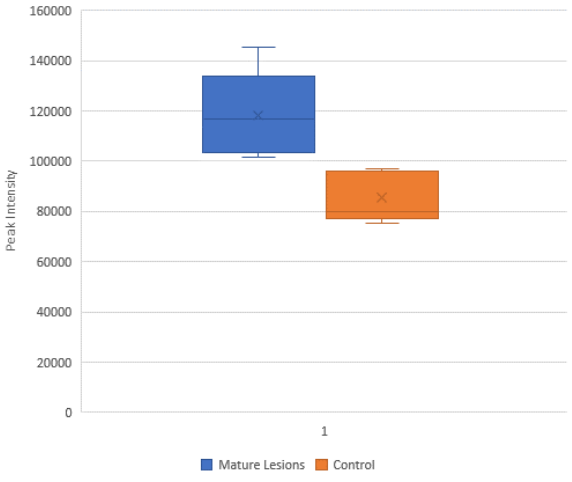

SUMMARY

Groups	Count	Sum	Average	Variance
Mature Lesions	5	590526.2	118105.2	3.01E+08
Control (Les)	5	426475.6	85295.12	99847211

ANOVA

Source of Variation	SS	df	MS	F	P-value	F crit
Between Groups	2.69E+09	1	2.69E+09	13.42581	0.006363	5.317655
Within Groups	1.6E+09	8	2E+08			
Total	4.29E+09	9				

Figure 3.24: Statistical analysis of the concentration of compound D in maize leaf samples with mature lesions and their control. Average metabolite concentration difference of compound D in leaves with mature lesions was significantly higher than the asymptomatic controls; p-value < 0.05.

The maize leaves portraying mature lesions were further subjected to metabolomical multivariate statistical analysis. This would allow overall comparison of the chromatograms and further highlight the change in the maize leaf metabolome in the later stages of GLS. The unsupervised PCA score plot shown in Figure 3.25 (A) indicates the treatments separating into their unique groups solely based on their individual GCMS chromatogram profiles, with one exception (one of the metabolites in this sample's chromatogram had an exaggerated peak intensity). This indicates that there is less intra-variation and considerable inter-variation in the sample's profiles. The statistical value Q2 also highlights the potential reliability of this data model to predict unknown samples with possible GLS infection. The supervised OPLS-DA plot in Figure 3.25 (B) correlates with the observation in the PCA plot further affirming the distinction between the groups in their GCMS chromatogram profile. Moreover, this illustrates that the metabolite changes that were observed in the symptomatic samples created a considerable change in the metabolome of the maize leaves. The statistical values (give them in brackets) suggest that the model can be reliably used to predict unknown samples under a similar premise.

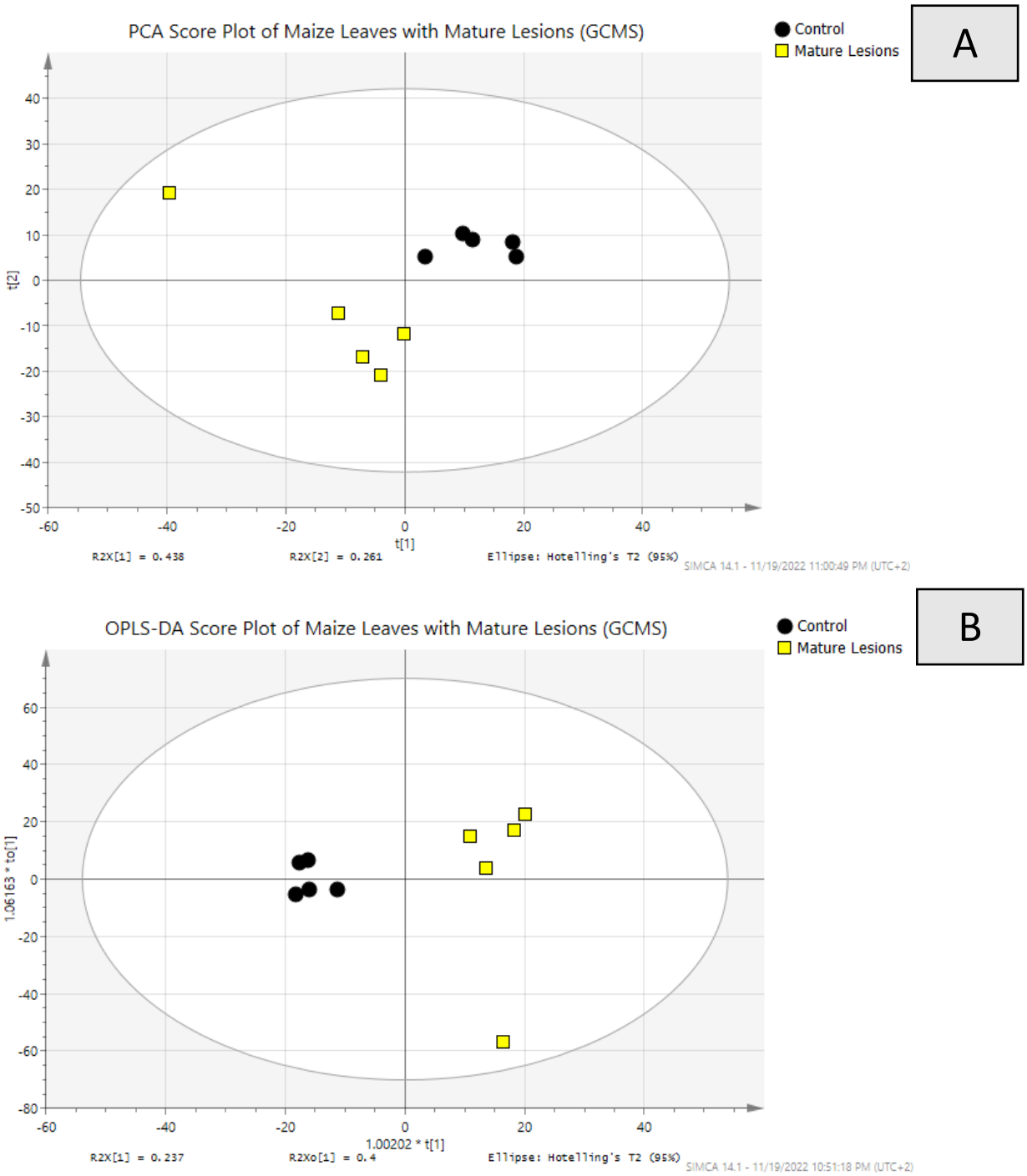

Figure 3.25: (A) GCMS chromatogram PCA score plot of leaf samples with mature lesions and accompanying controls. Clear separation of the mature lesions and control samples was observed. Multivariate statistical values: R2X = 0.94, Q2 = 0.70. (B) GCMS chromatogram OPLS-DA score plot of leaf samples with mature lesions and accompanying controls. Definitive separation of the two sample sets was observed. Multivariate statistical values R2X = 0.78, R2Y = 0.97, Q2 = 0.88).

3.4.3.3 Glasshouse trial

The maize leaves from the glasshouse trial i.e., inoculated maize leaves with mature lesions and asymptomatic control leaves, were also subjected to GCMS analysis. The sample chromatograms were stacked in Mnova (Figure 3.26) for comparison and identification of key changes in the metabolite profile. Intensive analysis of the chromatograms revealed several changes between the inoculated plants and the control. The first difference was observed at retention time 29.0 mins as shown in Figure 3.27, named compound C. The chromatogram data showed that the metabolite at this retention time had lower expressions in the inoculated maize leaves with mature lesions than in the asymptomatic controls. This observation corresponds to the observation made in the field trial leaf samples with mature lesions (Figure 3.21). Statistical analysis of the chromatogram numerical data (Figure 3.28) highlighted the difference in the peak intensity of the metabolite between the two sample sets. Based on the data's p-value ($p = 0.07$) the observed difference was insignificant under the 95% confidence interval, but it was significant under the 90% confidence interval. This means that there is a 90 % confidence that the concentration of compound C in the inoculated leaves with mature lesions is significantly lower than in the asymptomatic control samples. Subsequently, another key point difference in the chromatogram was observed at retention time 30.95 mins, illustrated in Figure 3.29. The metabolite was observed predominantly in the control samples and appeared to be present in minute amounts (to none) in the inoculated samples. Statistical analysis of the chromatogram numerical data (Figure 3.30) showed a p-value less than 0.05, indicating that the decreased concentration in the inoculated samples was significantly different from that in the control samples. Both these observations suggest that *C. zeina* hinders the production or expression of these metabolites in maize leaves.

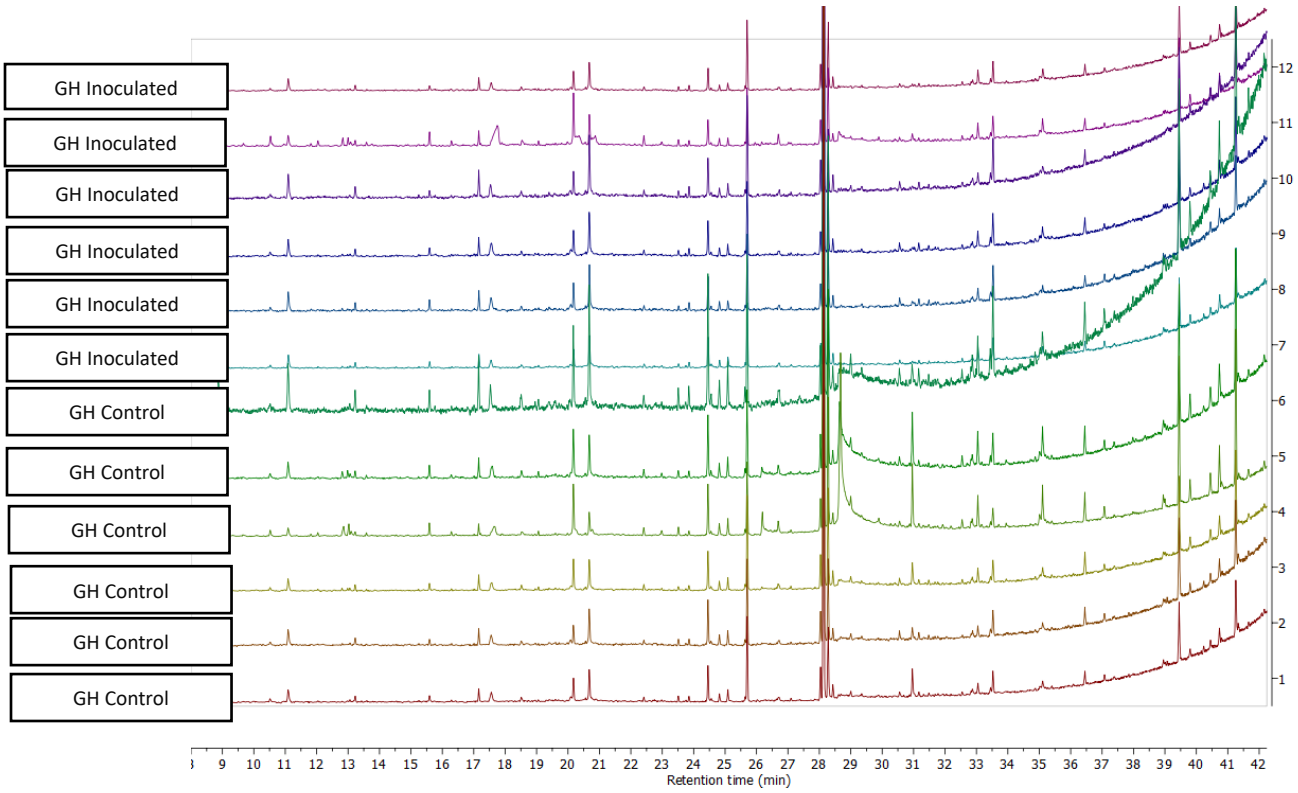

Figure 3.26: Stacked GCMS chromatograms of maize leaves sampled from the glasshouse trial.

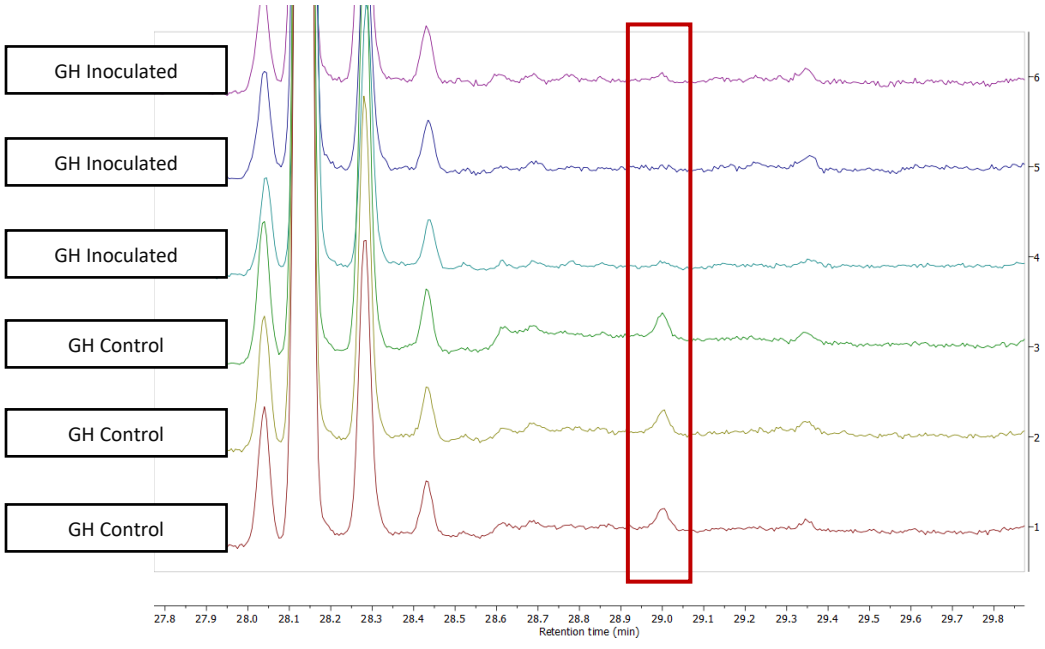

Figure 3.27: Expanded chromatogram region showing metabolite concentration change observed in the glasshouse trial leaf samples at retention time 29.0 mins. (red box) identified as a potential pathogen related biomarker. The metabolite concentration (peak intensity) is lower in the glasshouse inoculated leaves with mature lesions than in the uninoculated control samples.

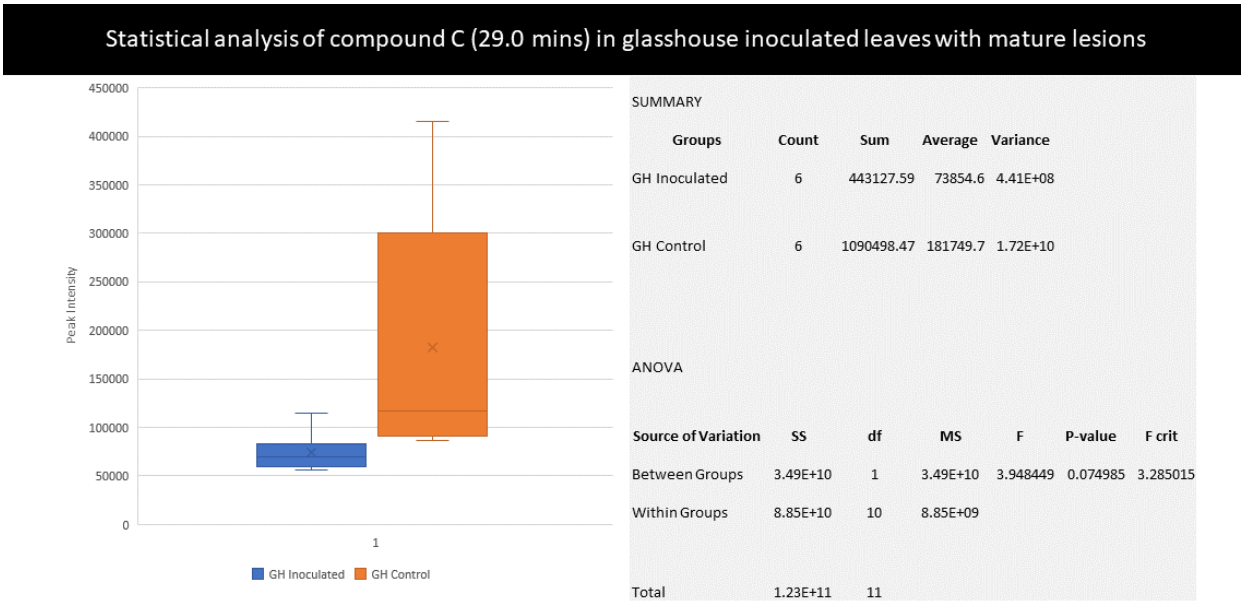

SUMMARY

Groups	Count	Sum	Average	Variance
GH Inoculated	6	443127.59	73854.6	4.41E+08
GH Control	6	1090498.47	181749.7	1.72E+10

ANOVA

Source of Variation	SS	df	MS	F	P-value	F crit
Between Groups	3.49E+10	1	3.49E+10	3.948449	0.074985	3.285015
Within Groups	8.85E+10	10	8.85E+09			
Total	1.23E+11	11				

Figure 3.28: Statistical analysis of the concentration of compound C in glasshouse inoculated maize leaves with mature lesions and their control. Average metabolite concentration difference of compound C in the inoculated leaves was not significantly lower than in the asymptomatic controls; p-value > 0.05.

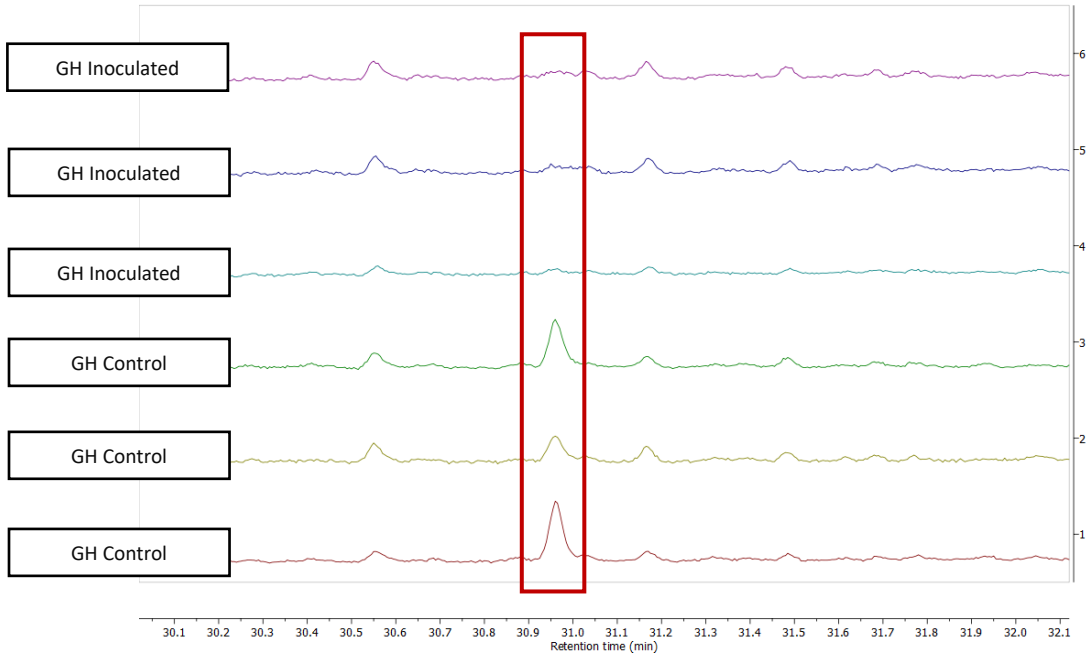

Figure 3.29: Expanded chromatogram region showing metabolite concentration change observed in the glasshouse trial leaf samples at retention time 29.0 mins. (red box) identified as a potential pathogen related biomarker. The metabolite concentration (peak intensity) is lower in the glasshouse inoculated leaves with mature lesions than in the uninoculated control samples. Using visual observations, it appears as if the peak is almost absent in the inoculated samples.

Statistical analysis of compound E (30.95 mins) in glasshouse inoculated leaves with mature lesions

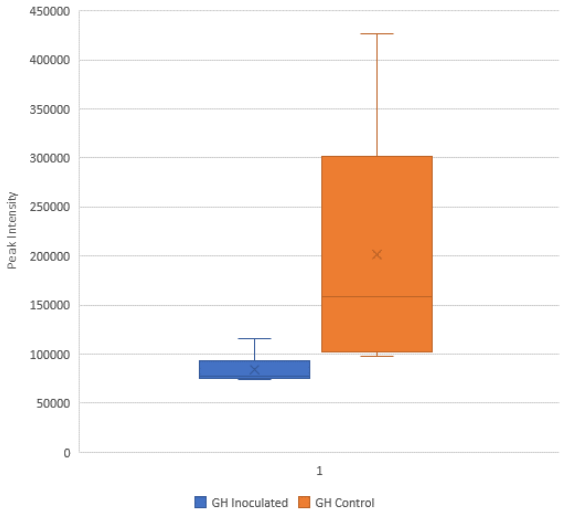

SUMMARY

Groups	Count	Sum	Average	Variance
GH Inoculated	6	506365.58	84394.26	2.55E+08
GH Control	6	1205715.53	200952.59	1.56E+10

ANOVA

Source of Variation	SS	df	MS	F	P-value	F crit
Between Groups	4.08E+10	1	4.08E+10	5.139419	0.046806	4.964603
Within Groups	7.93E+10	10	7.93E+09			
Total	1.2E+11	11				

Figure 3.30: Statistical analysis of the concentration of compound C in glasshouse inoculated maize leaves with mature lesions and their control. Average metabolite concentration difference of compound C in the inoculated leaves was significantly lower than in the asymptomatic controls; p-value < 0.05.

The glasshouse samples' chromatogram numerical data was further analysed using multivariate statistical analysis. This would allow overall comparison of the metabolomic profiles of the two sample sets and establish a correlation between *C. zeina* inoculation and change in leaf metabolome. The unsupervised PCA plot in Figure 3.31 (A) showed no clear separation between the sample sets, indicating that there is little inter-variation in the samples' chromatograms based on individual their metabolomic profiles. Furthermore, separation was observed between the samples within the same group, suggesting intra-variation amongst the replicates. Though the statistical values are high (R2X = 0.95; Q2 = 0.89), the plot trend is inconclusive in providing a clear indication on the metabolome change due to *C. zeina* inoculation. The supervised OPLS-DA plot shown in Figure 3.31 (B), which takes the average GCMS metabolomic profile of all the replicates within a designated treatment (group) showed a clear distinction between the two sample sets. This indicates the difference in the metabolomic profile between the inoculated and control groups. This leads us to believe that changes in the maize leaf metabolome can be attributed to *C. zeina*. Furthermore, the statistical values also suggest that the model can be reliably used to predict unknown samples under a similar premise. Moreover, this provides evidence that *C. zeina* inoculation has a considerable effect on the metabolomic profile of causing a notable distinction from the metabolic profile of asymptomatic maize leaves. Therefore, establishing a correlation between *C. zeina* and changes in the maize leaf's metabolome.

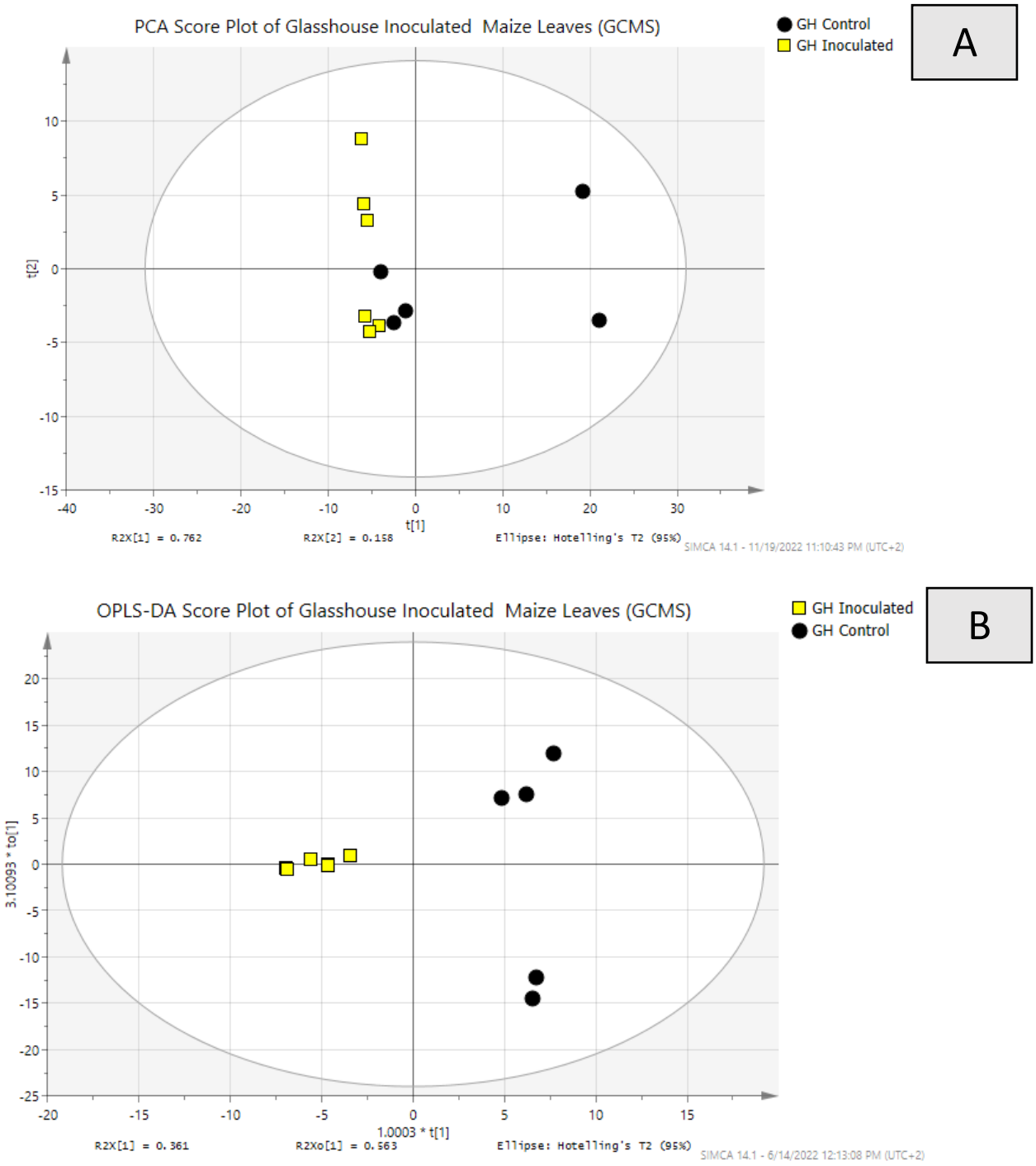

Figure 3.31: (A) GCMS chromatogram PCA score plot of glasshouse inoculated leaves with mature lesions and accompanying controls. Clear separation of the mature lesions and control samples was observed. Multivariate statistical values: R2X = 0.95, Q2 = 0.89. (B) GCMS chromatogram OPLS-DA score plot of leaf samples with mature lesions and accompanying controls. Definitive separation of the two sample sets was observed. Multivariate statistical values R2X = 0.97, R2Y = 0.97, Q2 = 0.86).

3.4.3.4 Comparative Analysis of Field Trial and Glasshouse Trial Chromatograms and Potential Biomarkers' Mass Spectra.

A comparative analysis was carried out on all the maize leaf sample GCMS chromatograms to determine similarities between the different classes of leaf samples, i.e., field trial and glasshouse trial samples. Representative chromatograms from each class were stacked in Mnova as illustrated by Figure 3.43. The comparison showed that the field trial samples had more metabolites in their chromatograms than the glasshouse samples. However, several metabolites were similar between the two classes but differed only in peak intensity or concentration. The glasshouse samples' plant material was less than the field trial samples' plant material, as only the inoculated regions were sampled and extracted for metabolites. Therefore, the metabolites were more concentrated in the field trial samples, i.e., same occurrence with different levels of expression.

The potential grey leaf spot metabolite biomarkers found in all classes were also compared, and their suggested identities were determined using their MS fragmentation patterns from the NIST 14 (NIST, USA) database as illustrated in Table 3.2. The database suggested that compound A shared similarities to hexadecanoic acid, 1-(hydroxymethyl)-1,2-ethanediyl ester (Figure 3.44), compound B shared similarities with 7-hexadecenal (Figure 3.45), compound C shared similarities with 9,12,15-octadecatrienoic acid (Figure 3.46), compound D shared similarities to 7,8-epoxylanostan-11-ol,3-acetoxy (Figure 3.47), and compound E shared similarities with methyl-5,11,14,17-eicosatetraenoate (Figure 3.48).The comparison indicated that the observation made for compound A in the chlorotic spots' chromatogram was also observed in the mature lesions' chromatogram. A similar observation was made for compound C in the mature lesions of the field trial and the glasshouse trial samples' chromatograms. The metabolite was present in a smaller concentration in the symptomatic (mature lesions samples). However, no similar metabolite trend was observed in the chlorotic spots and glasshouse chromatograms.

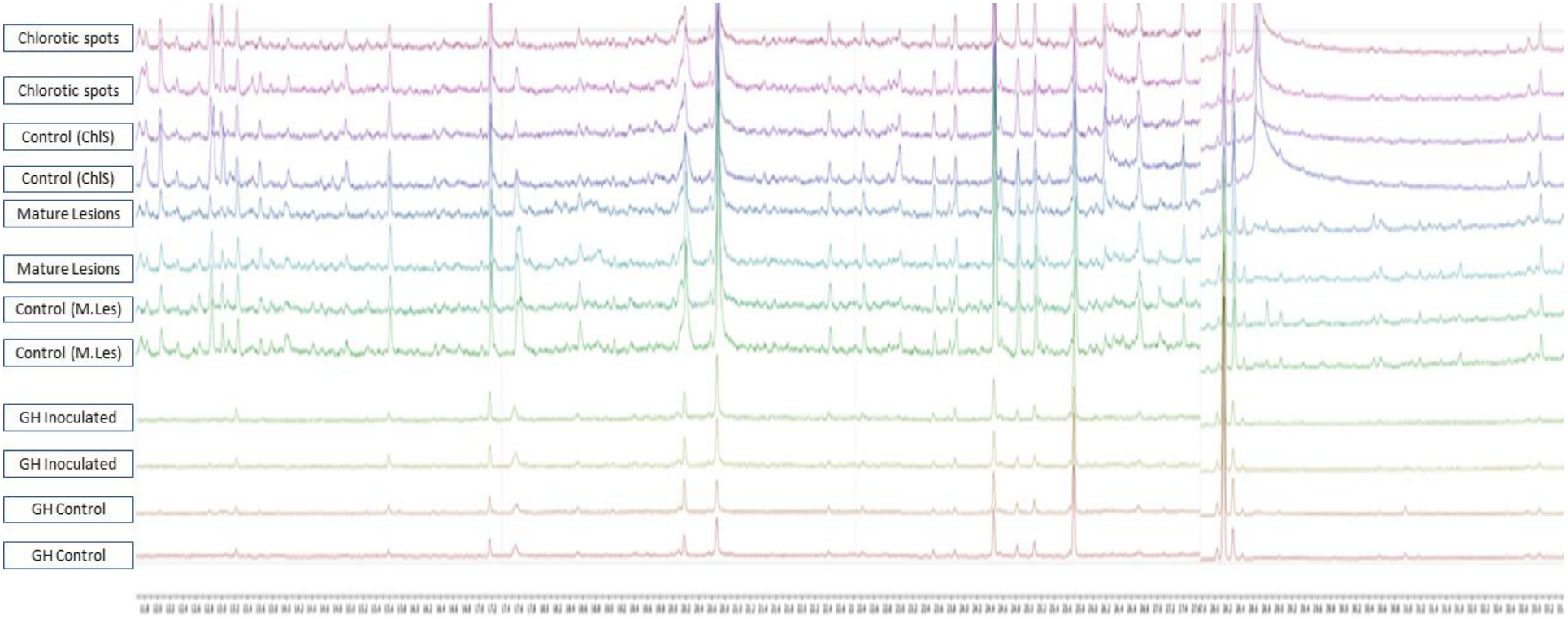

Figure 3.32: Stacked GCMS chromatograms of representatives of field trial maize leaves with chlorotic spots, field trial leaves with mature lesions, inoculated glasshouse leaves with mature lesions and their respective controls. This was to compare the symptomatic samples chromatograms and to compare the control samples' chromatograms metabolomic profile. The field trial control's spectra are labelled as follows: (M. Les) – Field Trial Mature Lesions; (ChlS) – Field Trial Chlorotic Spots. (GH) – Glasshouse. The major differences observed are that the field trial and the glasshouse trial samples have common metabolites in their profiles but expressed in different concentrations, i.e., more concentrated in the field trial samples.

Table 3.2: Comparison of potential grey leaf spot biomarkers identified in the GCMS chromatograms of the field trial maize leaf samples (chlorotic spots and mature lesions) and glasshouse trial maize leaf samples (C. zeina inoculated). All samples were compared to their appropriate controls.

Potential biomarker	Chromatogram retention time (mins.)	Chlorotic spots (Field Trial)	Mature lesions (Field Trial)	Mature lesions Glasshouse trial	Suggested compound match (NIST 14 database) and their similarity index (SI)
Compound A	27.4	Higher peak intensity in the symptomatic leaf samples. **p > 0.05**	Higher peak intensity in the symptomatic leaf samples. **p < 0.05**	Absent in all samples.	Hexadecanoic acid, 1-(hydroxymethyl)-1,2-ethanediyl ester **SI = 63.5** (See Figure 3.44)
Compound B	24.5	Same peak intensity in all samples.	Higher in symptomatic leaf samples. **p < 0.05**	Same peak intensity in all samples	7-Hexadecenal **SI = 86.2** (See Figure 3.45)
Compound C	29.0	Same peak intensity in all samples.	Higher peak intensity in the asymptomatic leaf samples. **p > 0.05**	Higher peak intensity in the asymptomatic leaf samples. **p > 0.05**	9,12,15-octadecatrienoic acid **SI = 87.6** (See Figure 3.46)
Compound D	30.2	Absent in all samples.	Present only in the symptomatic leaf samples. **p < 0.05**	Absent in all samples.	7,8-epoxylanostan-11-ol,3-acetoxy **SI = 71.4** (See Figure 3.47)
Compound E	30.95	Absent in all samples.	Same peak intensity in all samples.	Present only in the asymptomatic leaf samples. **p < 0.05**	Methyl-5,11,14,17-eicosatetraenoate **SI = 83.4** (See Figure 3.48)

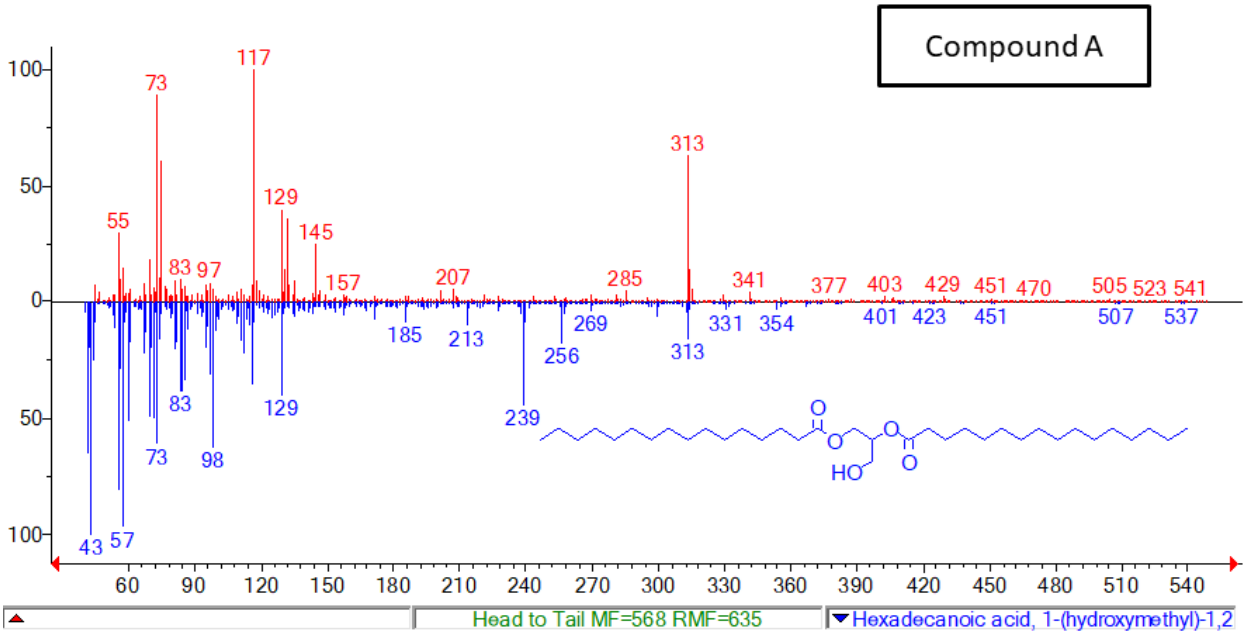

Figure 3.33: Suggested match for compound A based on MS spectrum comparison in NIST 14 database. The MS fragments of the unknown extracted metabolite are in red and the MS fragments for hexadecanoic acid, 1-(hydroxymethyl)-1,2 are blue.

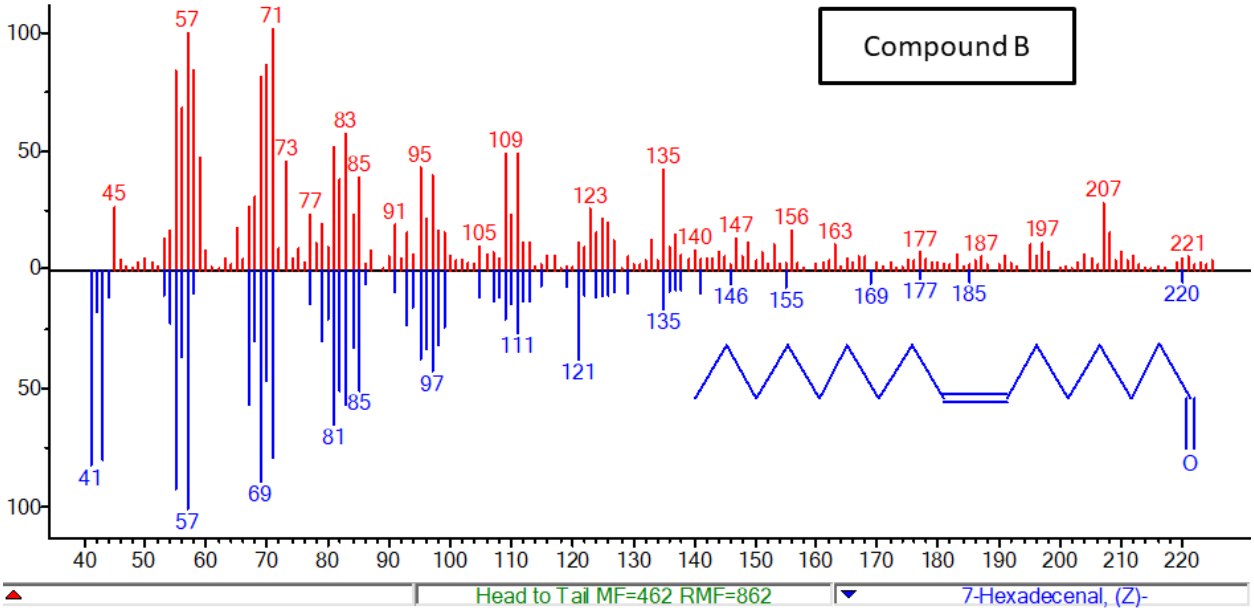

Figure 3.34: Suggested match for compound B based on MS spectrum comparison in NIST 14 database. The MS fragments of the unknown metabolite are in red and the MS fragments for 7-hexadecenal are in blue.

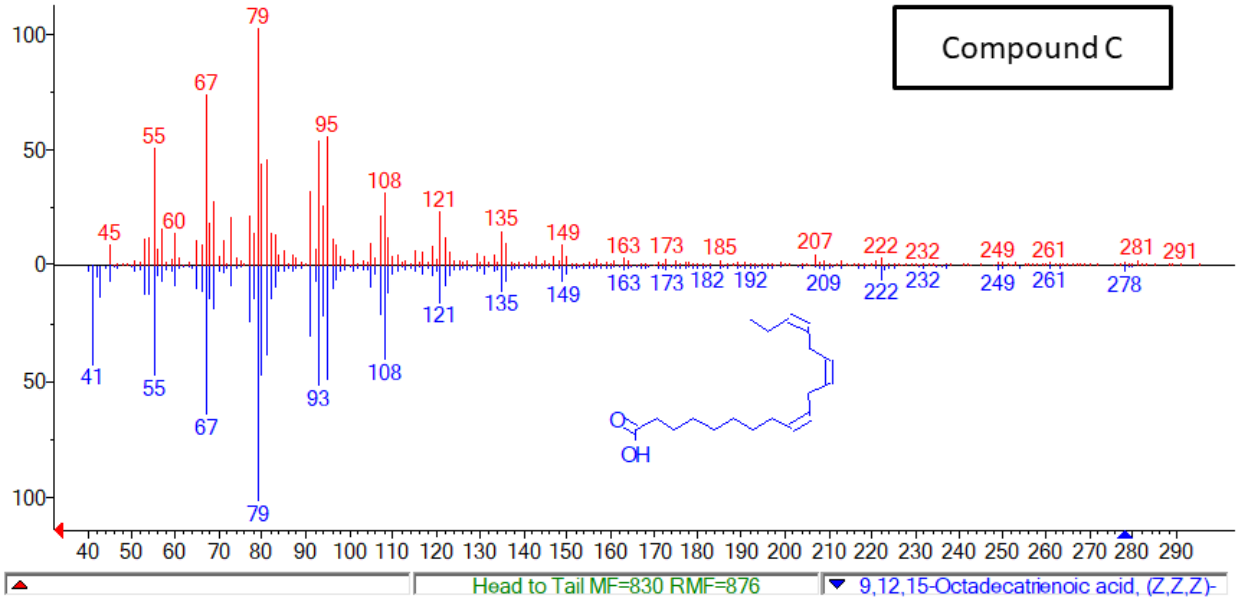

Figure 3.35: Suggested match for compound C based on MS spectrum comparison in NIST 14 database. The MS fragments of the unknown metabolite are in red and the MS fragments for 9,12,15-octadecatrienoic acid are in blue.

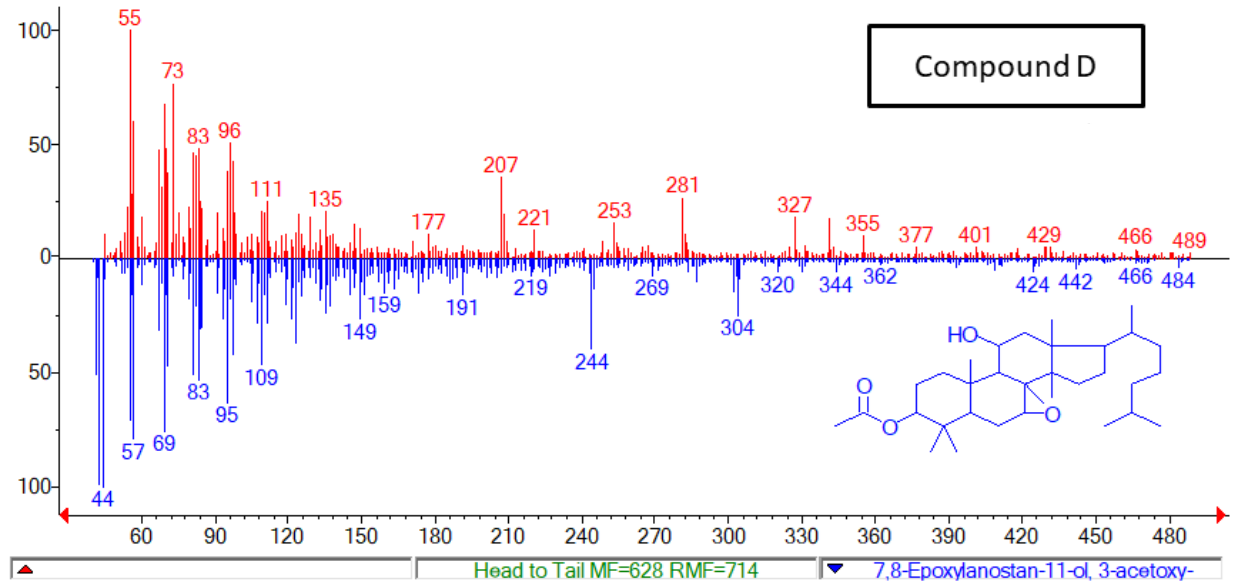

Figure 3.36: Suggested match for compound D based on MS spectrum comparison in NIST 14 database. The MS fragments of the unknown metabolite are in red and the MS fragments for 7,8-epoxylanostan-11-ol-acetoxy are in blue.

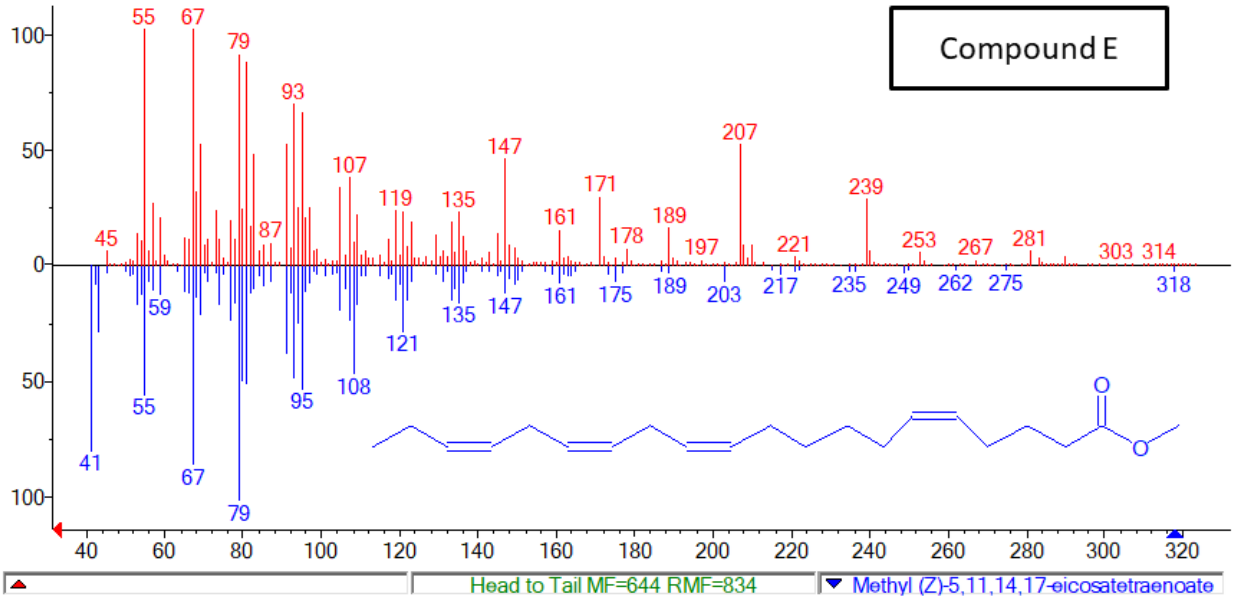

Figure 3.37: Suggested match for compound E based on MS spectrum comparison in NIST 14 database. The MS fragments of the unknown metabolite are in red and the MS fragments for methyl-5,11,14,17-eicosatetraenoate are in blue.

3.5 Discussion

This study assessed the efficacy of metabolomical analyses techniques, NMR and GCMS in the diagnosis of grey leaf spot caused by *C. zeina.* The study was done by analysing the metabolome of GLS symptomatic maize leaves from a field trial and inoculated leaves from a glasshouse trial, with their respective controls. The field trial provided two sets of symptomatic leaf samples, i.e., chlorotic spots and mature lesions. From the glasshouse trial only samples depicting mature lesions were collected for analysis. These would allow the analysis of metabolomic changes caused by grey leaf spot in the early and late stages of infection. The metabolomic fingerprint of the NMR spectra of the field trial leaves with chlorotic spots did not indicate any changes in the plant's metabolome as result of grey leaf spot. This indicates possibly that early stages of grey leaf spot infection do not induce observable changes in the metabolomic fingerprint of maize leaves with chlorotic spots. This however is inconclusive as a stronger NMR instrument might be able to detect metabolomic fingerprint changes in maize leaves during the early stages of *C. zeina* infection. It has is reported that maize leaves like many plants produce various metabolites as a form of defense at the onset of pathogen entry into the plant (Oikawa et al., 2001).

The GCMS analysis showed a single metabolite change (increased concentration in the symptomatic leaves) at retention time 27.4 mins. in the metabolomic profile of chlorotic spots leaf samples which was

named compound A. However, statistical analyses showed that the increase in compound A's concentration in these samples was not significantly different from that in the asymptomatic control samples.

Analyses of the metabolomic fingerprint of maize leaves with mature lesions using NMR analysis showed several changes in the spectra of symptomatic leaves. It was observed that certain functional groups in the NMR spectra of mature lesions leaf samples had a higher peak intensity that the healthy leaves. According to the specific functional group 1H NMR chemical shift reference chart by Gable (2019) the peak intensity differences were found in spectral regions where functional groups such as alcohols, esters, alkyl halides, alkenes and long saturated carbon chains are detected. All these functional groups can be found in maize sesquiterpenoid and diterpenoid phytoalexins e.g., zealexins, kauralexins and dolabralexins (Huffaker et al., 2011; Ding et al., 2020) (Figure 3.1), which have all been reported to play a role in maize fungal pathogen defense mechanisms.

The GCMS data of the mature lesions showed several metabolite differences between the symptomatic mature lesions and their relative controls, and these were identified as potential biomarkers. These metabolites of interest were named compounds A-D. It’s worthwhile to note that compound A was also detected in the leaf samples with chlorotic spots, thus indicating its potential significance in its association with grey leaf spot. Statistical analysis of these metabolites of interest in the mature lesions’ samples indicated that were significantly different from their relative control samples’ metabolites, except for compound C. The MS of the metabolites of interest were run through the NIST 14 database to determine the possible identity of the metabolites. The suggested metabolites from the database contained most or all the functional groups of interest detected in the NMR spectra.

The NMR spectra of the glasshouse leaf samples with mature lesions also showed several differences between the inoculated and control samples. Furthermore, a similar phenomenon was observed in the mature lesion samples of the glasshouse and field trial samples in the spectral region of 4.0-5.1 ppm. The observation made was that the NMR peaks in this region had higher intensities in the symptomatic samples than the asymptomatic (control) samples, in both trials. The chemical shifts of 3.90 – 5.05 ppm are regions where compounds containing functional groups such as alcohols, esters, alkyl halides and alkenes are detected (Gable, 2019). The GCMS analysis of the crude extracts from the glasshouse samples indicated some metabolite differences between the inoculated and uninoculated samples. The identified metabolites of interest were named compounds C and E. It is important to note that compound C was also found in the mature lesions’ samples from the field trial. Though statistical analysis deemed the

metabolite difference in the glasshouse samples as insignificant, this was the first observation of a concurring possible biomarker in both the glasshouse symptomatic samples and field trial mature lesions samples.

A similarity search in the NIST 14 database using the metabolite MS data of the identified biomarkers from the maize samples was carried out to determine the possible identities of these metabolites of interest. The database suggested that the compound A had a 63.5 % similarity to hexadecanoic acid, 1-(hydroxymethyl)-1,2-ethanediyl ester (Figure 3.44), a fatty acid ester. Despite the low similarity percentage, analyses of the MS fragmentation indicated that several mass fragments were present in both the target and database compound. This suggests that the low similarity could be attributed to the esterification of the fatty acid. Fatty acids have been reported to play a significant role in plant defense signaling mechanism (Walley et al., 2013). Studies have also indicated that levels of free fatty acids increase are triggered during early plant-microbe interactions depicting their vital role in this process (Trépanier et al., 2005). Additionally, it has been concluded that fatty acids in general play a role in impairing the growth of some plant microbial pathogens including mycelial growth and spore germination (Prost et al., 2005). A study done by Xing and Chin (2000) indicated that eggplants with increased levels of palmitoleic acid had enhanced resistance to *Verticillium dahlia*. This study indicated an enhanced level of compound A in maize leaves with chlorotic spots and mature lesions suggesting that grey leaf spot influenced the concentration increase. This suggests that this compound is involved in *C. zeina* – maize interaction. A study done by Arora and Kumar (2017) showed that hexadecanoic acid, 1-(hydroxymethyl)-1,2-ethanediyl ester isolated from *Cenchrus setigerus* (Poacea) displayed antioxidant activity *in vitro*. Another study by Kadhim et al. (2017) indicated that the same compound had antimicrobial activity. Khan and Javaid (2020) identified 1-(hydroxymethyl)-1,2-ethanediyl ester in *Trichoderma pseudokoningii*, a fungal biocontrol against various fungal pathogens. Since compound A share some chemical similarities to this compound, a possible explanation is that its production in maize was upregulated possibly in response to *C. zeina* infection. Since 1-(hydroxymethyl)-1,2-ethanediyl ester was also discovered in a fungus, it is possible that compound A may also be produced by the fungi hence the high concentration observation in the maize. The enhanced expression of compound A in the maize leaf samples with chlorotic spots further suggests its role in early infection of grey leaf spot. This leads to the belief that it can possibly be used in early detection of grey leaf spot in maize and provide an understanding the early mechanism of *C. zeina* in maize infection.

Based on the NIST 14 database search, compound B had 86.3 % similarity 7-hexadecenal (Figure 3.45). Enhanced expression of compound B was observed in the field trial maize leaves with mature lesions. This suggests its involvement in the later stages of grey leaf spot infection in maize. Ethyl acetate extract of *Solenostemma arghel* containing 7-hexadecenal showed high antifungal activity against *Penicillium funiculosum*, *Penicillium jensenii* and *Candida albicans* in *vitro* (Abdel-Motaal et al., 2022). Another study done by Olanrewaju et al. (2019) showed that a methanol extract of *Polyalthia longifolia* containing 7-hexadecenal portrayed antimicrobial activity. The similarity of compound B to 7-hexadecenal possibly suggests that it has possible antimicrobial activity in maize against *C. zeina*. Furthermore, the observed increase of compound expression in the field trial leaf samples with mature lesions suggests its involvement in pathogen defense of maize.

Compound C had 87.6 % similarity to 9,12,15-octadecatrienoic acid (Figure 3.46), commonly known as alpha linolenic acid. This compound had decreased concentrations in the leaf samples with mature lesions in both the field trial and the glasshouse trial. This brought about two possibilities; perhaps the pathogen caused a decrease in the expression of the compound during infection or possibly the plant repurposed resources to produce metabolites essential for the infection process. It has been reported that plants often produce secondary metabolites only when required, to conserve resources (Erb and Kliebenstein, 2020). A key process in plant response to biotic stresses is enhanced production of variety of oxylipins (Walley et al., 2013). Oxylipins are produced by enzymatic or autoxidation of polyunsaturated fatty acids and this leads to the production of phytohormone jasmonic acid (Kachroo and Kachroo, 2009). Alpha linolenic acid released from membrane lipids is a precursor for oxylipin biosynthesis via the octadecanoid pathway (Xue et al., 2008; Lim et al., 2017).

Studies have indicated that linolenic acid along with oleic acid regulate fungal development, seed colonization and mycotoxin production by *Aspergillus* spp. (Xue et al., 2008). This was observed in *A. niduans*, which metabolises linolenic acid to a series of of sporongenic molecules known as psi factors. These psi factors regulate the ratio of asexual and sexual spores production (Calvo et al., 1999). Furthermore, linolenic acid and hydroxylinolenic acid have been reported to cause an increase in asexual spore production in *A. nidulans*, *A. parasiticus* and *A. flavus* (Calvo et al., 1999; Calvo et al., 2001). Another study by Xue et al. (2008) showed that colonization of soybean seed by *C. kikuchii* correlated with the ratio of oleic acid/linolenic acid. This leads to the plausible conclusion that compound C was possibly used by the plant to synthesize defensive oxylipins against the infection. Another possibility is that since this observation was made in the later stages of infection, i.e., mature lesions stage, compound A was used by

the pathogen to synthesize more spores for its dissemination in the leaves. It's also probable to assume that both these scenarios might have occurred simultaneously, however, this study cannot provide evidence to distinguish which is true with certainty.

Compound D was observed in the field trial maize leaves showing mature lesions and not in the control samples, suggesting it's a pathogen or infection induced metabolite. The NIST 14 database search suggested that compound D had a 71.4 % similarity to 7,8-epoxylanostan-11-ol,3-acetoxy (Figure 3.47). Previously, 7,8-epoxylanostan-11-ol,3-acetoxy was identified in the methanol crude extract of *Phyllanthus amarus*, which exhibited antimicrobial effect against *Pseudomonas aeruginosa* and *Staphylococcus aureus* (Parker et al., 2009). The compound was also identified in ethanolic extracts of *Rhus muelleri* which depicted an antimicrobial effect against *Fusarium oxysorum f. sp. lycopersici* (De Rodríguez et al., 2015). Interestingly, the same metabolite was also identified in an ethyl acetate extract of *Trichoderma pseudokoningii* (Khan and Javaid, 2020). The study by Khan and Javaid (2020) showed that *T. pseudokoningii* had an antagonistic effect against the growth of *Macrophomina phaseolina*, a soil-borne pathogen that affects various plants. It was suggested that 7,8-epoxylanostan-11-ol,3-acetoxy maybe be involved in this biocontrol effect (Khan and Javaid, 2020). Since the compound shares some similarities with 7,8-epoxylanostan-11-ol,3-acetoxy, it is possible that the observation made in the maize leaf samples from the glasshouse trial were influenced by grey leaf spot disease. It's also plausible to suggest that since compound D is found in the symptomatic samples only, it may be a pathogen metabolite released during the infection process. On the contrary, it may also be produced by the plant itself as a defense mechanism. Either way, this indicates that compound D may be a potentially significant biomarker in grey leaf spot diagnosis in maize leaves.

Compound E had an 83.4 % similarity to methyl-5,11,14,17-eicosatetraenoate (Figure 3.48). Eicosapolyenoic acids are reported to be molecules that engage in plant signaling networks involved in fungal pathogen resistance. They trigger a response cascade in plants that includes transcriptional activation of phytoalexin synthesis genes, lignification, programmed cell death, and other hypersensitive responses against pathogens (Walley et al., 2013). A study by Ahmed et al. (2022) illustrated that methanolic extracts of *Pleurospermum candollei* containing methyl-5,11,14,17-eicosatetraenoate had antimicrobial effects. Since compound E has an 83.4 % similarity to methyl-5,11,14,17-eicosatetraenoate, it perhaps elicits similar antimicrobial effects on the fungal pathogen. However, in this study it was also observed that compound E was present in low concentrations in the inoculated glasshouse maize leaves

with mature lesions. This could mean that the increased concentration observed in the field trial samples could be the result of another metabolic process and not be a result of the fungal infection.

The evidence from this study illustrates that grey leaf spot caused by *C. zeina* leaves a footprint in the metabolome of maize leaves. It alters the metabolomic fingerprint of the leaves by affecting specific metabolites within the metabolome. It possibly does this by triggering certain defensive secondary metabolites and/or inhibiting the expression of others in its path to full infection. These metabolite footprints were picked up by the metabolomic analyses techniques NMR and GCMS. Furthermore, the altered metabolites of interest shared similarities with reported secondary metabolites involved in plant defense signaling or pathogen attack mechanisms. This indicates the potential capability of these metabolites in providing clarity on the infection mechanism of grey leaf spot in maize and possibly acting as potential biomarkers in future grey leaf spot diagnosis. The differences in the metabolomic changes between the different treatments (field trial chlorotic spots and mature lesions, and the glasshouse samples with mature lesions) also provides a gateway into understanding the metabolomic changes at the different stages of infection as well as different degrees of infection. Conclusively, it was found that metabolic fingerprint and metabolomic analyses are considerably powerful tools in diagnosing and assessing grey leaf spot infection in maize caused by *C. zeina*.

3.6 References

Abdel-Motaal, F.F., Maher, Z.M., Ibrahim, S.F., El-Mleeh, A., Behery, M., Metwally, A.A., 2022. Comparative studies on the antioxidant, antifungal, and wound healing activities of *Solenostemma arghel* ethyl acetate and methanolic extracts. Appl. Sci. 12. https://doi.org/10.3390/app12094121

Ahmed, M., Khan, K.-R., Ahmad, S., Aati, H.Y., Ovatlarnporn, C., Rehman, M.S., Javed, T., Khursheed, A., Ghalloo, B.A., Dilshad, R., Anwar, M., 2022. Comprehensive phytochemical profiling, biological activities, and molecular docking studies of *Pleurospermum candollei*: An insight into potential for natural products development. Molecules 27, 4113. https://doi.org/10.3390/molecules27134113

Ahuja, I., Kissen, R., Bones, A.M., 2012. Phytoalexins in defense against pathogens. Trends Plant Sci. 17, 73–90. https://doi.org/10.1016/J.TPLANTS.2011.11.002

Arora, S., Kumar, G., 2017. Gas chromatography-mass spectrometry (GC-MS) determination of bioactive constituents from the methanolic and ethyl acetate extract of *Cenchrus setigerus* Vahl (Poaceae) 6, 635–640.

Calvo, A.M., Gardner, H.W., Keller, N.P., 2001. Genetic connection between fatty acid metabolism and sporulation in *Aspergillus nidulans*. J. Biol. Chem. 276, 25766–25774. https://doi.org/10.1074/JBC.M100732200

Calvo, A.M., Hinze, L.L., Gardner, H.W., Keller, N.P., 1999. Sporogenic effect of polyunsaturated fatty acids on development of *Aspergillus spp*. Appl. Environ. Microbiol. 65, 3668–3673. https://doi.org/10.1128/AEM.65.8.3668-3673.1999

De Souza, L.P., Garbowicz, K., Brotman, Y., Tohge, T., Fernie, A.R., 2020. The acetate pathway supports flavonoid and lipid biosynthesis in *Arabidopsis*. Plant Physiol. 182, 857–869. https://doi.org/10.1104/PP.19.00683

Ding, Y., Weckwerth, P.R., Poretsky, E., Murphy, K.M., Sims, J., Saldivar, E., Christensen, S.A., Char, S.N., Yang, B., Tong, A. dao, Shen, Z., Kremling, K.A., Buckler, E.S., Kono, T., Nelson, D.R., Bohlmann, J., Bakker, M.G., Vaughan, M.M., Khalil, A.S., Betsiashvili, M., Dressano, K., Köllner, T.G., Briggs, S.P., Zerbe, P., Schmelz, E.A., Huffaker, A., 2020. Genetic elucidation of interconnected antibiotic pathways mediating maize innate immunity. Nat. plants 6, 1375–1388. https://doi.org/10.1038/S41477-020-00787-9

Doehlemann, G., Wahl, R., Horst, R.J., Voll, L.M., Usadel, B., Poree, F., Stitt, M., Pons-Kühnemann, J., Sonnewald, U., Kahmann, R., Kämper, J., 2008. Reprogramming a maize plant: transcriptional and metabolic changes induced by the fungal biotroph *Ustilago maydis*. Plant J. 56, 181–195. https://doi.org/10.1111/J.1365-313X.2008.03590.X

Erb, M., Kliebenstein, D.J., 2020. Plant secondary metabolites as defenses, regulators, and primary metabolites: The blurred functional trichotomy. Plant Physiol. 184, 39–52. https://doi.org/10.1104/PP.20.00433

Gable, K., 2019. 1H NMR chemical shift [WWW Document]. URL https://sites.science.oregonstate.edu/~gablek/CH335/Chapter10/ChemicalShift.htm (accessed 2.28.22).

Huffaker, A., Kaplan, F., Vaughan, M.M., Dafoe, N.J., Ni, X., Rocca, J.R., Alborn, H.T., Teal, P.E.A., Schmelz, E.A., 2011a. Novel acidic sesquiterpenoids constitute a dominant class of pathogen-induced phytoalexins in maize. Plant Physiol. 156, 2082–2097. https://doi.org/10.1104/pp.111.179457

Huffaker, A., Kaplan, F., Vaughan, M.M., Dafoe, N.J., Ni, X., Rocca, J.R., Alborn, H.T., Teal, P.E.A., Schmelz, E.A., 2011b. Novel acidic sesquiterpenoids constitute a dominant class of pathogen-induced phytoalexins in maize. Plant Physiol. 156, 2082. https://doi.org/10.1104/PP.111.179457

Jasso de Rodríguez, D., Trejo-González, F.A., Rodríguez-García, R., Díaz-Jimenez, M.L.V., Sáenz-Galindo, A., Hernández-Castillo, F.D., Villarreal-Quintanilla, J.A., Peña-Ramos, F.M., 2015. Antifungal activity in vitro of *Rhus muelleri* against *Fusarium oxysporum* f. sp. lycopersici. Ind. Crops Prod. 75, 150–158. https://doi.org/10.1016/J.INDCROP.2015.05.048

Jeandet, P., Hébrard, C., Deville, M.A., Cordelier, S., Dorey, S., Aziz, A., Crouzet, J., 2014. Deciphering the role of phytoalexins in plant-microorganism interactions and human health. Molecules 19, 18033. https://doi.org/10.3390/MOLECULES191118033

Kachroo, A., Kachroo, P., 2009. Fatty acid-derived signals in plant defense. Annu. Rev. Phytopathol. 47, 153–176. https://doi.org/10.1146/ANNUREV-PHYTO-080508-081820

Kadhim, M.J., Al-rubaye, A.F., Hameed, I.H., 2017. Determination of bioactive compounds of methanolic extract of *Vitis vinifera* determination of bioactive compounds of methanolic extract of *Vitis vinifera* using GC-MS. Int. J. Toxicol. Pharmacol. Res. 9, 113–126. https://doi.org/10.25258/ijtpr.v9i02.9047

Khan, I.H., Javaid, A., 2020. In *vitro* biocontrol potential of *Trichoderma pseudokoningii* against *Macrophomina phaseolina* . Artic. Int. J. Agric. Biol. https://doi.org/10.17957/IJAB/15.1494

Kodama, O., Miyakawa, J., Akatsuka, T., Kiyosawa, S., 1992. Sakuranetin, a flavanone phytoalexin from

ultraviolet-irradiated rice leaves. Phytochemistry 31, 3807–3809. https://doi.org/10.1016/S0031-9422(00)97532-0

Lim, G.H., Singhal, R., Kachroo, A., Kachroo, P., 2017. Fatty acid– and lipid-mediated signaling in plant defense. https://doi.org/10.1146/annurev-phyto-080516-035406 55, 505–536. https://doi.org/10.1146/ANNUREV-PHYTO-080516-035406

McMullen, M.D., Kresovich, S., Villeda, H.S., Bradbury, P., Li, H., Sun, Q., Flint-Garcia, S., Thornsberry, J., Acharya, C., Bottoms, C., Brown, P., Browne, C., Eller, M., Guill, K., Harjes, C., Kroon, D., Lepak, N., Mitchell, S.E., Peterson, B., Pressoir, G., Romero, S., Rosas, M.O., Salvo, S., Yates, H., Hanson, M., Jones, E., Smith, S., Glaubitz, J.C., Goodman, M., Ware, D., Holland, J.B., Buckler, E.S., 2009. Genetic properties of the maize nested association mapping population. Science 325, 737–740. https://doi.org/10.1126/SCIENCE.1174320

Meisel, B., Korsman, J., Kloppers, F.J., Berger, D.K., 2009. *Cercospora zeina* is the causal agent of grey leaf spot disease of maize in southern Africa. Eur. J. Plant Pathol. 124, 577–583. https://doi.org/10.1007/s10658-009-9443-1

Meyer, J., Berger, D.K., Christensen, S.A., Murray, S.L., 2017. RNA-Seq analysis of resistant and susceptible sub-tropical maize lines reveals a role for kauralexins in resistance to grey leaf spot disease , caused by Cercospora zeina 1–20. https://doi.org/10.1186/s12870-017-1137-9

Oikawa, A., Ishihara, A., Hasegawa, M., Kodama, O., Iwamura, H., 2001. Induced accumulation of 2-hydroxy-4,7-dimethoxy-1,4-benzoxazin-3-one glucoside (HDMBOA-Glc) in maize leaves. Phytochemistry 56, 669–675. https://doi.org/10.1016/S0031-9422(00)00494-5

Olanrewaju, I.O., Mordi, R.C., Echeme, J.O., Bolade, O.P., Bashir, M., Ekwuribe, S., Ayo-Ajayi, J.I., 2019. In *vitro* anti-microbial studies and GC/MS analysis of the leaf extract and fractions of *Polyalthia longifolia* (Engl. & Diels) Verde. https://doi.org/10.1088/1742-6596/1299/1/012087

Park, H.L., Yoo, Y., Hahn, T.R., Bhoo, S.H., Lee, S.W., Cho, M.H., 2014. Antimicrobial activity of UV-induced phenylamides from rice leaves. Molecules 19, 18139–18151. https://doi.org/10.3390/MOLECULES191118139

Parker, D., Beckmann, M., Zubair, H., Enot, D.P., Caracuel-Rios, Z., Overy, D.P., Snowdon, S., Talbot, N.J., Draper, J., 2009. Metabolomic analysis reveals a common pattern of metabolic re-programming during invasion of three host plant species by *Magnaporthe grisea*. Plant J. 59, 723–737. https://doi.org/10.1111/j.1365-313X.2009.03912.x

Pechanova, O., Pechan, T., 2015. Maize-Pathogen Interactions: An ongoing combat from a proteomics perspective. Int. J. Mol. Sci. 16, 28429. https://doi.org/10.3390/IJMS161226106

Prost, I., Dhondt, S., Rothe, G., Vicente, J., Rodriguez, M.J., Kift, N., Carbonne, F., Griffiths, G., Esquerré-Tugayé, M.T., Rosahl, S., Castresana, C., Hamberg, M., Fournier, J., 2005. Evaluation of the antimicrobial activities of plant oxylipins supports their involvement in defense against pathogens. Plant Physiol. 139, 1902–1913. https://doi.org/10.1104/PP.105.066274

Robertson, A., Mueller, D., 2007. Before applying fungicides to corn: Stop! Look! Consider! | Integrated crop management [WWW Document]. URL https://crops.extension.iastate.edu/encyclopedia/applying-fungicides-corn-stop-look-consider (accessed 5.26.22).

Sardans, J., Gargallo-Garriga, A., Urban, O., Klem, K., Walker, T.W.N., Holub, P., Janssens, I.A., Peñuelas,

J., 2020. Ecometabolomics for a better understanding of plant responses and acclimation to abiotic factors linked to global change. Metabolites 10, 1–20. https://doi.org/10.3390/METABO10060239

Schmelz, E.A., Huffaker, A., Sims, J.W., Christensen, S.A., Lu, X., Okada, K., Peters, R.J., 2014. Biosynthesis, elicitation and roles of monocot terpenoid phytoalexins. Plant J. 79, 659–678. https://doi.org/10.1111/TPJ.12436

Schmelz, E.A., Kaplan, F., Huffaker, A., Dafoe, N.J., Vaughan, M.M., Ni, X., Rocca, J.R., Alborn, H.T., Teal, P.E., 2011. Identity, regulation, and activity of inducible diterpenoid phytoalexins in maize. Proc. Natl. Acad. Sci. U. S. A. 108, 5455–5460. https://doi.org/10.1073/PNAS.1014714108/SUPPL_FILE/ST03.PDF

Trépanier, M., Bécard, G., Moutoglis, P., Willemot, C., Gagné, S., Avis, T.J., Rioux, J.A., 2005. Dependence of arbuscular-mycorrhizal fungi on their plant host for palmitic acid synthesis. Appl. Environ. Microbiol. 71, 5341–5347. https://doi.org/10.1128/AEM.71.9.5341-5347.2005

Triba, M.N., Le Moyec, L., Amathieu, R., Goossens, C., Bouchemal, N., Nahon, P., Rutledge, D.N., Savarin, P., 2015. PLS/OPLS models in metabolomics: the impact of permutation of dataset rows on the K-fold cross-validation quality parameters †. Mol. BioSyst 11, 13. https://doi.org/10.1039/c4mb00414k

Ube, N., Katsuyama, Y., Kariya, K., Tebayashi, S. ichi, Sue, M., Tohnooka, T., Ueno, K., Taketa, S., Ishihara, A., 2021. Identification of methoxylchalcones produced in response to CuCl2 treatment and pathogen infection in barley. Phytochemistry 184. https://doi.org/10.1016/J.PHYTOCHEM.2020.112650

Walley, J.W., Kliebenstein, D.J., Bostock, R.M., Dehesh, K., 2013. Fatty acids and early detection of pathogens. Curr. Opin. Plant Biol. 16, 520–526. https://doi.org/10.1016/J.PBI.2013.06.011

Xing, J., Chin, C.K., 2000. Modification of fatty acids in eggplant affects its resistance to Verticilliumdahliae. Physiol. Mol. Plant Pathol. 56, 217–225. https://doi.org/10.1006/PMPP.2000.0268

Xue, H.Q., Upchurch, R.G., Kwanyuen, P., 2008. Relationships between oleic and linoleic acid content and seed colonization by *Cercospora kikuchii* and *Diaporthe phaseolorum*. Plant Dis. 92, 1038–1042. https://doi.org/10.1094/PDIS-92-7-1038

4. The Use of Metabolomical Analyses To Diagnose The Effect of Fumonisin-Producing *Fusarium Verticillioides* On *Vigna Unguiculata* (Cowpea)

4.1 Introduction

Cowpea (*Vigna unguiculata* (L.) Walp.) also falls victim to fumonisins produced by *Fusarium verticillioides* as indicated by Kritzinger et al. (2003) and Kotze et al. (2016). Through the production of fumonisins, the fungus can cause necrosis and systemically disrupt the functions of the plant in its early stages thus hindering the plant's proliferation (Kamle et al., 2019). Fumonisins are structural analogs of sphinganine and sphingosine which are precursors in the production of sphingolipids (Merrill et al., 2001; Zeng et al., 2020). Sphingolipids carry out an array of functions necessary for the growth and proliferation of various eukaryotic organisms (Michaelson et al., 2016). It was discovered that the disease symptoms observed in plants contaminated with fumonisins were a result of changes in the level of various bioactive lipids and related biosynthetic processes (Zeng et al., 2020). Baldwin et al. (2014) carried out a study that indicated that FB_1 produced by *F. verticilloides* in maize roots could be transported to the leaves through transpiration mediated bulk flow without the fungi colonizing the leaves, causing disruption in leaf proliferation. This implies that it is possible to observe the effect of *F. verticilloides* in the leaves without detecting the fungus itself. This brings forth a challenge in diagnosing such a pathogen as it is possible that the site of infection and site of effect are spatially separated.

Cowpea has developed means to curb and control the effect of a causative pathogen primarily using secondary metabolites. An example is by using reactive oxygen species (ROS) catalysed by the enzyme peroxidase (Bhagat and Chakraborty, 1970). ROS oxidises hydroxy cinnamyl alcohols into free radical intermediates that play various roles in directly or indirectly reducing fungal pathogen viability and spread in cowpea (Passardi et al., 2005). A study done by Nandi et al. (2013) on the biochemical responses of cowpea infected with *Sclerotium rofsii* indicated an increase in peroxidase activity three days post

inoculation. It also showed enhanced activity of polyphenol oxidase, which produces polyphenols and quinones that inhibit the activity of the pathogen's extracellular enzymes and triggers signals for the adjacent unaffected cells (Nandi et al., 2013). It has been reported that peroxidases and polyphenol oxidases play a vital role in strengthening the cell wall barrier thus restricting pathogen entry into the plant cells (Bruce and West, 1989).

Phenyl ammonia lyase, which is involved in phenyl propanoid metabolism is used by cowpea in the production of flavonoid phytoalexins, which they use as antimicrobial molecules (Nandi et al., 2013). Xue et al. (1998) reported that in an effort to resist *Rhizoctonia* sp. infection, bean (*Phaseolus vulgaris* L.) plants produce pathogenenesis related proteins of β-1,3-glucanases and chitinases involved in the hydrolysis of β-1,3-glucans, and chitin respectively, which are vital components of fungal cell walls. Nandi et al. (2013) also observed an enhanced activity of these two enzymes in cowpea inoculated with *S. rofsii*.

The metabolomic changes of cowpea due to soil-borne pathogens have not been significantly explored. Kotze et al. (2016) showed that fumonisins produced by *F. verticillioides* have a significant impact on the growth and development of cowpea. However, little information is available on the specific metabolomic changes to the various parts of the plant. It has already been reported that both fumonisins and *F. verticillioides* conidia can translocate from the roots and elicit their effect in the leaves (Baldwin et al., 2014). This study aims to build on the work done by Kotze et al. (2016) by assessing the metabolomical changes that occur in cowpea leaves due to fumonisin-producing *F. verticillioides*, to better understand the negative effect on plant growth and development.

4.2 Aim

The aim of this study was to determine if metabolomical analyses can be used in diagnosing a systemic effect in cowpea after inoculation with a fumonisin-producing *Fusarium verticillioides* isolate. This was done by artificially inoculating the seeds and analysing the metabolomic profile of the leaves. The latter was achieved by imploring two main strategies i.e., metabolomic fingerprinting using Nuclear Magnetic Resonance (NMR) analysis and biomarker target analyses using Gas Chromatography coupled with Mass Spectrometry (GCMS). The objectives were to identify any metabolic changes that may occur in the cowpea leaf metabolome due to the infection and to identify potential biomarker metabolites that may be uniquely associated with *F. verticillioides* infection in cowpea. This would provide a gateway to understanding the systemic effect of fumonisins in cowpea leaves and possibly assist in early diagnosis leading to the development of early control measures.

4.3 Materials and Methods

4.3.1 Cowpea Phytotron Trial

Cowpea seeds (Bets Wit cultivar) were obtained from Barenbrug South Africa (Pty) Ltd, Pyramid, Pretoria, South Africa. *Fusarium verticillioides* strain MRC 8265 (Gelderblom et al., 1988) was sub-cultured from 15% glycerol stocks stored at -80 °C. This strain is known to produce fumonisins. The stocks were transferred aseptically onto Petri dishes containing potato carrot agar (PCA) and incubated in the dark at 25 °C for a period of 14 days. Thereafter, further subculturing was carried out to bulk up the pathogen and the Petri dishes were also incubated. Sterilized 0.02 % Tween solution was added to four-week-old cultures and a laboratory "hockey stick" was used to detach the conidia into the solution. The resultant conidial suspension was transferred to a 50 ml falcon tube. The conidial suspensions were adjusted to a concentration of $1x10^6$ conidia/ml using a haemocytometer.

Seed treatment was carried out according to the protocol by Kotze et al. (2016). Cowpea seeds were surface disinfected in 1% sodium hypochlorite, rinsed thrice with sterile distilled water and left to dry on a sterile paper towel in a laminar floor for 10 mins. The dried seeds were imbibed in the *F. verticillioides* conidia suspension using a disinfected falcon tube for 4 hrs and placed on a sterile paper towel in the laminar floor to dry for 10 mins. The control seeds were imbibed in 0.02 % Tween solution alone for the same duration and dried along with the inoculated seeds. The dried seeds were planted in plastic pots (10 cm diameter and 8.5 cm height) containing sterilized University of Pretoria obtained compost soil, . The inoculated and control samples comprised of six replicates with three seeds in each pot (6 pots x 3 seeds each). The pots were placed in a phytotron at the Plant Sciences Complex, in the Department of Plant and Soil Science set to 25 °C with a 16 hr light and 8 hr dark cycle at 80 % humidity.

Some seedlings were thinned, and the remainder were left to grow in the phytotron, where they were watered every two days until run off to keep the soil moist. Throughout the growth period several morphological observations such as germination rate, leaf size and colour were made. Approximately 10 weeks after planting all the leaves from each plant (both inoculated and control) were collected, placed in a brown bag and frozen over night at -80 °C. Thereafter, the frozen leaves were placed in a Virtis freeze-drier (SP Scientific, USA) in order to remove all the moisture. Freeze-dried material was then used for subsequent metabolite extraction and analyses.

4.3.2 Metabolite Extraction

The dried cowpea leaves were placed in a Büchi E-916 speed-extractor (Büchi E-916, Switzerland) for crude metabolite extraction using distilled methanol. The extraction parameters were set as follows: Dried

cowpea leaves were placed in 10 ml stainless steel tubes; the pressure set at 100 bar and temperature at 50 ^{o}C. Each extraction consisted of four cycles, with each one consisting of a 1 min heating phase, 9 mins solvent holding phase, and a discharge phase of 5 mins. A nitrogen gas purge was performed for 8 min at the end and the total extraction time was 1 hr and 32 mins. The extracts were dried using a Büchi Genevac (EZ-2 plus, England) at 40 ^{o}C, using the methanol protocol and dry extract masses were obtained. The chemical analyses techniques implored for analysing the metabolomic changes due *to F. verticillioides* were GCMS and NMR.

4.3.3 ^{1}H Nuclear Magnetic Resonance (NMR) Analysis

The cowpea leaf crude extracts from inoculated and uninoculated treatments were subjected to proton NMR (^{1}H NMR) analysis using an Oxford 200 MHz NMR instrument (Varian Incorporated, USA). This was done to analyse the cowpea leaves' metabolic fingerprint and metabolomical changes due to *F. verticillioides* infection and possible fumonisin contamination. A solution of 25 mg/ml was prepared from the crude extract using 80 % deuterated methanol and 20 % potassium phosphate buffer. Maleic acid (2 mg) was used as an internal standard. From the solution, 700 µl were transferred to a clean NMR glass tube which was placed in the NMR machine. The NMR parameters were set as follows: 512 scans were carried out on the sample consisting of 11 976 data points, an acquisition time of 2 seconds per scan and manual magnetic shimming was done for each individual sample. The obtained sample spectra were processed, analysed and compared using MestReNova (Mnova) version 14 (Mestrelab Research, Spain). The spectra's numerical data was exported to SIMCA-P version 14.1 (Sartorius Stedim Data Analytics AB, Sweden) for multivariate statistical analysis. Multivariate analysis provided principal component analysis plot (PCA) and orthogonal projection to latent structures discriminant analysis (OPLS-DA). PCA plots provide unsupervised data comparison of all samples while OPLS-DA plots provide supervised or sample group comparisons. This was done to establish a correlation between systemic *F. verticillioides* infection and observed cowpea metabolomic changes.

4.3.4 Gas Chromatography Mass Spectrometry (GCMS) Analysis

Cowpea leaf crude extracts from inoculated and uninoculated treatments were subjected to GCMS analysis in a Shimadzu GCMS-QP2010 SE instrument (Shimadzu Corporation, Japan). This was done to analyse the cowpea metabolic and metabolomic profile post *F. verticillioides* inoculation. These analyses were also aimed at identifying individual volatile metabolites' concentration change in cowpea due to *F. verticillioides* inoculation that can be used as potential biomarkers for infection diagnosis.

A solution of 1 mg/ml was prepared from the crude extract using distilled methanol and 1 ml was transferred to a GCMS glass vial. The samples were loaded on to the column using an AOC-20i+s auto-sampler. Compounds were separated in a Rtx- 5MS capillary column with dimensions of 29.3 m x 0.26 µm and a thickness of 0.25 µm. Splitless injections of 1 µl were preformed using an AOC-20i+s and the temperature for both the injector and detector were set at 270 °C. The oven was programmed at an initial temperature of 50 °C which was held for 2 min and thereafter the temperature was increased to 300 °C at a rate of 10 °C per min and it was held for 5 min making the total run time 32 min.

The acquisition for mass spectra was set at a mass range of 50.0 to 600.0 m/z. The chromatograms were analysed using the Shimadzu post-run analysis software and Mnova. Multivariate statistical analysis was also carried out in SIMCA-P. This was done to establish a correlation between systemic *F. verticillioides* infection and observed cowpea metabolomic changes. Numerical data of key metabolites identified as potential biomarkers from the chromatogram were exported to Microsoft Excel (Microsoft Corporation, USA) for further statistical analysis.

4.4 Results

4.4.1 Effect of Artificial Inoculation of Cowpea Seed with *F. Verticillioides* on Emergence and Growth.

All the seeds emerged around the same time thus no definitive correlation could be associated between *F. verticillioides* inoculation and rate of emergence. Once emerged, the cowpea seedlings were left to proliferate under observation for any further distinguishable phenotypic symptoms. The initial difference observed approximately 21 dap was that the inoculated seedlings had smaller leaves. This symptomatic trait became more noticeable at V5 growth stage (five fully emerged leaf pairs with leaf collars). Furthermore, around 42 dap the inoculated seedlings appeared to portray stunted growth when compared to the control plants. This became more and more evident as the growth progressed until the trial was concluded 10 weeks after planting. This led to a generalized possible conclusion that *F. verticillioides* seed inoculation does affect cowpea growth by prohibiting plant foliar and apical growth as highlighted in Figure 4.1. Moreover, after drying the leaves in the freeze drier, the dry mass recorded indicated that the average mass of inoculated leaf samples was lower than the dry mass of the control leaf samples (Table 1 and Figure 4.2). However, statistical analysis showed that the dry mass difference between the samples was not significant.

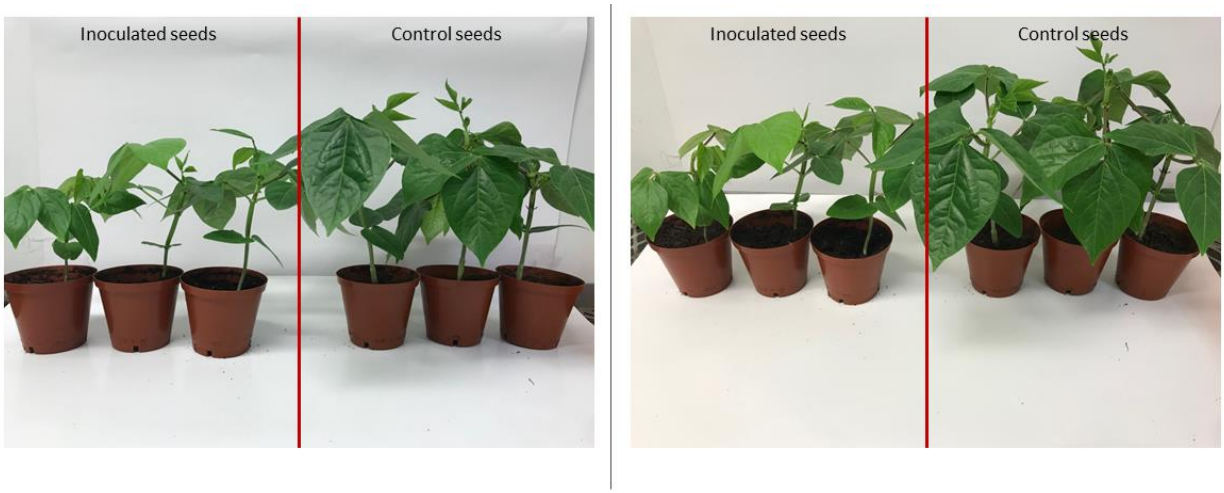

Figure 4.1: Cowpea plants showing the growth differences between the plants from seeds inoculated with F. verticillioides and control plants at 42 dap.

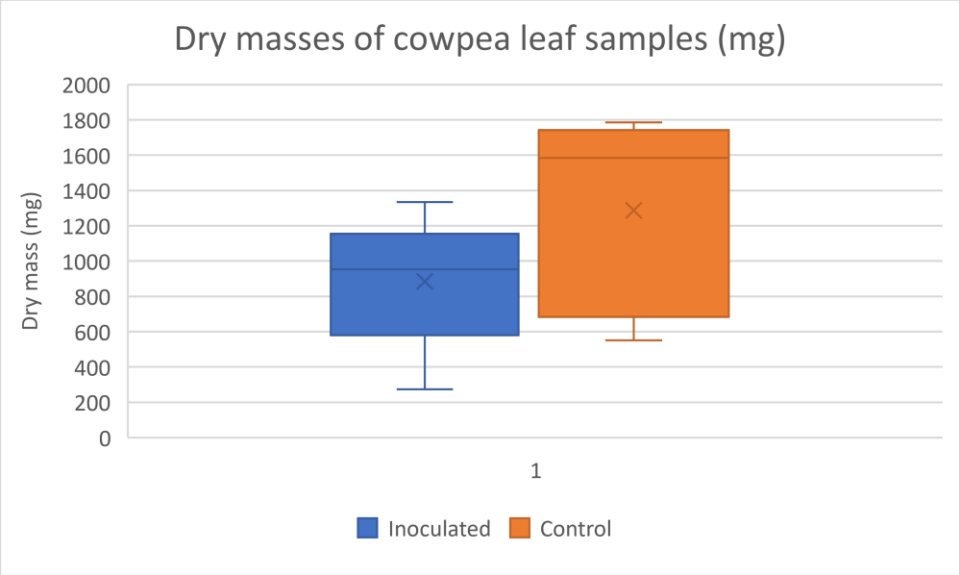

Average mass **(inoculated) = 884.76 mg**

Average mass **(control) = 1286.38 mg**

α = 0.05

p > 0.05

Figure 4.2: Dry mass of all cowpea leaf samples and the accompanying mass average for inoculated plants and the control (uninoculated) plants.

Table 4.1: Dry masses and metabolite extract masses of cowpea plants from seeds inoculated with *F. verticillioides* and their accompanying controls.

Cowpea Sample	Dry Mass (mg)	Extract Mass (mg)
Inoculated 1	273.6	82.5
Inoculated 2	953.0	224.7
Inoculated 3	1333.2	973.1
Inoculated 4	716.5	169.5
Inoculated 5	887.5	259.0
Control 1	550.4	149.4
Control 2	814.6	258.8
Control 3	1785.6	374.4
Control 4	1583.7	412.8
Control 5	1697.6	358.4

4.4.2 ^{1}H Nuclear Magnetic Resonance (NMR) Results

The leaf extracts were analysed on a ^{1}H NMR to assess the possible systemic effect of *F. verticillioides* infection on the cowpea metabolomic fingerprint. NMR spectra comparison was done in Mnova by stacking the treated and control samples' spectra. The spectra did not show any definitive differences between the inoculated and control samples (Figure 4.3). This observation suggests that cowpea seed inoculation with *F. verticillioides* had little to no influence on the metabolomic fingerprint of cowpea leaves according to NMR analysis, which is much less sensitive than GCMS analysis. The cowpea leaf extracts NMR spectra's numerical data was obtained (binned) and subjected to multivariate statistical analysis to establish a possible correlation between *F. verticillioides* inoculation and a metabolomic change in cowpea leaves. The unsupervised PCA score plot in Figure 4.4 (A) showed no clear separation between the samples. Though statistical values of the PCA plot (Q2 and R2) were good, the lack of separation between the sample sets led to an inconclusive resolve in determining the implications of *F. verticillioides* on the cowpea leaf metabolome. Furthermore, the supervised OPLS-DA plot (Figure 4.4 B) which accounts for the two sample groups, also showed no separation between the inoculated and the control samples. The negative Q2 statistical value further cements the suggestion that the leaf metabolome did not provide a definitive indication of the impact *F. verticillioides* has on cowpea, as determined by ^{1}H NMR analysis.

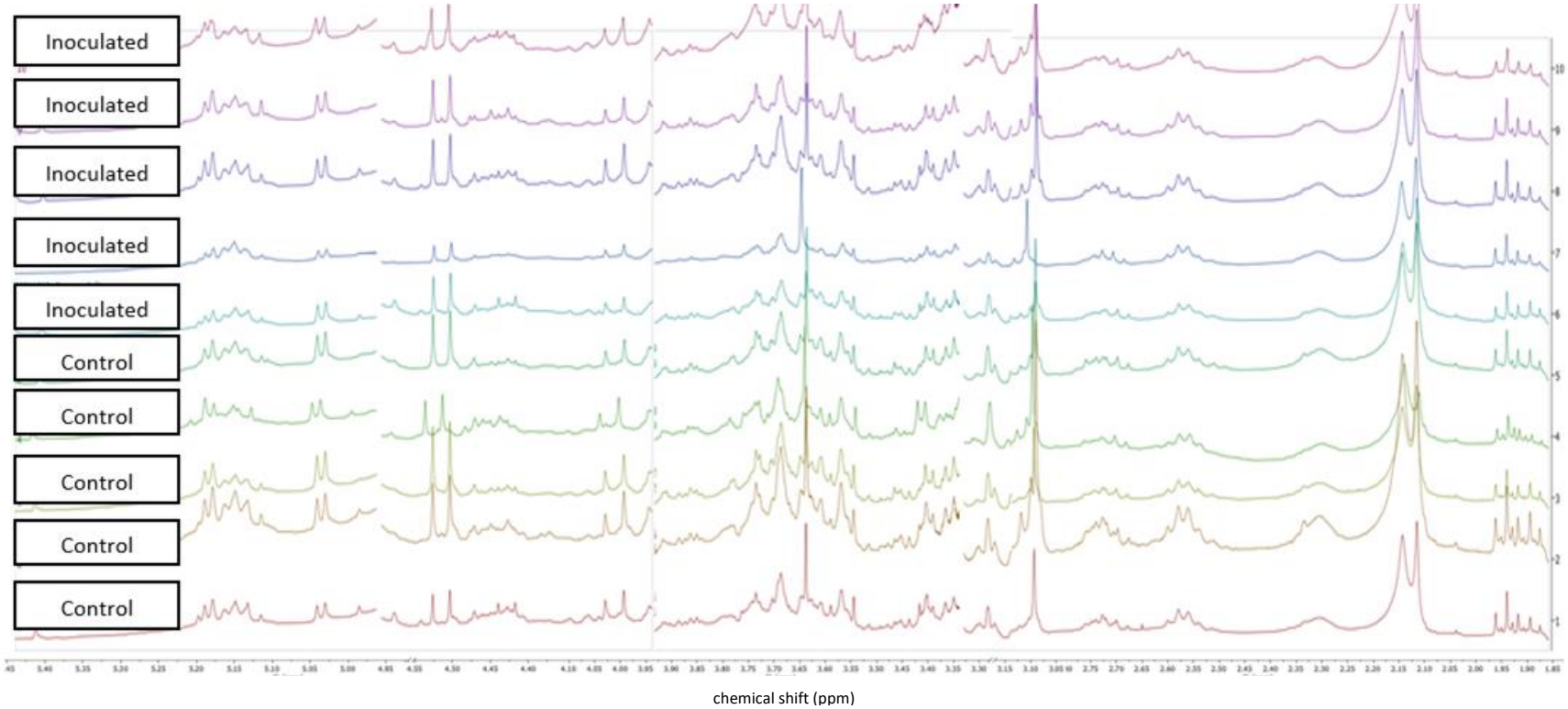

Figure 4.3: Stacked ^{1}H NMR spectra of cowpea leaf extracts from cowpea seeds inoculated with F. verticillioides and accompanying control samples. No definitive spectra differences were observed between the two sets of samples. The solvent (methanol) and internal standard (maleic acid) peaks were removed from the NMR spectra.

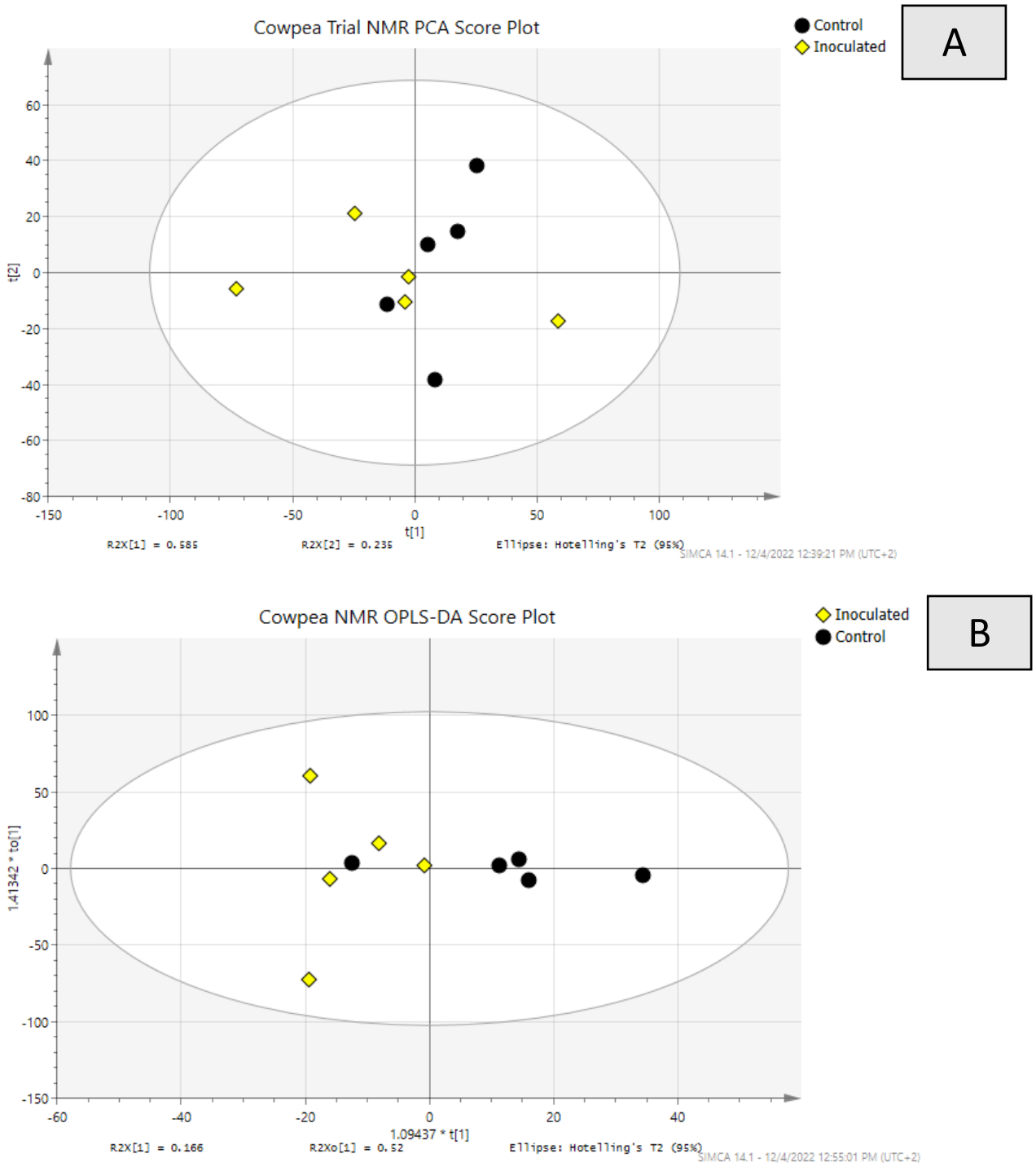

Figure 4.4: (A) 1H NMR PCA score plot of cowpea leaf extracts from cowpea seeds inoculated with F. verticillioides and accompanying controls. No definitive separation between the two sample sets. Multivariate statistical values: Q2 = 0.65; R2X = 0.82. (B) 1H NMR OPLS-DA Score plot of cowpea leaf extracts from cowpea seeds inoculated with F. verticillioides and accompanying controls. No definitive separation between the two sample sets. Multivariate statistical values: Q2 = -0.49; R2X = 0.69, R2Y = 0.54.

4.4.3 Gas Chromatography Mass Spectrometry (GCMS) Results

The cowpea crude leaf extracts were also subjected to GCMS analysis to assess the effect of *F. verticillioides* on individual metabolites in cowpea leaves. This would potentially lead to the identification of infection related biomarkers that may be used in future *F. verticillioides* infection diagnosis.

The chromatograms of all samples of leaves inoculated *with F. verticillioides* were stacked for comparison in Mnova (Figure 4.5). Several metabolite differences were observed between the two sample sets. The first metabolite difference was observed at retention time 27.35 mins. The peak intensity of the metabolite was observed to be higher in the inoculated samples as shown in Figure 4.6. Statistical analysis of the chromatogram's numerical data (Figure 4.7) indicated a significant increase in the concentration of this compound in the inoculated samples. This metabolite was named **Metabolite A**, due to the identity being unknown.

Another distinguishing observation in the chromatogram was observed at 29.65 mins. rt (Figure 4.8). The metabolite was present at a considerably larger concentration in the inoculated cowpea samples and in trace amounts to almost absent in the control cowpea samples. This indicated evidence of a potentially *F. verticillioides* triggered metabolite concentration increase in cowpea leaves. Statistical analysis of the numerical data indicated the margin of difference of the metabolite between the two sample sets, illustrating its significance (Figure 4.9). The metabolite obtained was named **Metabolite B**.

Subsequently, at retention time 30.95 mins another distinguishing observation was made but different from the previous observations (Figure 4.10). The specific metabolite peak intensity was considerably lower in the inoculated cowpea samples indicating a metabolite concentration decrease post inoculation. However, statistical analysis of the chromatogram numerical data indicated that the margin of difference of the metabolite between the sample sets, though considerable, was not significant (Figure 4.11). The metabolite was named **Metabolite C**.

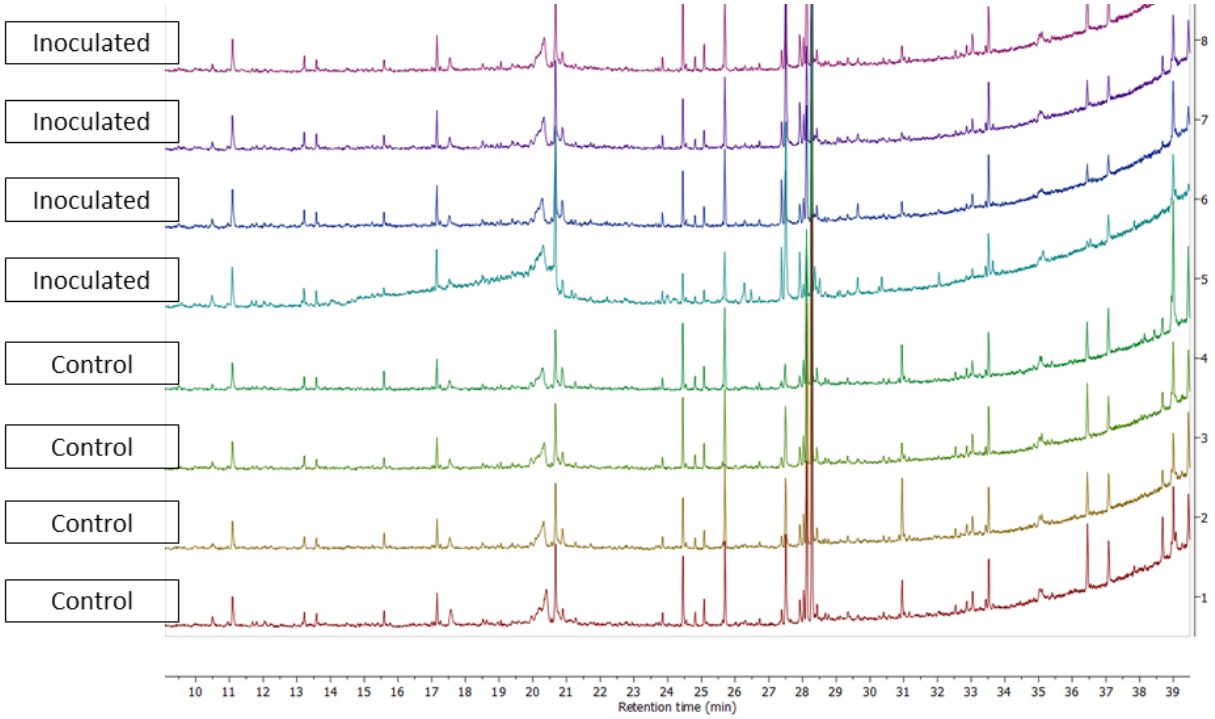

Figure 4.5: Stacked GCMS chromatograms of leaf extracts samples with chlorotic spots and their accompanying controls. At first glance, no clear definitive metabolite differences were observed in the chromatograms of the leaves with chlorotic spots and the asymptomatic controls.

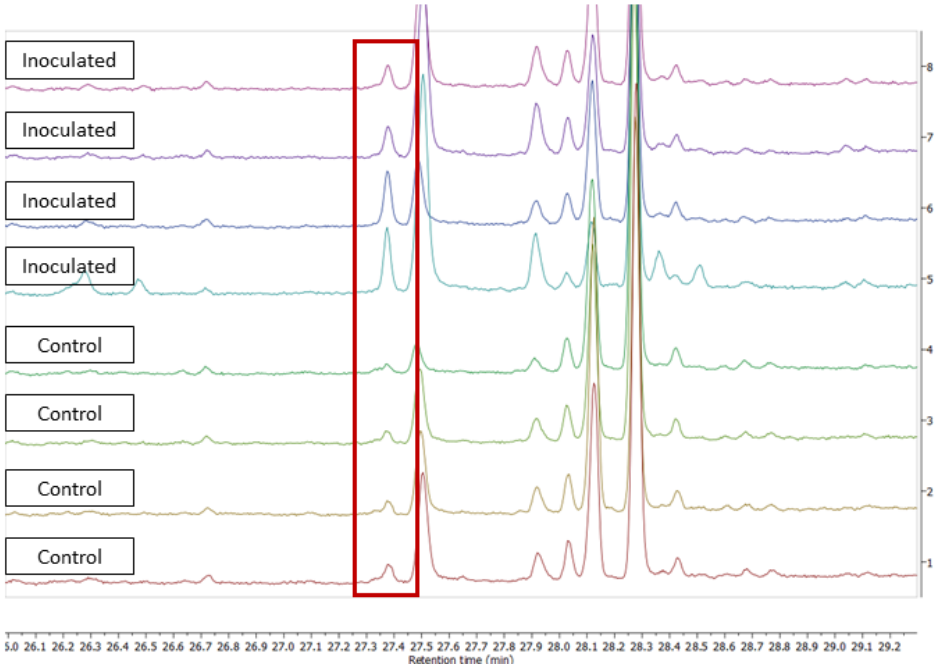

Figure 4.6: Expanded chromatogram region showing a metabolite concentration change observed in the cowpea leaf extracts from inoculated cowpea seeds at retention time 27.35 mins. (red box) identified as a potential pathogen related biomarker. The metabolite concentration (peak intensity) is higher in the inoculated samples than in the control samples.

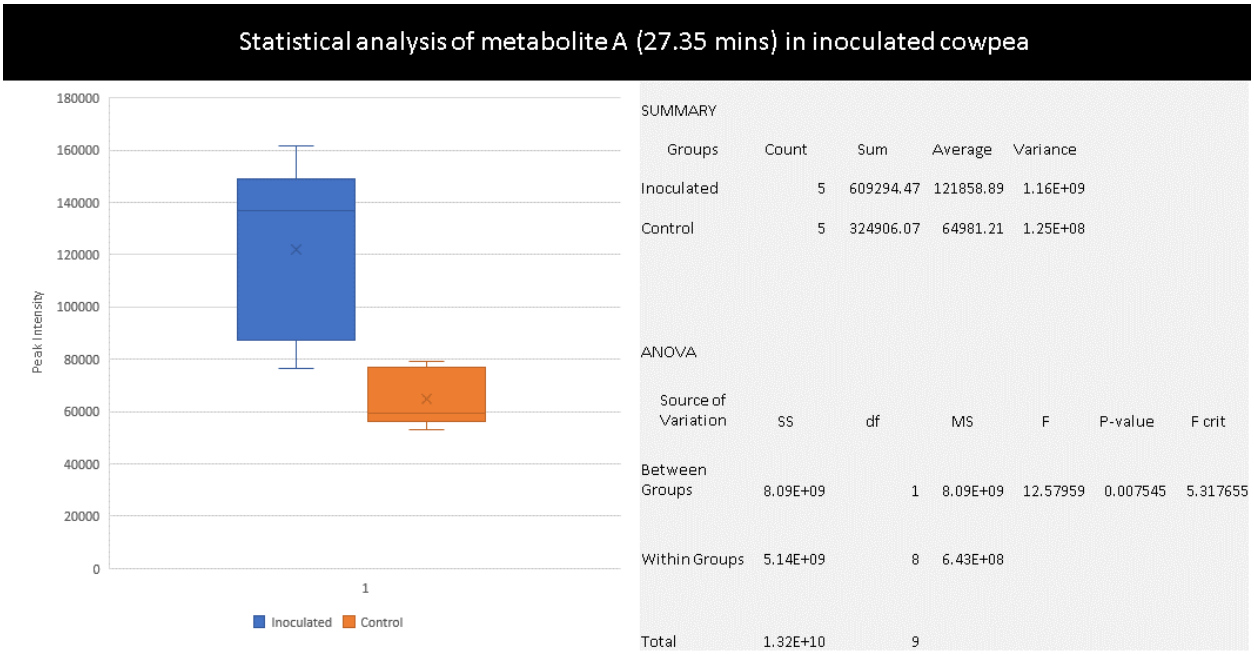

SUMMARY

Groups	Count	Sum	Average	Variance
Inoculated	5	609294.47	121858.89	1.16E+09
Control	5	324906.07	64981.21	1.25E+08

ANOVA

Source of Variation	SS	df	MS	F	P-value	F crit
Between Groups	8.09E+09	1	8.09E+09	12.57959	0.007545	5.317655
Within Groups	5.14E+09	8	6.43E+08			
Total	1.32E+10	9				

Figure 4.7: Statistical analysis of the concentration of metabolite A in the cowpea leaf extracts from inoculated cowpea seeds and their control (α = 0.05). Average metabolite concentration difference of metabolite A between the inoculated and controls was significant, p-value < 0.05.

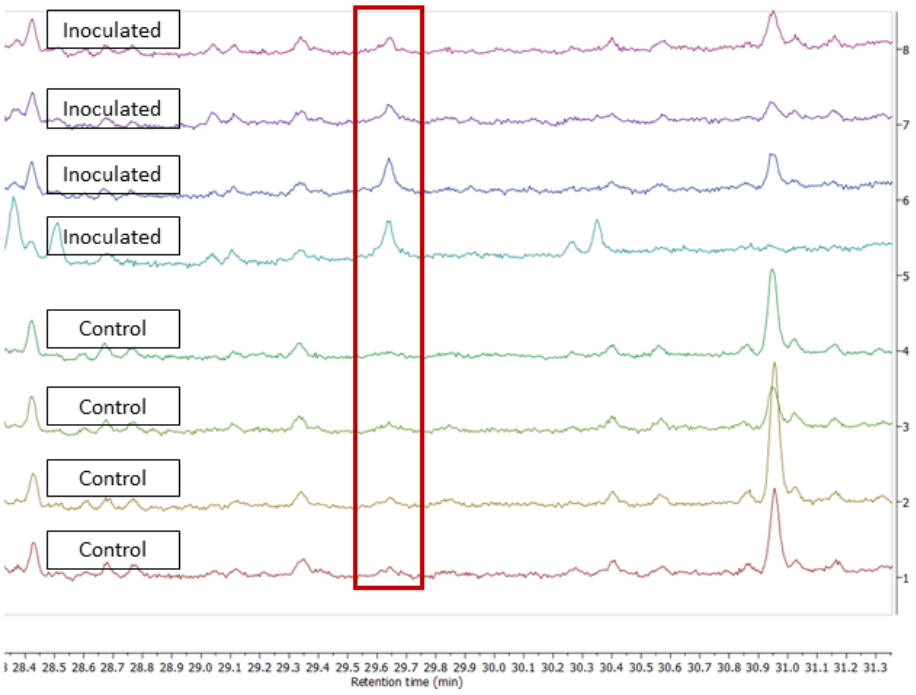

Figure 4.8: Expanded chromatogram region showing a metabolite concentration change observed in the cowpea leaf extracts from inoculated cowpea seeds at retention time 29.6 mins. (red box) identified as a potential pathogen related biomarker. The metabolite concentration (peak intensity) is higher in the inoculated samples than in the control samples.

Statistical analysis of metabolite B (29.64 mins) in inoculated cowpea

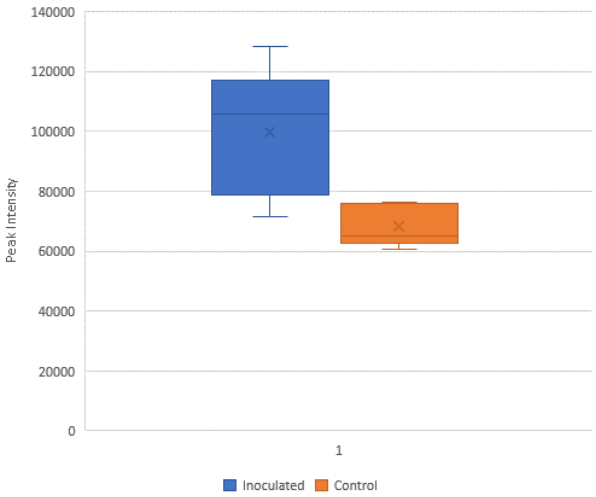

SUMMARY

Groups	Count	Sum	Average	Variance
Inoculated	5	497971.57	99594.31	4.65E+08
Control	5	342354.05	68470.81	51367675

ANOVA

Source of Variation	SS	df	MS	F	P-value	F crit
Between Groups	2.42E+09	1	2.42E+09	9.370878	0.015554	5.317655
Within Groups	2.07E+09	8	2.58E+08			
Total	4.49E+09	9				

Figure 4.9: Statistical analysis of the concentration of metabolite B in the cowpea leaf extracts from inoculated cowpea seeds and their control (α = 0.05). Average metabolite concentration difference of metabolite B between the inoculated and controls was significant, p-value < 0.05.

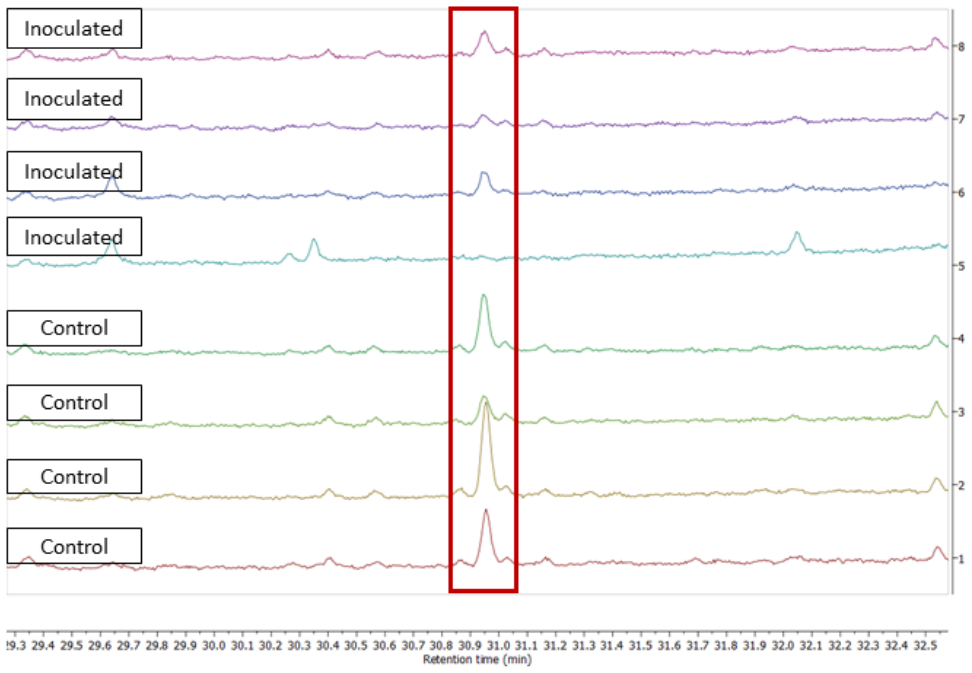

Figure 4.10: Expanded chromatogram region showing a metabolite concentration change observed in the cowpea leaf extracts from inoculated cowpea seeds at 30.95 mins. (red box) identified as a potential pathogen related biomarker. The metabolite concentration (peak intensity) is lower in the inoculated samples than in the controls.

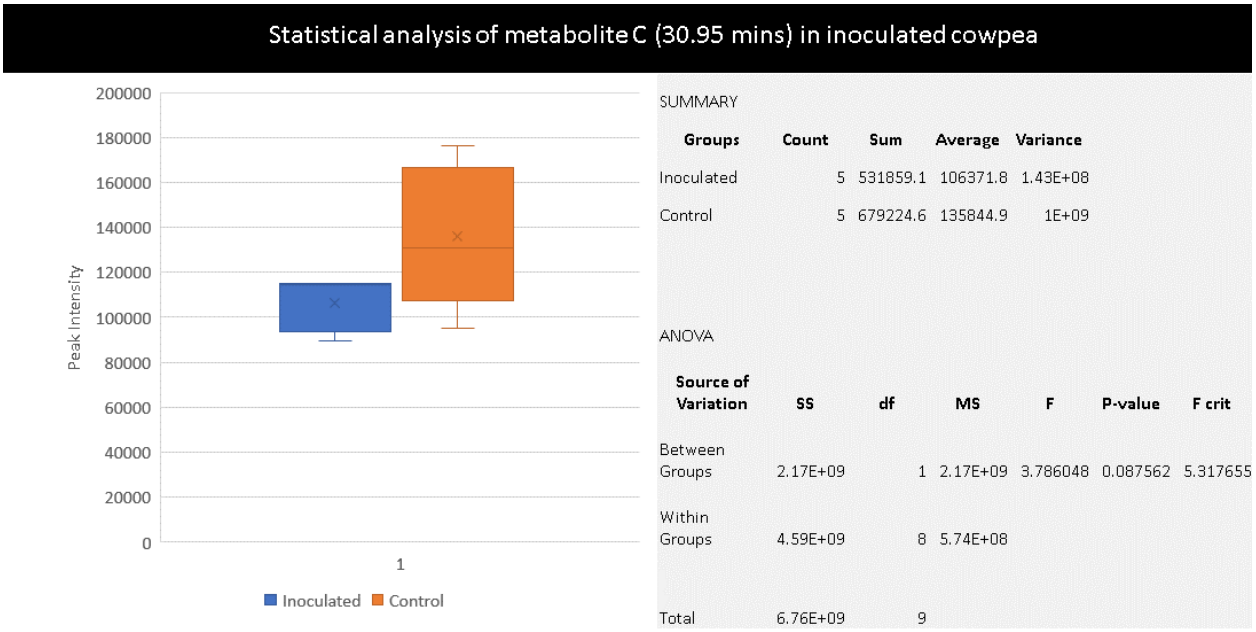

SUMMARY

Groups	Count	Sum	Average	Variance
Inoculated	5	531859.1	106371.8	1.43E+08
Control	5	679224.6	135844.9	1E+09

ANOVA

Source of Variation	SS	df	MS	F	P-value	F crit
Between Groups	2.17E+09	1	2.17E+09	3.786048	0.087562	5.317655
Within Groups	4.59E+09	8	5.74E+08			
Total	6.76E+09	9				

Figure 4.11: Statistical analysis of the concentration of metabolite C in the cowpea leaf extracts from inoculated cowpea seeds and their control (α = 0.05). The average metabolite concentration difference of metabolite C between the inoculated and controls was not significant, p-value > 0.05.

The cowpea leaf extracts chromatograms' numerical data was further subjected to multivariate statistical analysis to determine the possible correlation between *F. verticillioides* inoculation and change in the metabolomic profile in cowpea leaves. The unsupervised PCA plot (Figure 4.12 A) showed some separation between the two sample sets, though not definitive, solely based on each sample's individual GCMS chromatogram. This indicated that *F. verticillioides* inoculation had a certain degree of influence on the cowpea metabolomic profile that caused the slight observed distinction between the sample sets. However, the statistical value, Q2 was very low suggesting that the model could not be used to definitively diagnose unknown cowpea leaf samples inoculated with *F. verticillioides* under similar premises. The supervised OPLS-DA plot, which compares the average metabolomic profiles of the replicates within a set, highlighted clear separation between the two sample sets (Figure 4.12 B). This highlighted a clear distinction in the metabolic profiles of the *F. verticillioides* inoculated cowpea samples and the uninoculated cowpea samples. Furthermore, this suggests that *F. verticillioides* had a considerable influence on the metabolomic profile of cowpea samples creating a notable distinction from the untampered metabolomic profile in the uninoculated samples. The statistical values indicated that the data model could be reliably used to predict or diagnose unknown cowpea leaf samples inoculated with *F. verticillioides* under similar premises. Moreover, it establishes a correlation between *F. verticillioides* inoculation and the observed change in the cowpea leaf metabolome.

The mass spectra of the identified potential biomarkers were run through NIST 14 database to check for similarities to known compounds based on their MS fragmentation patterns (summarized in table 4.2). Based on the database it was suggested that metabolite A shared similarities with 1,3-dimethoxypropan-2-yl palmitate (Figure 4.13), metabolite B shared similarities to butyl-9,12,15-octadecatrienoate (Figure 4.14), and metabolite C methyl-5,11,14,17, eicosatretranoate (Figure 3.15).

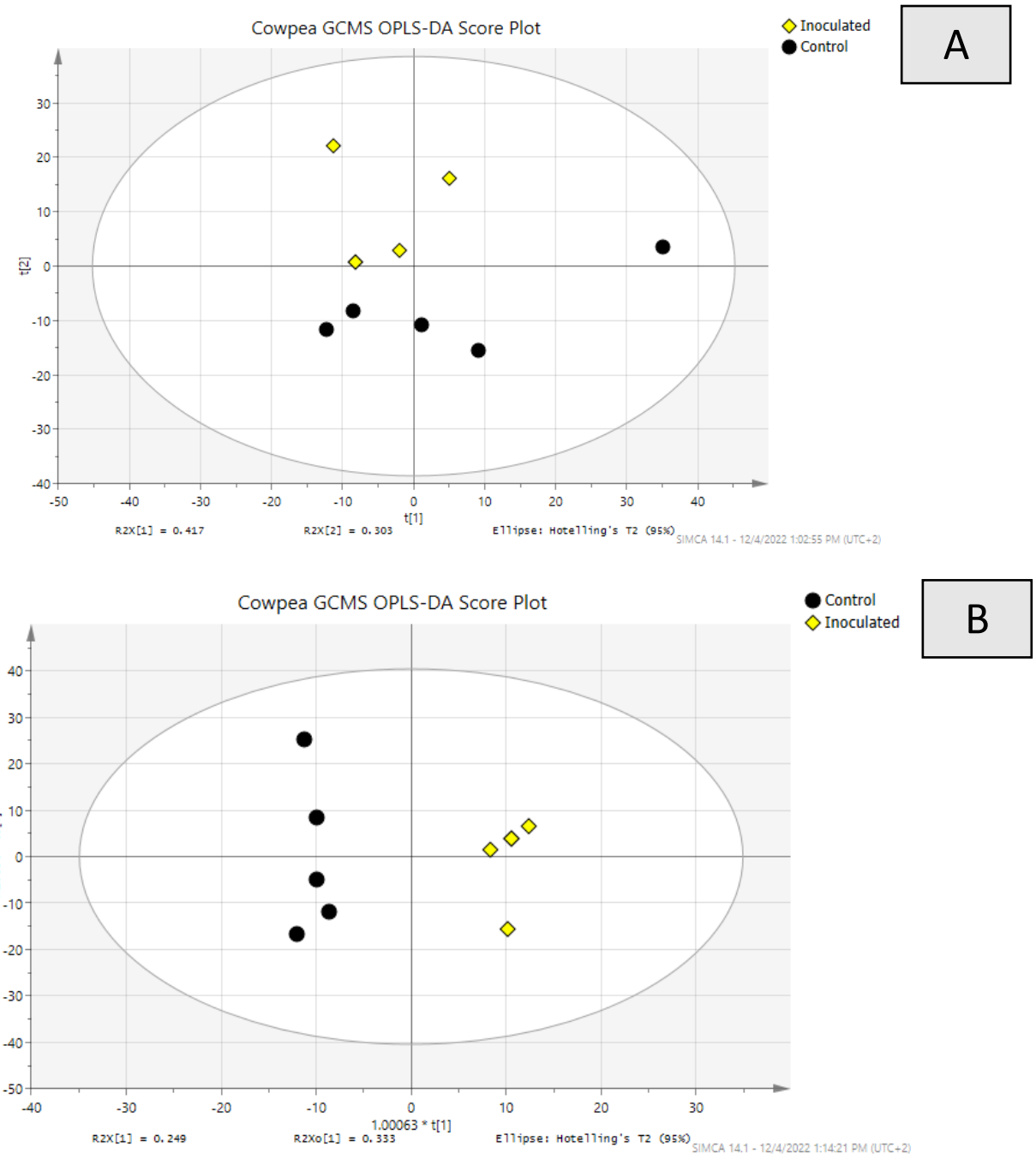

Figure 4.12: (A) GCMS chromatogram PCA score plot of cowpea leaf extracts from cowpea seeds inoculated with F. verticillioides and accompanying controls. Clear separation of the mature lesions and control samples was observed. Multivariate statistical values: Q2 = 0.01; R2X = 0.64. (B) GCMS chromatogram OPLS-DA score plot of cowpea leaf extracts from cowpea seeds inoculated with F. verticillioides and accompanying controls. Definitive separation of the two sample sets was observed. Multivariate statistical values Q2 = 0.90; R2X = 0.92, R2Y = 1.

Table 4.2: Identified potential biomarkers associated with cowpea leaves after seed inoculation with F. verticillioides with suggested matches from the NIST 14 database (α = 0.05).

Potential Biomarker	Chromatogram retention time (mins.)	Observation	Suggested compound match and their similarity index (SI)
Metabolite A	27.38 **p < 0.05**	Higher concentration in inoculated samples	1,3-Dimethoxypropan-2-yl palmitate **SI = 63.9** (See Figure 4.13)
Metabolite B	29.64 **p < 0.05**	Present predominantly in inoculated samples only	Butyl-9,12,15-octadecatrienoate **SI = 73.0** (See Figure 4.14)
Metabolite C	30.95 **p> 0.05**	Lower concentration in inoculated samples.	Methyl-5,11,14,17, eicosatretranoate **SI = 81.7** (See Figure 4.15)

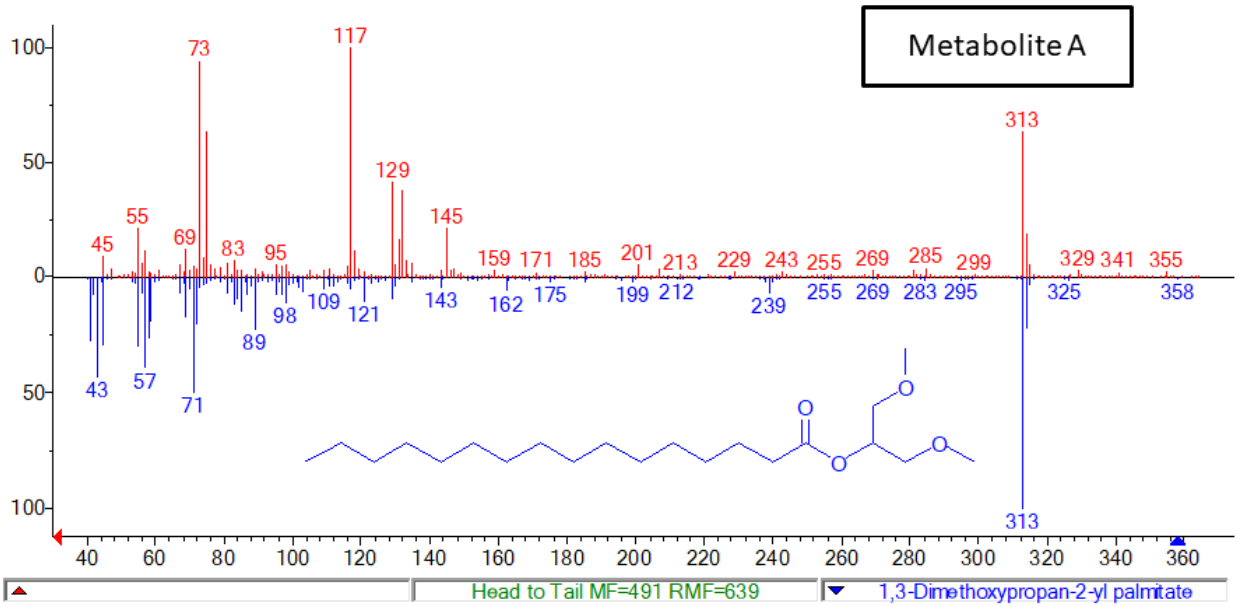

Figure 4.13: Suggested match for metabolite A based on MS spectrum comparison in NIST 14 database. The MS fragments of the unknown metabolite are in red and the MS fragments for 1,3 dimethoxypropan-2-yl palmitate are blue.

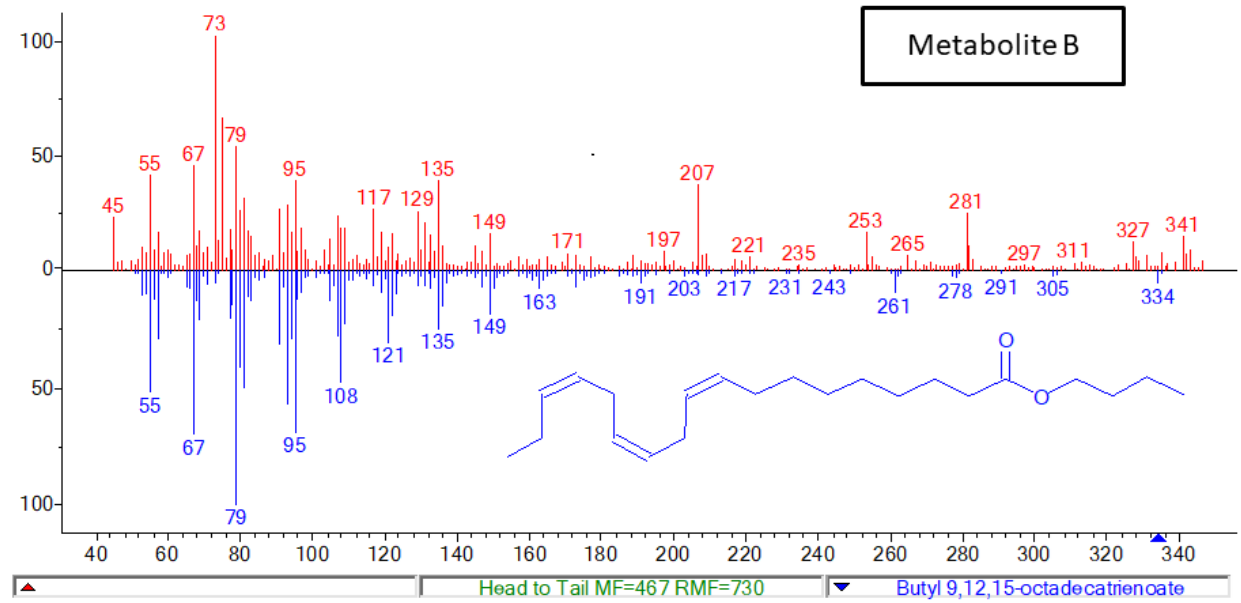

Figure 4.14: Suggested match for metabolite B based on MS spectrum comparison in NIST 14 database. The MS fragments of the unknown metabolite are in red and the MS fragments for butyl-9,12,15-octadecatrienoate are blue.

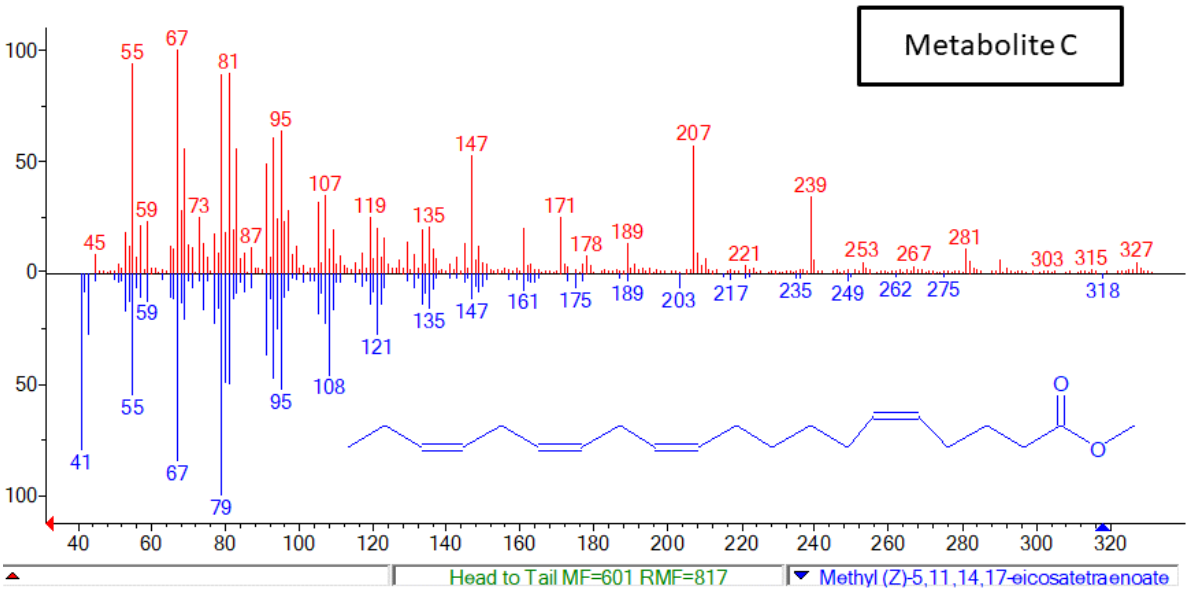

Figure 4.15: Suggested match for metabolite C based on MS spectrum comparison in NIST 14 database. The MS fragments of the unknown metabolite are in red and the MS fragments for methyl-5,11,14,17- eicosatretranoate are blue.

4.5 Discussion

This study was aimed at assessing the efficacy of metabolomical analyses in diagnosing systemic cowpea infection following inoculation of the seed by an fumonisin-producing *F. verticillioides* strain. The trial showed that inoculated plants were smaller than the uninoculated plants, but the dry masses didn't differ significantly. The average dry mass of the leaves from the inoculated samples was lower than the control leaf samples Though this difference was deemed statistically not significant the general observed trend indicated that inoculated samples had a decreased mass. These results correlate with the results obtained by Kotze et al. (2016) who observed that cowpea seeds inoculated with *F. verticillioides* (strains: MRC 8265, 8271, 8272) yielded plants with stunted growth compared to uninoculated plants. As mentioned earlier, FB_1 is a structural analog of sphinganine and sphingosine (Figure 2.8), which are precursors in ceramide biosynthesis (Merrill et al., 2001; Zeng et al., 2020). Sphingolipids carry out functions that include acting as structural components for the plasma membrane and endomembrane systems, secondary messengers and bioactive molecules for plant cell signaling for development, stress response (biotic and abiotic) and programmed cell death (apoptosis) (Zeng et al., 2020). Kritzinger et al. (2006) discovered that cowpea seeds artificially treated with varying concentrations of FB_1 had decreased seed germination. Transmission electron microscopy (TEM) demonstrated that FB_1 led to the plasma membrane being separated from the cell wall, formation of irregular sized vacuoles and abundance of

lipid bodies next to the cell wall (Kritzinger et al., 2006). It has also been widely reported that *F. verticillioides* through FB_1 affects the lipid biosynthesis pathway thus affecting the plant growth (Williams et al., 2007). It has also been reported that FB_1 inhibits H^+ ATPase thus affecting ATP production, a vital component of plant metabolism (Gutiérrez-Nájera et al., 2005). Studies have indicated that fumonisins disrupt cell functions of the plant in the early development stage that's hindering the plant's growth (Zeng et al., 2020).

To analyse the systemic impact of *F. verticillioides* inoculation on cowpea leaves, metabolomic fingerprints of the leaf extracts were analysed using ^1H NMR and GCMS. The NMR spectra showed no difference between the inoculated and uninoculated cowpea leaf samples. This suggests that systemically, *F. verticillioides* has little to no effect on the metabolomic fingerprint of cowpea leaves. Another reason may be that the metabolite differences were in minute quantities that could not be detected by the NMR instrument (Nagana Gowda and Raftery, 2021). The leaf extracts were further subjected to GCMS analysis to identify leaf metabolites that may be impacted by *F. verticillioides* seed inoculation, that may be potential biomarkers in diagnosing *F. verticillioides* infection. There were several differences between the chromatograms of the inoculated samples and the uninoculated samples. The most definitive differences identified were at retention times 27.38, 29.64 and 30.95 mins. Due to their unknown identities, they were named metabolites A, B and C, respectively. The mass spectrum for these metabolites were obtained and a possible match was obtained in the NIST 14 database (summarized in Table 4.2).

According to the database, metabolite A was 63.9 % similar to 1,3-dimethoxypropan-2-yl palmitate, metabolite B was 73.0 % similar to butyl-9,12,15-octadecatrienoate, and metabolite C was 81.7 % similar to methyl-5,11,14,17-eicosatretranoate. 1,3-dimethoxypropan-2-yl palmitate is a palmitic acid derivative, an important fatty acid involved in fatty acid synthesis and lipid oxidation (David et al., 2020). A study by Ma et al. (2021) showed that palmitic acid had inhibitory effects on mycelial growth and spore production of *Fusarium oxysporum* f.sp. *niveum*, a soil-borne fungus that infects watermelon (*Citrullus lanatus*). Studies have shown that palmitic acid has antioxidant and anti-inflammatory effects (Arora & Kumar, 2017; Kadhim et al., 2017). Since metabolite A shares some similarity with 1,3-dimethoxypropan-2-yl palmitate, it may also have the same effect as the compound detected in cowpea leaves. Therefore, it is possible that it has the same antifungal effect as 1,3-dimethoxypropan-2-yl palmitate, leading to the observed increase in expression in the inoculated leaf samples. Hence, the observed increase in its expression in the inoculated samples. Furthermore, this also suggests that it is a *F. verticillioides* triggered metabolite, indicating the systemic impact of this pathogen in altering the leaf metabolome of cowpea.

Butyl-9,12,15-octadecatrienoate is a derivative of 9,12,15-octadecatrienoic acid or alpha-linolenic acid, a vital fatty acid in plant defense signaling (Xue et al., 2008). Alpha-linolenic is a precursor for phyto-oxylipin biosynthesis, which is vital for plant's cell signaling during pathogen invasion (Upchurch, 2008). Oxylipins are produced when polyunsaturated fatty acids undergo autoxidation or enzymatic oxidation to produce phytohormones such as jasmonic acid (Lim et al., 2017). Studies have shown that linolenic acid plays a role in seed colonization and mycotoxin production by *Aspergillus* spp. (Lim et al., 2017). Calvo et al. (1999) observed that linolenic acid and its derivative hydroxylinolenic acid caused an increase in the asexual production of spores in *A. nidulans, A. parasiticus* and *A. flavus* (Calvo et al., 1999; Calvo et al., 2001). Studies have further suggested that linolenic acid plays a role in signaling conidiation in *A. parasiticus* (Upchurch, 2008). Another study by Xue et al. (2008) indicated that colonization of soybean (*Glycine max*) seed by *Cercospora kikuchii* led to a decrease in the plant levels of linoleic acid. In this study it was observed that metabolite B was predominantly expressed only in the inoculated cowpea samples. Furthermore, the database suggested that it shares similarities with butyl-9,12,15-octadecatrienoate, a derivative of alpha linolenic acid. It is plausible to assume that it may also share similar activity with the suggested compound. Thus metabolite B may be defense signaling molecule that was upregulated in response to *F. verticillioides* infection in cowpea; hence the observed increase in concentration in the inoculated samples. Another possibility is that since metabolite B shares similarities to a derivative of alpha-linolenic acid, it may be a byproduct in linolenic acid metabolism by *F. verticillioides* during conidiation in cowpea. Based on this observation, it is plausible to suggest that metabolite B expression could possibly have been triggered by *F. verticillioides*.

Methyl-5,11,14,17-eicosatetraenoate is an eicosapolyenoic acid, a group of fatty acids involved in signaling immune responses in plants (Walley et al., 2013). These compounds may serve as plant defense signaling molecules that induce resistance to pathogens during early infection stages (Bostock et al., 2011). This will trigger the activation of phytoalexin synthesis genes, hypersensitive responses against pathogens and lignification (Walley et al., 2013). Studies have also indicated that methyl-5,11,14,17-eicosatetraenoate has an antimicrobial effect (Ahmed et al., 2022). Since metabolite C shares similarities with methyl-5,11,14,17-eicosatetraenoate, it is plausible that it shares similar signaling activities with the compound. However, in this study it was observed that metabolite C expression was decreased in the inoculated samples. This contradicts the expected observation because if it has signaling properties, it should be upregulated upon pathogen infection. However, studies have shown that some fungi release toxins that target the plant's signaling mechanisms thus weakening the plant's defense (Wang et al., 2014). Thus, it's possible that *F. verticillioides* hindered the expression of metabolite C to improve its

colonization in the cowpea leaves. Additionally, this is another possible indication of *F. verticillioides* triggered metabolome change in cowpea leaves.

Most of the suggested matches from the database were long chain carbon lipid-based molecules. *Fusarium verticillioides* elicits its effect through fumonisins, the most prominent being FB_1 (Blacutt et al., 2018). It has been widely reported that fumonisins disrupt the sphingolipid biosynthesis pathway (Riley and Merrill, 2019). This leads to the alteration in the levels of various bioactive lipids and associated processes (Zeng et al., 2020). Sphingolipids play an important role as secondary messengers in plant response to biotic stress, thus perturbation in their synthesis affects the signal transduction route in plants, causing the plant to be more susceptible to pathogen invasion (Beccaccioli et al., 2021). FB_1 is a structural analog of sphinganine and sphingosine, used in ceramide biosynthesis (Merrill et al., 2001). It competitively inhibits ceramide synthase and this leads to an accumulation of the precursors that were meant to partake in the biosynthesis process (Zeng et al., 2020). It is possible that the upregulated metabolites (metabolite A and B) observed in the inoculated samples were precursors to the biosynthetic pathway blocked by FB_1 produced by *F. verticillioides*. Additionally, the database suggests that they contain long carbon chains, and these are attributes of lipid biosynthesis precursors.

The results from this study illustrate that seed infection of cowpea by a fumonisin-producing *F. verticillioides* isolate causes a systemic change to the metabolome of the plant as observed by the metabolite changes in the leaves. This corresponds to the discovery by Baldwin et al. (2014) that indicated that FB1 produced by *F. verticilloides* in the roots could be transported to the leaves through transpiration mediated bulk flow without the fungi colonizing the leaves, causing disruption in leaf proliferation. Furthermore, the study highlighted the proficiency of metabolomic profiling in detecting the systemic metabolite changes elicited by *F. verticillioides*. This Illustrates the capabilities of metabolomical analyses in diagnosing systemic *F. verticillioides* infection where the site of infection and the site of effect are in different plant organs. Three inoculation-related potential biomarkers where identified and further analysis could assert these as *F. verticillioides* infection biomarkers, which could prove useful in the future diagnosis of *F. verticillioides* infection. Thus, it can be concluded that metabolomic analyses is an effective tool in the systemic diagnosis of *F. verticillioides* infection in cowpea. Additionally, it is possibly a powerful tool in understanding systemic metabolomic changes caused by *F. verticillioides* (fumonisins) cowpea infection and its associated impact on lipid metabolism in plants.

4.6 References

Ahmed, M., Khan, K.-R., Ahmad, S., Aati, H.Y., Ovatlarnporn, C., Rehman, M.S., Javed, T., Khursheed, A., Ghalloo, B.A., Dilshad, R., Anwar, M., 2022. Comprehensive phytochemical profiling, biological activities, and molecular docking studies of pleurospermum candollei: An insight into potential for natural products development. Molecules 27, 4113. https://doi.org/10.3390/molecules27134113

Arora, S., Kumar, G., 2017. Gas Chromatography-Mass Spectrometry (GC-MS) determination of bioactive constituents from the methanolic and ethyl acetate extract of *Cenchrus setigerus* Vahl (Poaceae) 6, 635–640.

Baldwin, T.T., Zitomer, N.C., Mitchell, T.R., Zimeri, A.M., Bacon, C.W., Riley, R.T., Glenn, A.E., 2014. Maize seedling blight induced by *Fusarium verticillioides*: Accumulation of fumonisin B1 in leaves without colonization of the leaves. J. Agric. Food Chem. 62, 2118–2125. https://doi.org/10.1021/JF5001106/ASSET/IMAGES/LARGE/JF-2014-001106_0007.JPEG

Beccaccioli, M., Salustri, M., Scala, V., Ludovici, M., Cacciotti, A., D'angeli, S., Brown, D.W., Reverberi, M., 2021. The effect of *Fusarium verticillioides* fumonisins on fatty acids, sphingolipids, and oxylipins in maize germlings. Int. J. Mol. Sci. 22, 1–17. https://doi.org/10.3390/IJMS22052435

Bhagat, I., Chakraborty, B., 1970. Defense response triggered by *Sclerotium rolfsii* in tea plants. Ecoprint An Int. J. Ecol. 17, 69–76. https://doi.org/10.3126/ECO.V17I0.4119

Blacutt, A.A., Gold, S.E., Voss, K.A., Gao, M., Glenn, A.E., 2018. *Fusarium verticillioides* : Advancements in understanding the toxicity , virulence , and niche adaptations of a model Mycotoxigenic pathogen of maize 312–326.

Bostock, R.M., Savchenko, T., Lazarus, C., Dehesh, K., 2011. Plant signaling & behavior eicosapolyenoic acids novel MAMPs with reciprocal effect on oomycete-plant defense signaling networks. https://doi.org/10.4161/psb.6.4.14782

Bruce, R.J., West, C.A., 1989. Elicitation of lignin biosynthesis and isoperoxidase activity by pectic fragments in suspension cultures of castor bean. Plant Physiol. 91, 889–897. https://doi.org/10.1104/PP.91.3.889

Calvo, A.M., Gardner, H.W., Keller, N.P., 2001. Genetic connection between fatty acid metabolism and sporulation in *Aspergillus nidulans*. J. Biol. Chem. 276, 25766–25774. https://doi.org/10.1074/JBC.M100732200

Calvo, A.M., Hinze, L.L., Gardner, H.W., Keller, N.P., 1999. Sporogenic effect of polyunsaturated fatty acids on development of *Aspergillus spp*. Appl. Environ. Microbiol. 65, 3668–3673. https://doi.org/10.1128/AEM.65.8.3668-3673.1999

David, L., Kang, J., Dufresne, D., Zhu, D., Chen, S., 2020. Multi-omics revealed molecular mechanisms underlying guard cell systemic acquired resistance. Int. J. Mol. Sci. 22, 1–22. https://doi.org/10.3390/IJMS22010191

Gelderblom, W.C., Jaskiewicz, K., Marasas, W.F., Thiel, P.G., Horak, R.M., Vleggaar, R., Kriek, N.P., 1988. Fumonisins--novel mycotoxins with cancer-promoting activity produced by *Fusarium moniliforme*. Appl. Environ. Microbiol. 54.

Gutiérrez-Nájera, N., Muñoz-Clares, R.A., Palacios-Bahena, S., Ramírez, J., Sánchez-Nieto, S., Plasencia, J., Gavilanes-Ruíz, M., 2005. Fumonisin B1, a sphingoid toxin, is a potent inhibitor of the plasma

membrane H+-ATPase. Planta 221, 589–596. https://doi.org/10.1007/S00425-004-1469-1

Kadhim, M.J., Al-rubaye, A.F., Hameed, I.H., 2017. Determination of bioactive compounds of methanolic extract of *Vitis vinifera* determination of bioactive compounds of methanolic extract of *Vitis vinifera* using GC-MS. Int. J. Toxicol. Pharmacol. Res. 9, 113–126. https://doi.org/10.25258/ijtpr.v9i02.9047

Kamle, M., Mahato, D.K., Devi, S., Lee, K.E., Kang, S.G., Kumar, P., 2019. Fumonisins: Impact on agriculture, food, and human health and their management strategies. Toxins 2019, Vol. 11, Page 328 11, 328. https://doi.org/10.3390/TOXINS11060328

Kotze, R.G., Crampton, B.G., Kritzinger, Q., 2016. Effect of fumonisin B 1 on the emergence , growth and ceramide synthase gene expression of cowpea (*Vigna unguiculata* (L .) Walp). Eur. J. Plant Pathol. https://doi.org/10.1007/s10658-016-1089-1

Kritzinger, Q., Aveling, T.A.S., Marasas, W.F.O., Rheeder, J.P., Van Der Westhuizen, L. V., Shephard, G.S., 2003. Mycoflora and fumonisin mycotoxins associated with cowpea [*Vigna unguiculata* (L.) Walp] seeds. J. Agric. Food Chem. 51, 2188–2192. https://doi.org/10.1021/jf026121v

Kritzinger, Q., Aveling, T.A.S., Van Der Merwe, C.F., 2006. Phytotoxic effects of fumonisin B1 on cowpea seed. Phytoparasitica 34, 178–186. https://doi.org/10.1007/BF02981318

Lim, G.H., Singhal, R., Kachroo, A., Kachroo, P., 2017. Fatty acid– and lipid-mediated signaling in plant defense. https://doi.org/10.1146/annurev-phyto-080516-035406 55, 505–536. https://doi.org/10.1146/ANNUREV-PHYTO-080516-035406

Ma, K., Kou, J., Khashi U Rahman, M., Du, W., Liang, X., Wu, F., Li, W., Pan, K., 2021. Palmitic acid mediated change of rhizosphere and alleviation of *Fusarium* wilt disease in watermelon. Saudi J. Biol. Sci. 28, 3616–3623. https://doi.org/10.1016/J.SJBS.2021.03.040

Merrill, A.H., Sullards, M.C., Wang, E., Voss, K.A., Riley, R.T., 2001. Sphingolipid metabolism: roles in signal transduction and disruption by fumonisins. Environ. Health Perspect. 109, 283–289. https://doi.org/10.1289/ehp.01109s2283

Nagana Gowda, G.A., Raftery, D., 2021. NMR Based Metabolomics. Adv. Exp. Med. Biol. 1280, 19. https://doi.org/10.1007/978-3-030-51652-9_2

Nandi, S., Dutta, S., Mondal, A., Nath, A.A.R., Chattopadhaya, A., Chaudhuri, S., 2013. Biochemical responses during the pathogenesis of *Sclerotium rolfsii* on cowpea. African J. Biotechnol. 12, 3968–3977. https://doi.org/10.5897/AJB2013.12405

Passardi, F., Cosio, C., Penel, C., Dunand, C., 2005. Peroxidases have more functions than a Swiss army knife. Plant Cell Rep. 24, 255–265. https://doi.org/10.1007/S00299-005-0972-6

Riley, R.T., Merrill, A.H., 2019. Ceramide synthase inhibition by fumonisins: a perfect storm of perturbed sphingolipid metabolism, signaling, and disease. J. Lipid Res. 60, 1183–1189. https://doi.org/10.1194/JLR.S093815

Upchurch, R.G., 2008. Fatty acid unsaturation, mobilization, and regulation in the response of plants to stress. Biotechnol. Lett. 30, 967–977. https://doi.org/10.1007/S10529-008-9639-Z

Walley, J.W., Kliebenstein, D.J., Bostock, R.M., Dehesh, K., 2013. Fatty acids and early detection of pathogens. Curr. Opin. Plant Biol. 16, 520–526. https://doi.org/10.1016/J.PBI.2013.06.011

Wang, X., Jiang, N., Liu, J., Liu, W., Wang, G.L., 2014. The role of effectors and host immunity in plant-necrotrophic fungal interactions. Virulence 5, 722–732. https://doi.org/10.4161/VIRU.29798

Williams, L.D., Glenn, A.E., Zimeri, A.M., Bacon, C.W., Smith, M.A., Riley, R.T., 2007. Fumonisin disruption of ceramide biosynthesis in maize roots and the effects on plant development and *Fusarium verticillioides*-induced seedling disease. J. Agric. Food Chem. 55, 2937–2946. https://doi.org/10.1021/jf0635614

Xue, H.Q., Upchurch, R.G., Kwanyuen, P., 2008. Relationships between oleic and linoleic acid content and seed colonization by *Cercospora kikuchii* and *Diaporthe phaseolorum*. Plant Dis. 92, 1038–1042. https://doi.org/10.1094/PDIS-92-7-1038

Xue, L., Charest, P.M., Jabaji-Hare, S.H., 1998. Systemic Induction of peroxidases, 1,3-beta-glucanases, chitinases, and resistance in bean plants by binucleate R*hizoctonia* species. Phytopathology 88, 359–365. https://doi.org/10.1094/PHYTO.1998.88.4.359

Zeng, H.Y., Li, C.Y., Yao, N., 2020. Fumonisin B1: A tool for exploring the multiple functions of sphingolipids in Plants. Front. Plant Sci. 11, 1649. https://doi.org/10.3389/FPLS.2020.600458/BIBTEX

5. General Discussion and Future Prospects

5.1 General Discussion

Metabolomical analyses provides a high throughput assessment, identification and quantification of all metabolites, endogenous and exogenous, within biological samples (Smolinska et al., 2012). Plants being sessile organisms extensively depend on secondary metabolites for their survival, development, and proliferation. Plants are susceptible to a variety of fungal pathogens and implore secondary metabolites for various signal transductions to resist or curb fungal infection (Ray et al., 2017). One of the biggest challenges of fungal disease diagnosis in plants is that fungi upon entering their plant host, can remain dormant until ideal conditions arise and then they become rapidly pathogenic. This study assessed whether metabolomic analyses can be used as a tool to detect fungal infection in plants based on specific changes in the plant's metabolome. It also aimed to determine specific metabolites unique to the subject fungal diseases that may potentially act as biomarkers for future disease diagnosis. To achieve this two extensively studied fungal pathogens and their respective target plants were selected. *Cercospora zeina* a well-known maize foliar pathogen that causes grey spot leaf in maize (*Zea mays*) and fumonisin producing *Fusarium verticillioides* in cowpea (*Vigna unguiculata*). Investigations on these two pathogen-plant systems have been reported by e.g., Meisel et al. (2009) and Kritzinger et al. (2006), respectively.

For the maize pathosystem two sets of samples were collected from a field trial based foliar symptoms, i.e., chlorotic spots indicating early stages of *C. zeina* infection and mature lesions indicating later stages *C. zeina* infection. A separate artificial inoculation of maize with *C. zeina* was carried out in a glasshouse to correlate to the metabolomic changes found in the field trial. For the cowpea patho-system an artificial seed inoculation of *F. verticillioides* was carried out in a phytotron and the leaves of the resulting plants were analysed for metabolomic changes. These two pathogens have completely different modes of actions. *Cercospora zeina* enters through the leaf stomata and elicits its virulence in the leaves, i.e., the site of infection is also the site of pathogenicity (Meisel et al. 2009). On the other hand *F. verticillioides* is a soil-borne pathogen which can infectseeds and through translocation, its virulence systemically affects above ground parts of the plant (Kotze et al. 2016). Metabolomical analyses techniques ^{1}H Nuclear Magnetic Resonance (NMR) and Gas Chromatography Mass Spectrometry (GCMS) were implored to determine changes in the plant's metabolome and specific metabolite changes in the plants' fingerprints.

In maize, the metabolomic analyses revealed that early infection stages (chlorotic spots) had little to no effect on the metabolomic fingerprint of the maize leaves as depicted by the NMR spectral data of field trial maize leaves with chlorotic spots. Furthermore, the metabolomic profile data from GCMS analysis of the same samples suggested that there are no significant changes to the specific metabolites in the leaves due to grey leaf spot. Thus, it can be postulated based on this study that early stages of grey leaf spot characterized by chlorotic spots on the maize leaves, do not have a significant impact on the metabolome of the maize leaves. However, analysis of the later stages of grey leaf spot infection in maize leaves from the same field trial showing mature lesions suggested that *C. zeina* caused a definitive change in the metabolomic fingerprint of maize leaves. This is highlighted by the differences in the NMR spectral data of field trial maize leaves with mature lesions and their accompanying asymptomatic controls, as well as the clear groupings between the sample sets in the statistical plots from multivariate analysis in SIMCA. According to Gable (2019), these changes were observed in the regions with the functional group signals of alcohols, esters, alkyl halides and alkenes. These are structural characteristics of some of the reported maize antimicrobial metabolites such as zealexins, kauralexins and dolabralexins (Huffaker et al., 2011; Ding et al., 2020). Furthermore, several specific metabolite changes were observed in the leaves metabolomic profile from the GCMS chromatograms. This was indicated by the separate groupings observed in the SIMCA statistical plots of the symptomatic and asymptomatic maize leaves based on their chromatograms. These metabolites that changed (due to *C. zeina*) were identified as potential biomarkers for grey leaf spot and due to their unknown identities, they were allocated generic names (compound A-E) for future identifications. Using NIST 14 metabolite database, it was showed that the identified potential biomarkers observed in the maize leaves with mature lesions shared some structural similarities to reported metabolites with known antimicrobial effects. This led to the suggestion that possibly these potential biomarkers may also play a role in maize defense against *C. zeina.*

Glasshouse maize trial was carried out to compare to the metabolomical changes observed in the maize leaves upon artificial inoculation by *C. zeina*. From the glasshouse trial, the maize leaves with mature lesions were collected and analysed for metabolomical changes. Metabolomical analysis using ^{1}H NMR showed that *C. zeina* artificial inoculation on maize leaves induced various changes in the metabolomical fingerprint of the maize leaves. Furthermore, it was also discovered that the fingerprint regions on the NMR spectra of the greenhouse maize leaves with mature lesions correlated with most of the changes observed in the maize leaves with mature lesions from the field trial. This further cemented the suggestion that these regions could possibly be the functional groups of some antimicrobial metabolites found in maize. It is also plausible that these metabolites could have been produced by *C. zeina* to assist in its

virulence in maize leaves, as it has been reported that some fungal pathogens metabolise host metabolites to assist in the virulence process by targeting host defense (Wang et al., 2014). The metabolomic profile of the greenhouse maize leaves with mature lesions obtained indicated various changes in the concentrations of specific metabolites. Several metabolites were identified as potential grey leaf spot biomarkers as their concentration and possible expression changed in the symptomatic maize leaves. Based on a NIST 14 database search, it was found that these metabolites shared some similarities with various known antimicrobial metabolites. However, most of them did not correspond to the potential biomarkers identified in the field trial samples. This lack of correlation could be attributed to the difference in degree of disease prevalence in the field trial and in the glasshouse, with the glasshouse plants' leaves having less severe lesions. A single potential biomarker was observed in both the field trial and greenhouse trial maize leaves with mature lesions, and it was compound C eluting at 29.0 retention time in the GCMS analysis. This metabolite was significantly lower in the symptomatic samples of both sample sets. This correlation led to the conclusion that this metabolite may be strongly linked to *C. zeina* infection in maize.

In the cowpea trial it was observed that the plants grown from cowpea seeds inoculated with *F. verticillioides* were considerably smaller than their uninoculated (control) counterparts, but the dry mass averages of the treatment and control leaves did not differ significantly. The observed decrease in the leaf area and the average leaf dry mass of the inoculated plants compared to the control plants could possibly be attributed to *F. verticillioides*. Despite the observed morphological differences, the metabolomic fingerprint analysis of the cowpea leaves using ^{1}H NMR did not indicate any changes to the leaves' metabolome due to *F. verticillioides* seed inoculation. However, metabolomic profile analysis of the same cowpea leaves using GCMS showed that the expression of three metabolites in the leaves was altered in the leaves of inoculated cowpea plants. Furthermore, a NIST 14 database comparison indicated that the identified metabolites shared various similarities with reported fatty acids. This led to the notion that these metabolites are strongly linked to *F. verticillioides* infection of cowpea seeds as it has been widely reported that this pathogen disrupts the sphingolipid biosynthesis pathway which is responsible for the synthesis of various fatty acids (Riley and Merrill, 2019b). Furthermore, it also affirms the discovery by Baldwin et al. (2014) that suggested that *F. verticillioides'* virulence spreads to various parts of its host plant through translocation of either its conidia or fumonisins (mycotoxin), thus disrupting cell functions in those plant organs.

From these findings, it is plausible to suggest that metabolomical and chemical fingerprint analyses successfully distinguished maize leaves infected with grey leaf spot caused by *C. zeina* from their healthy counterparts based on specific changes observed in the metabolomic fingerprint and profile of the maize leaves. It also successfully distinguished cowpea leaves from plants that were grown from seeds inoculated with *F. verticillioides*. These two findings show that metabolomical analyses is capable of diagnosing plant fungal diseases where the site of infection and site of virulence are the same, as well as systemic infections where the site of infection and the site of virulence are spatially separate. Furthermore, metabolomical and chemical fingerprint analyses led to the identification of potential pathogen related biomarkers in both instances that shared similarities to various reported antifungal metabolites. The potential biomarkers, with further analyses, can possibly be used to identify these pathogens in their hosts and assist in understanding the mode of action of these pathogens for the development of improved control measures. Unfortunately, it failed to definitively identify metabolomical changes in the early stages of grey leaf spot (chlorotic spots on maize leaves). However, the preliminary data obtained showed much potential and upon further exploration by metabolomical analyses biomarkers might be identified for early fungal disease diagnosis. Although much more extensive study is still required to cement these findings, it can be concluded with much credibility that this study provided a gateway into the application of metabolomical and chemical footprint analyses in plant fungal disease diagnosis that can prove to be fruitful in further studies.

5.2 Future Prospects

This study provided some evidence which suggested that metabolomic analysis has great potential in detecting fungal diseases in plants. However, further intensive research is still required to definitively conclude this hypothesis. For the maize study, two different levels of infection were analysed using metabolomical techniques. A single collection was carried out for the maize leaves with chlorotic spots and mature lesions from the field trial. This can be improved by carrying out multiple collections of maize leaf samples and analyse a wider sample range over multiple time points in a season. This could result in more definitive metabolomical changes in the early and later stages of grey leaf spot. Another experiment could be conducted simultaneously in a glasshouse with artificially inoculated maize leaves with *C. zeina*, and then include collecting leaf samples with chlorotic spots. These would then be compared to the field trial's leaves with chlorotic spots. This would provide a wholesome picture on the possible metabolomical changes in the early stages of grey leaf spot and lead to the possible identification of a more specific *C. zeina* biomarker.

For cowpea, a strategy that can be implored is sampling different parts of the plant, i.e., roots, stems, and leaves. This would possibly indicate the metabolomical changes effected by *F. verticillioides* from the roots (point of inoculation) to the leaves. If would potentially indicate how the mycotoxin produced by the fungi is translocated from the roots to the leaves where its virulence was observed, and maybe lead to the identification of a more *F. verticillioides* specific biomarker. Another strategy would be to emulate the study done by Kritzinger et al. (2006) and Kotze et al. (2016) and treat the seeds with pure fumonisin B_1 toxin. The above ground parts of the plant (i.e., stem and leaveas) will then be analysed to determine the metabolomical changes due to exposure to the toxin. The findings can be compared to the findings of the *F. verticillioides* cowpea seed treatment to observe possible similarities. If a common metabolomic change in cowpea is observed in the two sets of treatments, a definitive pathway can be established on how *F. verticillioides* uses fumonisins to elicit its virulence on plant hosts. Furthermore, this may lead to the identification of a biomarker that can be used to diagnose various fungal diseases caused by fumonisin producing fungi and shed light on the metabolical processes involved in their virulence for better disease control.

In terms of metabolomical analyses, analyses, improvements can be made by imploring more analytical techniques. Proton NMR analysis provided an overview of the possible types of affected compounds in the pant metabolome but was not conclusive in providing the actual identity of the compounds affected by fungal inoculation. GCMS analysis carried out in this study provided possible compounds that maybe by the fungal infection, but further refinement is still required to confidently identify the set compound. A first point of improvement would be to use liquid chromatography mass spectrometry (LCMS). The ^{1}H NMR analyses showed that various polar functional groups were upregulated in the maize leaves with mature lesions in both maize leaves from the field trial and from the glasshouse trial. Furthermore, most of the reported maize antimicrobial secondary metabolites e.g., DIMBOA, dobralexin, zealexins, etc., are all polar compounds that can be detected by LCMS. This can then be followed by preparatory liquid chromatography where the compounds of interest are isolated and subjected to further analyses for conclusive identification. This can be coupled with analysing on a GCMS with a polar column like DB-Wax, as these are considered efficient in separating polar compounds that's been derivatized (methylated) (Förster et al., 2022). Various other more sensitive metabolomical analytical techniques such as GCMS quantitative time of flight (QTOF) methods can be implored to give more accurate compounds identities of the identified potential biomarkers. This study provided a gateway that can be used as a starting point for an improved analytical study that will demonstrate the full potential of metabolomical analyses in fungal disease diagnosis in plants.

5.3 References

Baldwin, T.T., Zitomer, N.C., Mitchell, T.R., Zimeri, A.M., Bacon, C.W., Riley, R.T., Glenn, A.E., 2014. Maize seedling blight induced by *Fusarium verticillioides*: Accumulation of fumonisin B1 in leaves without colonization of the leaves. J. Agric. Food Chem. 62, 2118–2125. https://doi.org/10.1021/JF5001106/ASSET/IMAGES/LARGE/JF-2014-001106_0007.JPEG

Ding, Y., Weckwerth, P.R., Poretsky, E., Murphy, K.M., Sims, J., Saldivar, E., Christensen, S.A., Char, S.N., Yang, B., Tong, A. dao, Shen, Z., Kremling, K.A., Buckler, E.S., Kono, T., Nelson, D.R., Bohlmann, J., Bakker, M.G., Vaughan, M.M., Khalil, A.S., Betsiashvili, M., Dressano, K., Köllner, T.G., Briggs, S.P., Zerbe, P., Schmelz, E.A., Huffaker, A., 2020. Genetic elucidation of interconnected antibiotic pathways mediating maize innate immunity. Nat. plants 6, 1375–1388. https://doi.org/10.1038/S41477-020-00787-9

Förster, C., Handrick, V., Ding, Y., Nakamura, Y., Paetz, C., Schneider, B., Castro-Falcón, G., Hughes, C.C., Luck, K., Poosapati, S., Kunert, G., Huffaker, A., Gershenzon, J., Schmelz, E.A., Köllner, T.G., 2022. Biosynthesis and antifungal activity of fungus-induced O-methylated flavonoids in maize. Plant Physiol. 188, 167–190. https://doi.org/10.1093/PLPHYS/KIAB496

Gable, K., 2019. 1H NMR chemical shift [WWW Document]. URL https://sites.science.oregonstate.edu/~gablek/CH335/Chapter10/ChemicalShift.htm (accessed 2.28.22).

Huffaker, A., Kaplan, F., Vaughan, M.M., Dafoe, N.J., Ni, X., Rocca, J.R., Alborn, H.T., Teal, P.E.A., Schmelz, E.A., 2011. Novel acidic sesquiterpenoids constitute a dominant class of pathogen-induced phytoalexins in maize. Plant Physiol. 156, 2082–2097. https://doi.org/10.1104/pp.111.179457

Kotze, R.G., Crampton, B.G., Kritzinger, Q., 2016. Effect of fumonisin B 1 on the emergence , growth and ceramide synthase gene expression of cowpea (*Vigna unguiculata* (L .) Walp). Eur. J. Plant Pathol. https://doi.org/10.1007/s10658-016-1089-1

Kritzinger, Q., Aveling, T.A.S., Marasas, W.F.O., Rheeder, J.P., Van Der Westhuizen, L. V., Shephard, G.S., 2003. Mycoflora and fumonisin mycotoxins associated with cowpea [*Vigna unguiculata* (L.) Walp] seeds. J. Agric. Food Chem. 51, 2188–2192. https://doi.org/10.1021/jf026121v

Kritzinger, Q., Aveling, T.A.S., Van Der Merwe, C.F., 2006. Phytotoxic effects of fumonisin B1 on cowpea seed. Phytoparasitica 34, 178–186. https://doi.org/10.1007/BF02981318

Meisel, B., Korsman, J., Kloppers, F.J., Berger, D.K., 2009. *Cercospora zeina* is the causal agent of grey leaf spot disease of maize in southern Africa. Eur. J. Plant Pathol. 124, 577–583. https://doi.org/10.1007/s10658-009-9443-1

Ray, M., Ray, A., Dash, S., Mishra, A., Achary, K.G., Nayak, S., Singh, S., 2017. Fungal disease detection in plants: Traditional assays, novel diagnostic techniques and biosensors. Biosens. Bioelectron. https://doi.org/10.1016/j.bios.2016.09.032

Riley, R.T., Merrill, A.H., 2019. Ceramide synthase inhibition by fumonisins: a perfect storm of perturbed sphingolipid metabolism, signaling, and disease. J. Lipid Res. 60, 1183–1189. https://doi.org/10.1194/JLR.S093815

Smolinska, A., Blanchet, L., Buydens, L.M.C., Wijmenga, S.S., 2012. NMR and pattern recognition methods in metabolomics: From data acquisition to biomarker discovery: A review. Anal. Chim.

Acta 750, 82–97. https://doi.org/10.1016/J.ACA.2012.05.049

Wang, X., Jiang, N., Liu, J., Liu, W., Wang, G.L., 2014. The role of effectors and host immunity in plant-necrotrophic fungal interactions. Virulence 5, 722–732. https://doi.org/10.4161/VIRU.29798

6. Appendix

Appendix A : Glasshouse trial real time temperature and humidity readings

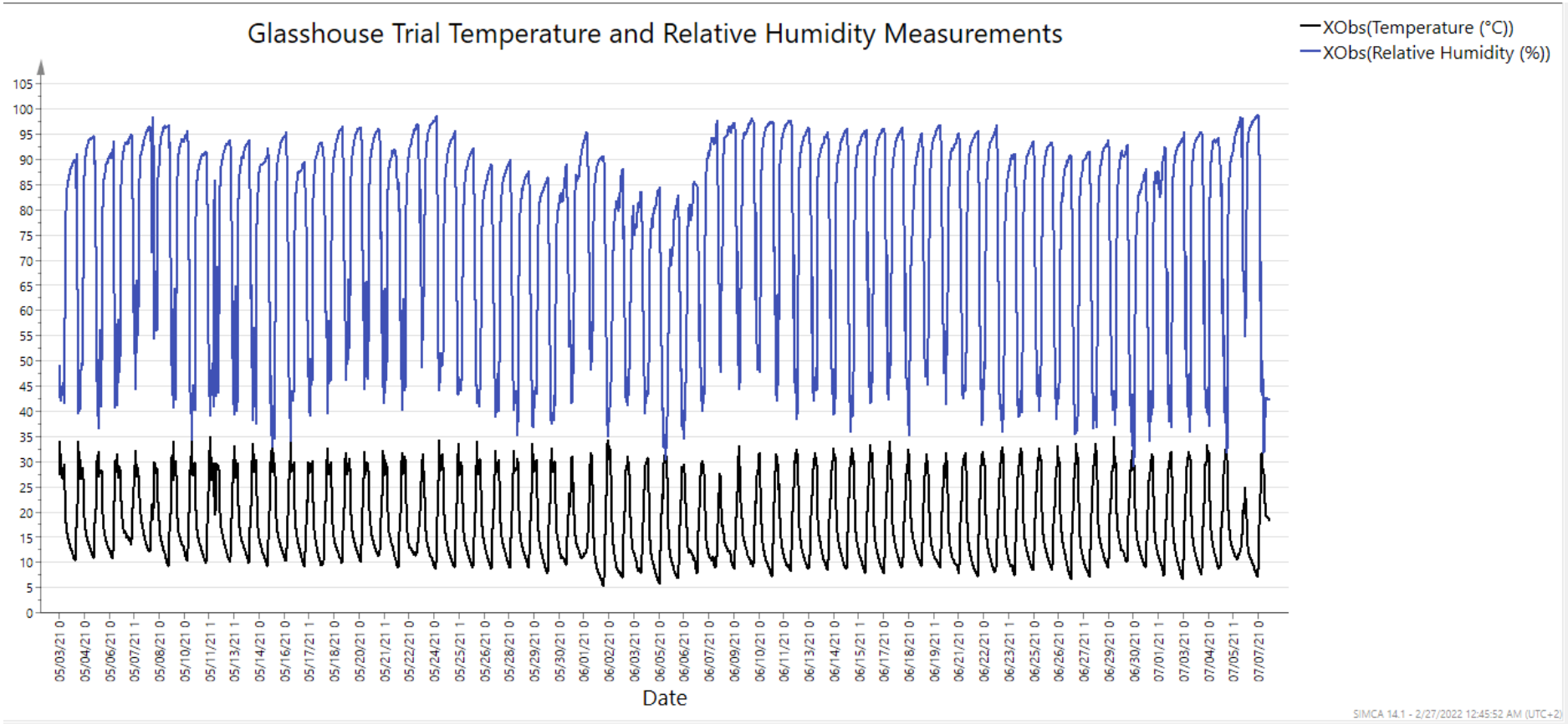

Figure 6.1: HOBO measurements of glasshouse temperature (°C, bottom graph) and relative humidity (top graph) for the duration of the trial.

Appendix B : Full mass spectra of all potential *Cercospora zeina* biomarkers identified in maize.

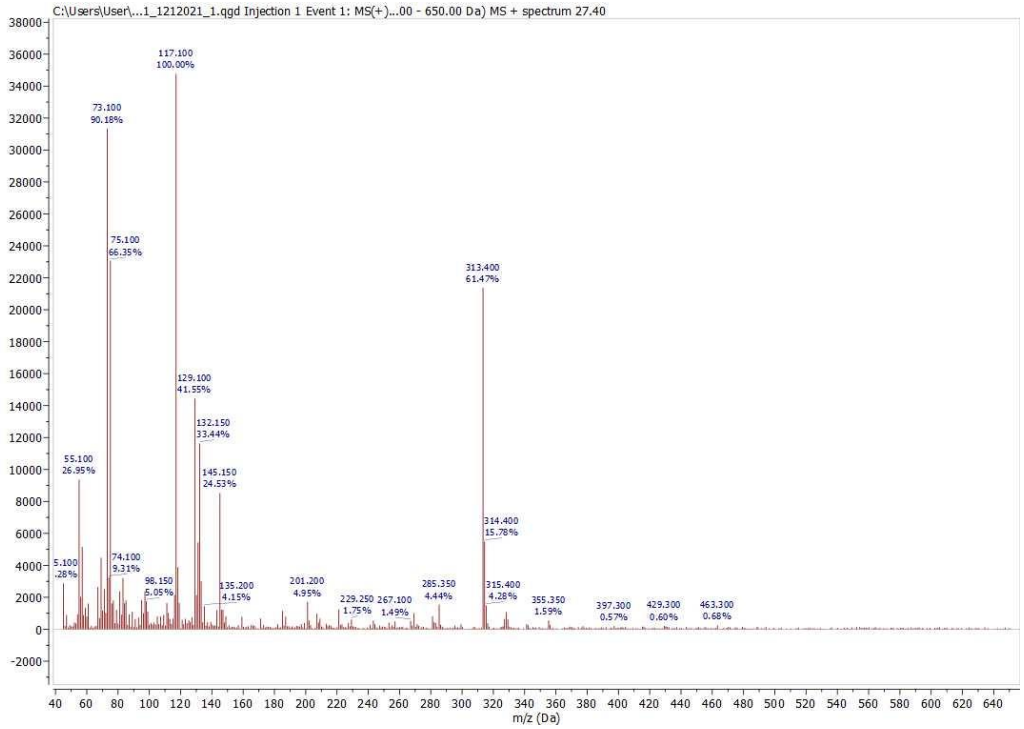

Figure 6.2: Mass spectrum of Compound A identified as a potential biomarker for grey leaf spot in the maize field trial chlorotic spots and mature lesions samples. It was identified at 27.4 minutes retention time in the leaf chromatogram.

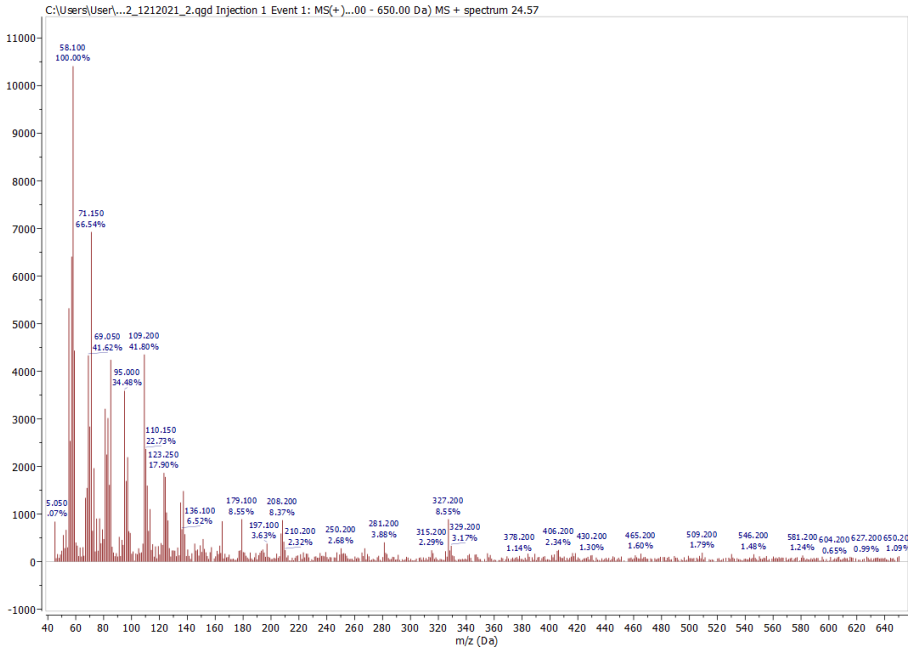

Figure 6.3: Mass spectrum of Compound B identified as a potential biomarker for grey leaf spot in the maize field trial mature lesions samples. It was identified at 24.5 minutes retention time in the leaf chromatogram.

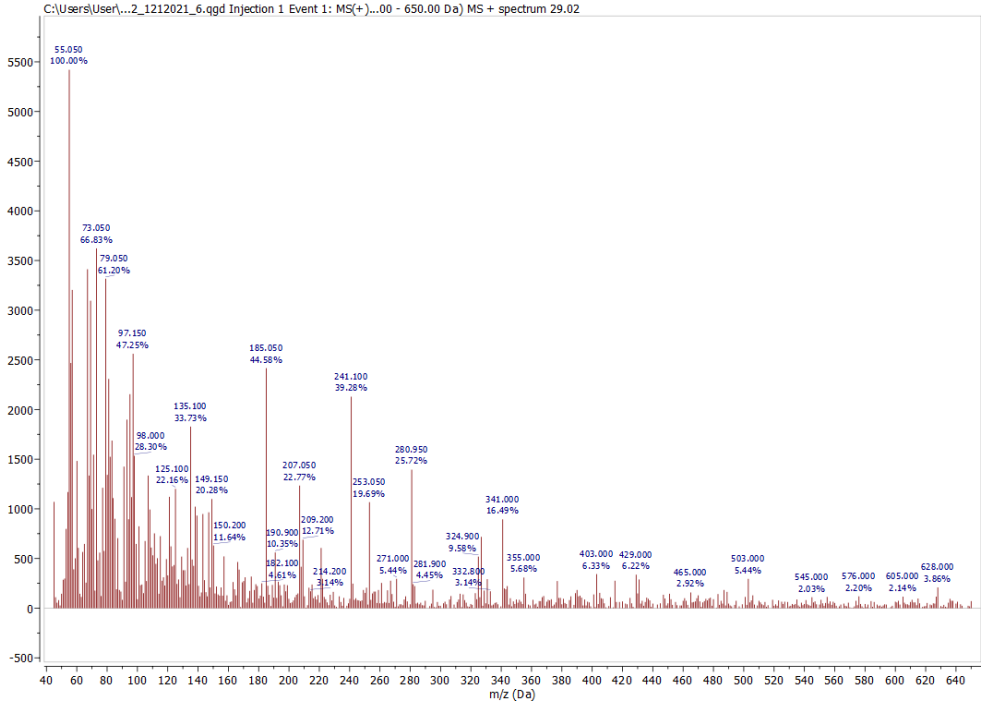

Figure 6.4: Mass spectrum of Compound C identified as a potential biomarker for grey leaf spot in both the leaf samples from the maize field trial with mature lesions and glasshouse trial with mature lesions. It was identified at 30.2 minutes retention time in the leaf chromatogram.

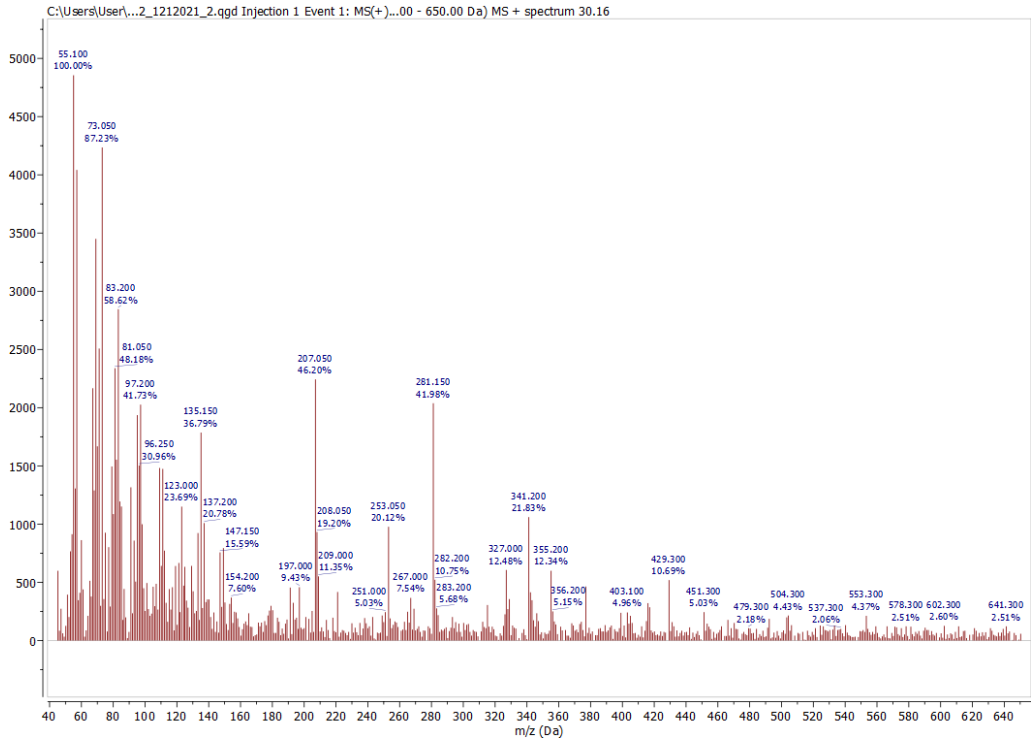

Figure 6.5: Mass spectrum of Compound D identified as a potential biomarker for grey leaf spot in symptomatic leaf samples from field trial with mature lesions. It was identified at 30.2 minutes retention time in the leaf chromatogram.

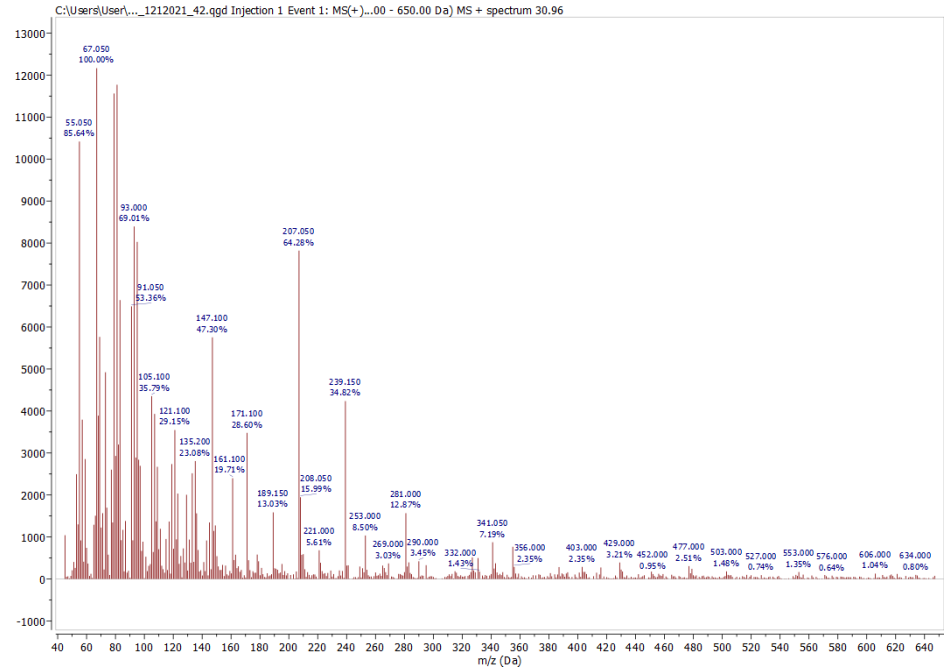

Figure 6.6: Mass spectrum of Compound D identified as a potential biomarker for grey leaf spot in symptomatic leaf samples from glasshouse trial with mature lesions. It was identified at 30.95 minutes retention time in the leaf chromatogram.

Appendix C : Full mass spectra of all potential biomarkers identified in cowpea artificially inoculated with *Fusarium verticillioides.*

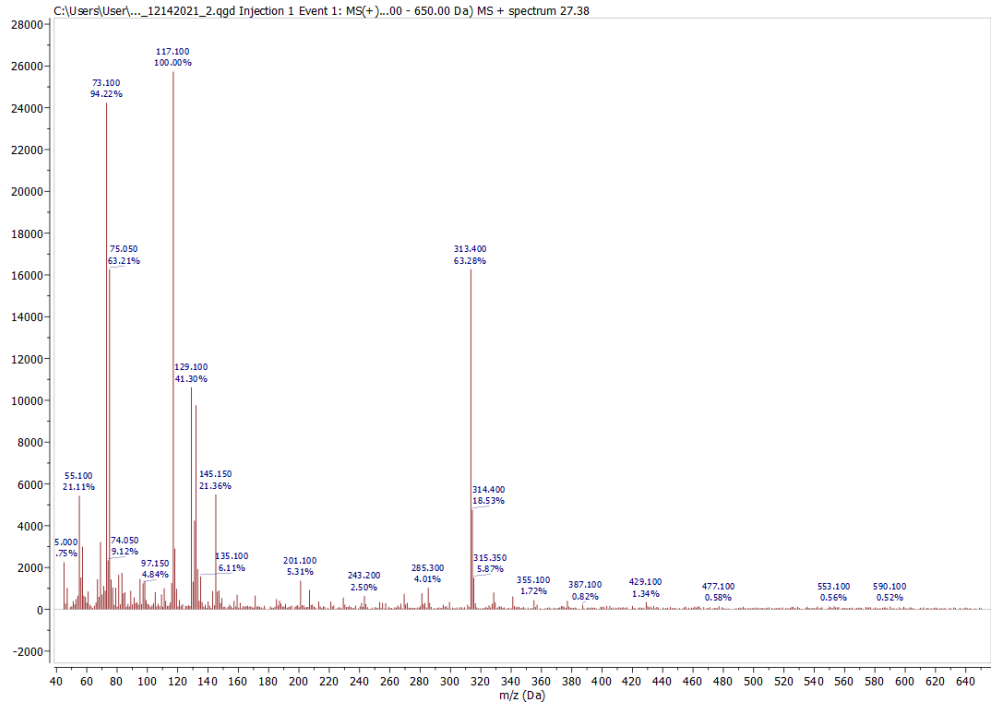

Figure 6.7: Mass spectrum of Metabolite A identified as a potential biomarker identified in the leaves of Fusarium verticillioides inoculated cowpea seeds. It was identified at 27.35 minutes retention time in the leaf chromatogram.

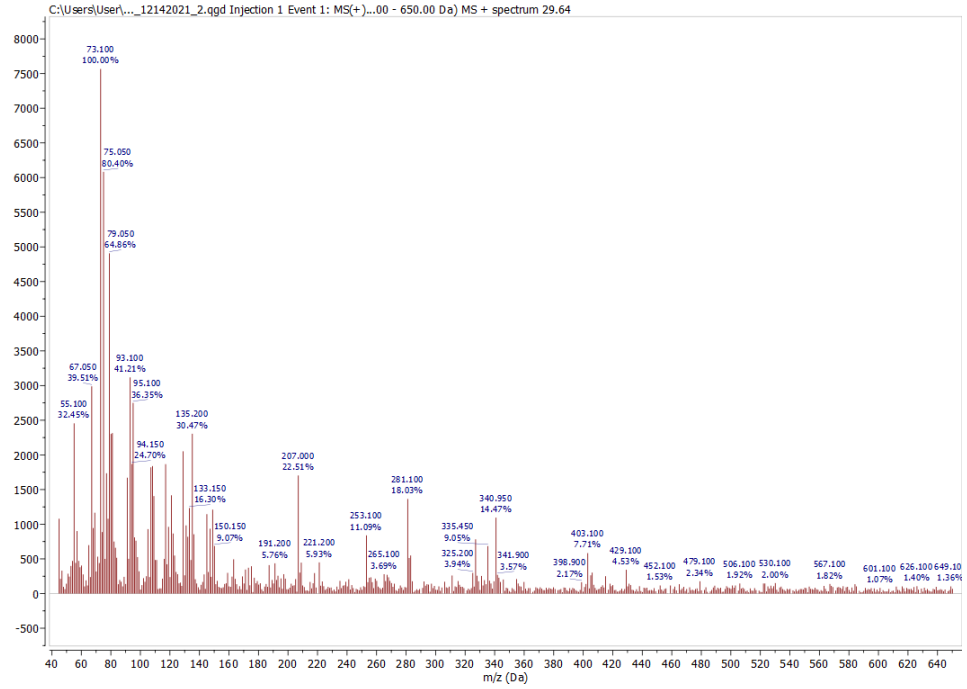

Figure 6.8: Mass spectrum of Metabolite B identified as a potential biomarker identified in the leaves of Fusarium verticillioides inoculated cowpea seeds. It was identified at 27.60 minutes retention time in the leaf chromatogram.

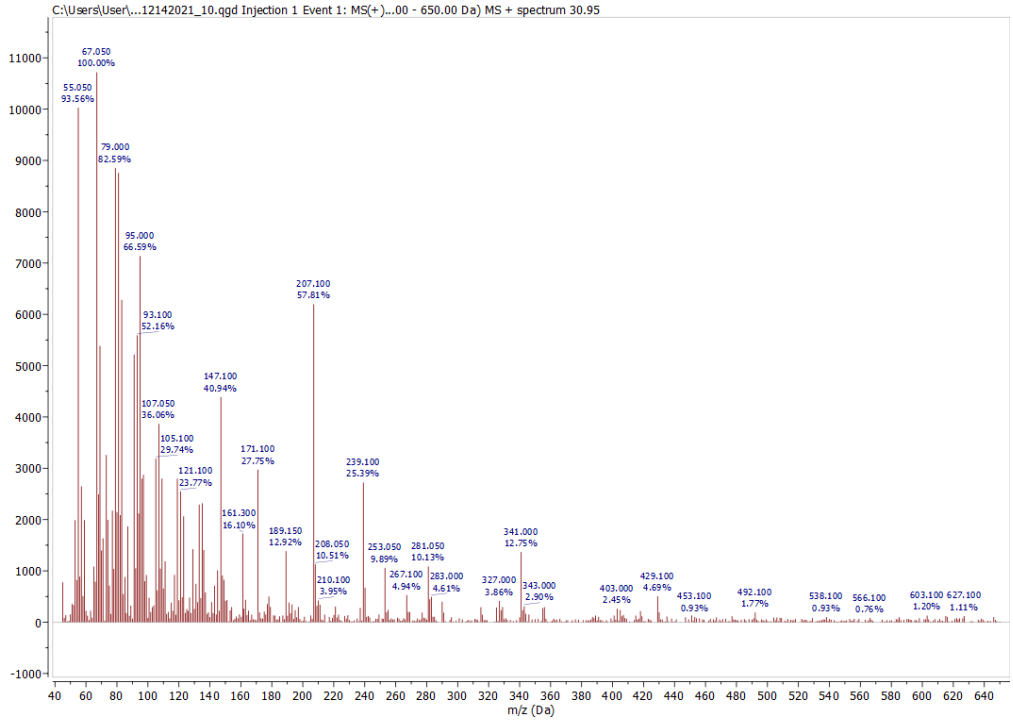

Figure 6.9: Mass spectrum of Metabolite A identified as a potential biomarker identified in the leaves of Fusarium verticillioides inoculated cowpea seeds. It was identified at 30.95 minutes retention time in the leaf chromatogram.